ABSTRACT

GRAHAM, BENJAMIN PHILLIP. Influence of Cortical Microtubules on the Diameter and Tip Shape of Cotton Fiber. (Under the direction of Dr. Candace H. Haigler).

Plant cell morphogenesis is critical to plant form and function. How plants achieve their shape is an active field of investigation, in part due to its potential for facilitating advances in the agriculture and textile industries. Cells with specialized shapes, like pollen tubes and root hairs, are critical for reproduction and nutrient uptake. Other unique plant cells are used directly by humans, such as the cotton fibers studied here. Cotton fibers are single cells that differentiate and elongate from the seed epidermis of *Gossypium* species. Two species of cotton, *Gossypium barbadense* and *G. hirsutum*, are the most widely cultivated species of cotton. The fibers of *G. barbadense* are longer, stronger, and have a smaller diameter relative to fibers of *G. hirsutum*. *Gossypium hirsutum* is more productive, but its fibers are of a lower quality due, in part, to its higher average fiber diameter. How plant cell shape formation is governed is a field of active investigation with many unanswered questions. Here, I seek to better understand cotton fiber morphogenesis in order to understand how to improve the quality of the world's leading renewable source for textile products.

First, I will review several specialized plant cell types characterized by two different growth modes, tip growth and anisotropic diffuse growth, in order to look for clues regarding their shape regulation that may be relevant to cotton fiber. The role of the cytoskeleton and cell wall in establishing/determining the cell shape of root hairs, pollen tubes, moss protonema, *Arabidopsis* trichome branches, and cotton fibers is discussed. Microtubules are a particular focus due to their potential influence on cellulose microfibril deposition and alignment, a process fundamental to cell shape formation. Of the cell types reviewed, *Arabidopsis* trichome branches may offer the most insight into early cotton fiber shape formation.

In the second chapter, a direct comparison of microtubule function in growth control between three cotton fiber tip types was conducted. These fiber tips vary in their natural diameter with the smallest being the single tip type found on *G. barbadense*. In contrast, two fiber tip types are found on *G. hirsutum*, the *tapered* and *hemisphere* types, with a small and large tip diameter respectively. An *in vitro* ovule culture system for *G. barbadense* developed in our lab aided the experimental comparisons between three tip types within two species. Ovules cultured

at 2 days post anthesis (DPA) with a microtubule antagonist, colchicine, were examined 48 hours later in order to look for differences in microtubule-mediated controls of expansion in different apical zones. Immunofluorescence was used to verify that colchicine abolished the microtubules. The results were consistent with a zonal regulation of microtubule-mediated expansion from the apex to 200 µm back for *G. hirsutum tapered* tips.

The third chapter expands on the initial results in a thorough examination of how microtubules regulate the diameter of the three fiber tip types, while also investigating how microtubules change and affect tip shape over time. Two microtubule antagonists (colchicine and oryzalin) and a microtubule stabilizer (Taxol) were added to ovule cultures at 1 and 2 DPA, followed by measurements 48 hours later. During this time cotton fiber shape is highly dynamic, and disrupting microtubules typically caused fiber swelling with a greater effect occurring with earlier treatment. A transient relationship between the apical dome size and microtubule organization was established in young *G. hirsutum tapered* fibers. Cumulatively, the results set the stage for identifying and testing potential molecular mechanisms for decreasing the diameter of *G. hirsutum* fibers as a means of making higher quality textiles more economical.

Influence of Cortical Microtubules on the Diameter and Tip Shape of Cotton Fiber

by
Benjamin Phillip Graham

A dissertation submitted to the Graduate Faculty of
North Carolina State University
in partial fulfillment of the
requirements for the degree of
Doctor of Philosophy

Plant Biology

Raleigh, North Carolina
2019

APPROVED BY:

_____	_____
Candace H. Haigler Committee Chair	Marcela Rojas-Pierce
_____	_____
Imara Perera	Vasu Kuraparthy

DEDICATION

This work is dedicated to my family, without whom this would not have been possible. To my parents, for their constant encouragement and for teaching me that those pursuing great success should be prepared for great hardship. To my wife, for enduring every trial with me while remaining steadfast in her support of this endeavour. To my children, for reminding me of where dreams begin and for providing the raucous laughter and endless joy that overshadowed any adversity I faced along the way.

BIOGRAPHY

Benjamin Phillip Graham was born in Charleston, South Carolina on May 8th, 1980. As a teenager, he moved to northeastern North Carolina where he finished high school in Camden County. After high school, Ben was admitted to the Honors Program at University of North Carolina at Wilmington to study biology, where he remained for only three semesters. Following his departure from college, Ben moved back to Charleston, SC and joined the work force. He spent his work weeks fulfilling various roles in local restaurants, from cooking to management, and his weekends traveling the country with a local rock band that he managed. It was during this time that Ben met his future wife. After marrying, Ben and his wife moved to Tucson, AZ where they stayed for several years exploring the landscapes of the Sonoran Desert and surrounding region. Ready to settle down, they returned to North Carolina in 2008 to start a family. Soon after returning to the east coast, Ben enrolled at Elizabeth City State University, in Elizabeth City, NC, where he finished his undergraduate degree, earning a B.S. in General Biology. While earning his degree, Ben worked for the university conducting research on the population genetics of local submerged aquatic vegetation under the direction of Dr. Margaret Young. He also supervised lab courses taught by his advisor where he developed his passion for research and teaching. In November of 2011, Ben and his wife celebrated the birth of their son. Ben graduated from ECSU in December of 2012 and remained a research technician there until joining the graduate program in the Plant and Microbial Biology Department at North Carolina State University in August of 2013. As a graduate student pursuing his Ph.D., Ben studied the cellular and molecular biology of cotton fiber shape determination as a research assistant in the lab of Dr. Candace Haigler. Not letting graduate school stand in the way, Ben and his family welcomed the addition of their second child, a daughter, in July of 2016. His passion for teaching drove him to participate in the Preparing the Professoriate teaching program at NCSU in 2017. Ben thrives while learning new things and hopes to convey that passion and excitement to new students as he continues on his path as an educator and scientist.

ACKNOWLEDGMENTS

I am very grateful to my advisor, Dr. Candace Haigler, for providing me with this opportunity and patiently guiding me through graduate school. I would also like to thank Dr. Margaret Young of Elizabeth City State University for preparing me for this journey and supporting me along the way. Thanks to Dr. Mike Stiff and Dr. Rich Tuttle for being wonderful mentors, dedicating many hours to my training, and helping me get my research off the ground. I would like to thank Dr. Larry Blanton for his constant encouragement, endless scientific witticisms, and great advice on navigating the logistics of graduate school. I would also like to thank Dr. Marcela Rojas-Pierce, Dr. Vasu Kuraparthy, and Dr. Imara Perera for serving on my committee and providing their support and counsel over the years. I thank Cotton Incorporated, Cary NC, for research support, including a Research Assistantship provided through Dr. Haigler's grant during my Ph.D. graduate program. Laser scanning confocal microscopy was performed in and supported by the staff of the Cellular and Molecular Imaging Facility supported by NC State and the National Science Foundation. The Phytotron staff plays a big role in helping to manage our cotton growing program, without which my work would not have been possible. Other researchers assisting with data collection are recognized in pertinent places below.

TABLE OF CONTENTS

LIST OF TABLES

Chapter 1

Chapter 2

Chapter 3

LIST OF FIGURES

Chapter 2

Appendix

CHAPTER 1

A Review of the Cytoskeleton in Anisotropic Plant Cell Shape Determination

Introduction

Anisotropic growth is a fundamental feature of cell morphology in animal, fungal, and plant systems. Expansion of a cell in a discrete, controlled direction allows for the formation of neurons, fungal hyphae, and a variety of specialized plant cells. This review will discuss our current understanding of how the cytoskeleton facilitates polar elongation in several plant cell types with different growth modes. Specifically, information regarding the processes governing the shape and size of the apical dome at the tips of the elongating cell types will be assessed for consistency with new observations in young cotton fibers.

Cotton fiber overview

Cotton fibers are single interphase cells that elongate from the epidermal cells of a developing fertilized ovule in some *Gossypium* species. Two *Gossypium* species in particular, *G. hirsutum* and *G. barbadense*, make up the bulk of the world's cotton production (Constable et al., 2015). Cotton fibers begin development near the day of anthesis by differentiating from epidermal cells and expanding isodiametrically above the epidermal surface. During the next two days fiber cells transition to polar elongation and tip shape modification. Cotton fibers elongate for roughly three weeks before transitioning to a stage of secondary cell wall deposition and maturity. This total process occurs over a period of about 50 days (Haigler et al., 2012; Stiff & Haigler, 2012).

Fibers produced by the two different species differ in their quality with *G. barbadense* producing more desirable fibers for textile products (Naylor et al., 2014). The superior qualities of *G. barbadense* fiber include greater length, strength, and lower fineness. Fineness is a measurement of mass per unit length (μg m^{-1}, or mtex). A lower fineness value is preferred because finer cotton leads to thin yet strong yarns. For example, the fineness values of two elite cotton cultivars studied extensively in the Haigler lab are 176 or 139 for *G. hirsutum* cv Deltapine 90 or *G. barbadense* cv Phytogen 800, respectively (Avci et al., 2013). Lower fineness results from smaller fiber diameter and/or a thinner secondary cell wall, which is not desirable

since secondary cell wall cellulose contributes to individual fiber strength and deep fabric dyeing. Correspondingly, the maturity ratios (describing the extent of wall thickening) of modern *G. hirsutum* or *G. barbadense* fibers typically exceed 0.9 (Avci et al., 2013).

Given high maturity, the lower fineness of *G. barbadense* fibers is mainly attributed to their lower perimeter as compared to *G. hirsutum*. (Perimeter is also approximated by the diameter of cotton fibers, which are nearly circular). Our lab recently showed variation in cotton fiber tip diameter, with young *G. barbadense* fibers having only one tip type, whereas *G. hirsutum* exhibits two distinct tip morphologies classified as *tapered* or *hemisphere* with smaller and larger diameters, respectively (Stiff & Haigler, 2016). These differences correlate with narrow fibers in mature *G. barbadense* cotton as compared to wider fibers (on average) in *G. hirsutum* cotton. For example, mature *G. hirsutum* cv. Deltapine90 had a calculated diameter of 16.78 µm, whereas 14.75 µm was the comparative value for *G. barbadense* cv. Phytogen 800 fiber (Avci et al., 2013). How the larger cell diameter in some *G. hirsutum* fibers, which occur in a mixture with narrower fibers, may impact the quality of downstream products is an important area of future exploration.

The cause of the two different fiber cell phenotypes occurring side-by-side on the same *G. hirsutum* ovule is unknown. Unfortunately, *G. barbadense* is the less productive species with a smaller cultivation range than *G. hirsutum*. This leads to *G. hirsutum* comprising roughly 90% of cotton cultivated globally (Constable et al., 2015). The natural question that forms in response to this is: how do we increase the quality of the more productive cotton? Since quality is linked to the cell shape, we must first understand what biological processes govern this property.

Control of Plant Cell Shape

Among the plant cells in a single plant body, many different shapes can be assumed depending on the location and function of the cell. Plant cells can be shaped like blocks, tubes, puzzle pieces, hairs, and even stars (Geitmann & Ortega, 2009). Extensive coordination between processes governing cell wall assembly and remodeling, intracellular trafficking, and signal transduction must be maintained in order to facilitate such outcomes. Different cell shapes are generally the result of the irreversible expansion of the cell wall in a tightly regulated fashion. Cell expansion occurs when turgor pressure increases within the cell causing an omnidirectional strain on the plant cell wall. Growth in discrete directions can occur when the cell wall is

resistant to turgor pressure in some regions while yielding to it in others. These concepts have been recently reviewed in detail (Guerriero et al., 2014; Bidhendi & Geitmann, 2016; Cosgrove, 2018; Eng & Sampathkumar, 2018).

The primary cell wall of dicotyledonous angiosperms, like cotton, is a complex composite of pectins, hemicelluloses (mainly xyloglucan), glycoproteins, and cellulose microfibrils. Some of these components are synthesized within the cell and secreted to specifically identified locations within the cell wall (Zhu et al., 2015). Cellulose, on the other hand, is synthesized from mobile plasma membrane-embedded protein complexes (Paradez et al., 2006). Cellulose is formed as a linear chain of glucose molecules synthesized via β-1,4 glucan linkages. Once extruded, the glucan chains can coalesce into high tensile strength cellulose microfibrils. The cellulose synthase complexes (CSCs) are assembled within the Golgi apparatus of the cell and delivered to the plasma membrane at specific locations (Crowell et al., 2010; Zhang et al., 2016).

During cell growth, methyl-esterified pectin is often secreted into the cell wall at the points of cell expansion. Expansion also occurs as a result of cell wall loosening via enzymatic activity (Cosgrove, 2018). As the cell continues to grow, the pectin can become more rigid through the enzymatic action of pectin methyl-esterase (PME) (Bosch et al., 2005). This enzyme removes the methyl group allowing pectins to crosslink with calcium ions (Ca^{2+}), which increases the stability of the pectin matrix when at the proper pH and barring enzymatic cell wall loosening (Palin & Geitmann, 2012). Cellulose microfibrils form structural supports embedded within the pectin matrix and are capable of interacting with non-cellulosic cell wall components (Park & Cosgrove, 2012). Both pectins and the hemicelluloses are sugar-based polymers that are branched and contain more sugar moiety types than cellulose. Hemicelluloses, such as xyloglucan, are associated with aiding the plant cell wall in maintaining its integrity via interactions with other wall components (Xiao et al., 2016). Plant cell morphogenesis is an active subject of study where much remains unclear.

The majority of plant cells expand via diffuse growth. Cells undergoing diffuse growth exhibit isodiametric cell expansion where cell wall synthesis takes place on all or most faces of the cell. Directional or anisotropic growth can also occur via diffuse growth. Cells of plant hypocotyls and within the root elongation zone develop in this way. The elongation of these cells, while simultaneously controlling their diameter, is what contributes to the overall plant

size. The current model of diffuse growth describes a primary cell wall with transversely oriented cellulose microfibrils that coincide with cortical microtubules. The transversely aligned cellulose acts to reinforce the cell wall preventing diametric expansion (Cosgrove, 2018).

Another form of polar elongation, tip growth, occurs when the majority of cell wall synthesis occurs at one end of an anisotropically expanding cell. Root hairs, pollen tubes, and moss protonema are classified as this type. Cells of this type concentrate new cell wall synthesis at the apex of the growing cell with no diametric expansion behind the apex. Typically, cells of this type have a cytoskeleton that is longitudinally oriented, coinciding with the growing axis of the cell (Ketelaar et al., 2003; Vidali & Bezanilla, 2012). The cells are also reinforced outside of the growing region by cellulose and other cell wall components. However, the cellulose microfibrils may not be transverse like in diffuse growing cells.

A mixed-mode of growth termed apically-biased diffuse growth, which exhibits elements of both tip- and diffuse growth, has been proposed for *Arabidopsis thaliana* trichome branches and cotton fibers. These cells have transversely oriented cellulose microfibrils, like diffuse growing cells, but exhibit a higher degree of cell wall synthesis in the apical region (Yanagisawa et al., 2015; Stiff & Haigler, 2016; Yu et al., 2019). For cotton fibers, treatment with a cell wall-degrading enzyme mixture caused bursting of cotton fibers predominantly at the apex, indicating new cell wall material is likely being secreted there. Consistently, in pulse-chase experiments with a cell wall-binding fluorophore, new cell wall synthesis at the apex was supported by its decreased fluorescence during the chase period (Stiff & Haigler, 2016).

Cell shape is ultimately determined by the zonal extension, or restriction, of the cell wall during turgor driven growth. Whether or not the cell wall succumbs to, or resists, turgor pressure depends on its biochemical makeup. Variations in cellulose and matrix polysaccharides can affect how the cell wall reacts to stress. What determines deposition sites and how the cell wall composition is coordinated to facilitate organized expansion is currently unclear. It is becoming clearer, however, that the cytoskeleton is highly involved in influencing cell wall composition and cell shape.

The Cytoskeleton

A central element influencing plant cell shape is the cytoskeleton. The cytoskeleton is primarily composed of microtubules, actin filaments, and their associated proteins. The

cytoskeleton is critical for mitosis and cytokinesis in eukaryotic organisms. In interphase cells, the cytoskeleton is required for organelle and vesicle trafficking, endo- and exocytosis, and structural support.

Microtubules are comprised of filamentous polymers of α- and β-tubulin dimers, termed protofilaments, that coalesce laterally into a hollow tube-like lattice (Zhang et al., 2015). Microtubule assembly is polar in that new tubulin dimer subunits are added to the growing plus end in a guanosine triphosphate (GTP)-dependent process. The many functions of microtubules, and their associated proteins, in plants have been extensively discussed in recent years (Bashline et al., 2014; Hashimoto, 2015; Krtková et al., 2016; Elliott & Shaw, 2018). Briefly, microtubules have been shown to function in the deposition and recycling of CSCs into, and from, the plasma membrane (Crowell et al., 2009). This is achieved via a transport and recycling endomembrane network including Golgi vesicles and the small, poorly defined compartments, called either cellulose synthase compartments (SmaCCs), or microtubule-associated cellulose synthase compartments (MASCs) (Zhu et al., 2015; Li et al., 2015).

Microtubule-associated motor proteins, such as the KINESIN-4A isoform known as FRAGILE FIBER 1, are capable of trafficking cell wall material to the plasma membrane. KINESIN-4A transports non-cellulosic matrix polysaccharides in elongating *Arabidopsis* cells while showing a similar distribution along microtubules in *G. hirsutum* cotton fibers (Kong et al., 2015; Zhu et al., 2015). Another motor protein, KINESIN 13A, enables the distribution of Golgi-stacks and plays a role in trichome branching and cell size in *Arabidopsis*. Mutants of KINESIN 13A produce trichomes with extra branches, more clustered Golgi-stacks, and larger petals compared to wild type (Fujikura et al., 2014; Lu et al., 2005). KINESIN 13A has an orthologue in *G. hirsutum* that can rescue the mutant trichome phenotype in *Arabidopsis*. This shows a high degree of functional similarity within two types of epidermal cell extensions from different species (Lu et al., 2005).

The most direct influence of microtubules on cell wall structure may be the guidance of CSCs during some stages of cellulose microfibril deposition (Paradez et al., 2006). A linker protein characterized in *Arabidopsis*, CELLULOSE SYNTHASE-INTERACTIVE PROTEIN1 (CSI1), is capable of interacting with membrane-embedded CSCs and cortical microtubules, potentially influencing the orientation and efficiency of cellulose microfibril deposition (Gu et al., 2010; Li et al., 2012). This has been documented in elongating hypocotyl cells, but not in

more unique elongating cells such as trichomes, pollen tubes, or cotton fibers. However, in cells exhibiting close alignment of cellulose microfibrils and microtubules this mechanism may be plausible. There is evidence that properly aligned cellulose microfibrils can be formed without an aligned cortical microtubule array. Mutations in MOR1, a microtubule organizing protein, led to disrupted microtubule arrays, decreased anisotropy, and increased diametric expansion. The cellulose microfibrils in MOR1 mutants, however, were still aligned in a manner similar to the wild type (Whittington et al., 2001). This has led to the hypothesis that microtubule guidance of CSCs may partially function to increase the length of the deposited microfibril, while not be completely necessary for normal microfibril alignment. A reduction in microfibril length would reduce the strength of the cell wall, potentially allowing for increased diametric expansion (Baskin, 2005). Based on these limited examples, it is clear that microtubules are critical to plant cell shape and that there is still much to learn about how these processes are coordinated.

The well-studied counterpart to microtubules in the cytoskeleton is actin. Actin is a globular protein that can rapidly polymerize and depolymerize forming highly dynamic filaments. These filaments are integral for transporting vesicles containing cell wall material to the points of active growth in a cell. The primary motor protein associated with actin filaments and vesicle trafficking is myosin. (Reddy & Day, 2001; Paterson et al., 2012) The myosin-dependent movement of vesicles via actin produces the cytoplasmic streaming effect that can be observed in some living plant cells. Actin is considered critical for tip growth since pharmacological actin perturbation inhibits cell elongation (Harries et al., 2005; Vidali et al., 2001). The function and dynamics of actin in plants have been reviewed in-depth (Blanchoin et al., 2010; Henty-Ridilla et al., 2013; Szymanski & Staiger, 2018).

Similar to microtubules, the proteins that interact with actin filaments are vital to their function. Although actin is capable of nucleating on its own, the process is selectively aided by two actin nucleation regulators: the ACTIN RELATED PROTEIN 2/3 (ARP2/3) complex, and a class of actin-binding proteins, called formins. The ARP2/3 complex is a seven-subunit complex including two subunits, ARP 2 and ARP 3, having structural similarities to globular actin. Actin requires three monomers of globular actin to begin polymerization. The ARP2/3 complex acts as the first two monomers so that only a single globular actin monomer is needed to begin this process (Blanchoin et al., 2000). Other subunits of the ARP2/3 complex are thought to be involved with the targeting of the complex and interaction with other proteins, including

microtubules (Goley & Welch, 2006; Havelková et al., 2015). Profilins and formins are also important actin-interacting proteins. Profilins bind monomeric actin and promote the exchange of ADP (adenosine diphosphate) with ATP (adenosine triphosphate) so that ATP-dependent actin filament polymerization can take place more efficiently (Paavilainen et al., 2004). Formins contain two characteristic protein domains, one binds the actin-binding protein profilin, while the other promotes actin nucleation (Sagot et al., 2002). Formins can be membrane-bound, effectively promoting the formation of nascent actin at specific locations at the plasma membrane (Vidali et al., 2009).

Taken together, it is clear to see that the cytoskeleton is involved in many cellular processes. Understanding the driving forces behind the spatial regulation of cytoskeletal components when targeting processes necessary for morphogenesis is critical to advancing progress in the area. Continuing to explore the interaction between the cell membrane and the cytoskeleton may provide insight into how the cytoskeleton can be used in targeting cell wall synthesis and remodeling. Being able to use this information to manipulate plant cell morphogenesis would create many opportunities for advancements in the agriculture and textile industries.

Cell Models for Anisotropic growth

The following will examine the role of the cytoskeleton in several plant cell types that are morphologically similar to cotton fibers. Recent work investigating how microtubules influence the shape of root hairs, moss protonema, *Arabidopsis* trichome branches, and cotton fibers will be compared. All of these cell types undergo anisotropic growth, producing tube-like or conical cellular extensions, and exist outside of collective tissue-forming cell groups. The cellular processes of cotton fiber are among the least studied of these examples due to the difficulty of conducting genetic perturbation experiments in cotton. These other cell systems will be probed for similarities to cotton fiber and clues providing insight into cotton fiber morphogenesis. An overview of the cell types and their disrupted phenotypes can be found in Table 1.

A key experimental tool in understanding the control of anisotropic growth in model cells has been treatment with cytoskeletal antagonists, which essentially conducts a loss-of-function experiment without genetic manipulation. Popular microtubule antagonists include colchicine, oryzalin, and Taxol. Colchicine is a microtubule disrupting agent that binds at the interface

between the α- and β-tubulin monomers within the dimeric repeating units of the protofilaments. Colchicine may hinder microtubule polymerization at low concentrations or cause de-polymerization at high concentrations (Stanton et al., 2011). Oryzalin, a dinitroaniline class herbicide, binds only to plant α-tubulin at a non-conserved binding site (Dostal et al., 2014), thereby disrupting lateral associations between protofilaments and inhibiting microtubule rescue during reorientation (Morrissette et al., 2004). In contrast to the microtubule disruptors, Taxol stabilizes microtubules by binding to a conserved site in β-tubulin, promoting microtubule polymerization, stability, and/or bundling. Taxol-bound tubulin stabilizes protofilaments, increasing their propensity to accept additional monomers at the plus-end (Stanton et al. 2011) and inhibits the peeling apart of protofilaments at the minus-end (Downing, 2000).

Frequently used actin antagonists include latrunculins and cytochalasins. Latrunculin B, isolated from a sea sponge, binds to globular actin monomers preventing incorporation into polymerized actin filaments (Helal et al., 2013). Cytochalasin D is one of several derivatives of an alkaloid compound produced by fungus. Cytochalasin D binds to the growing end of actin filaments inhibiting actin polymerization (Scherlach et al., 2010).

Root hairs

Root hairs are necessary to increase the surface area of roots in order to more efficiently absorb water and nutrients from the substrate in which a plant grows. Root hairs are unicellular trichomes that are cylindrical extensions of a single epidermal cell. Excellent reviews have been published in recent years covering root hair systems biology, overall development, and actin in root hairs (Libault et al., 2010; Ketelaar, 2013; Grierson et al., 2014; Mendrinna & Persson, 2015, respectively).

Early studies characterizing microtubule dynamics in the differentiating and elongating root hair used a green fluorescent protein (GFP) reporter fused to MICROTUBULE ASSOCIATED PROTEIN 4 (MAP4) to observe the microtubules *in vivo* in *Arabidopsis* root hairs (Van Bruaene et al., 2004). The authors made observations at the onset of root hair differentiation during bulge formation of trichoblasts, during late-stage growth, and of full-grown root hairs to compare the microtubule arrangement throughout development. Although cortical microtubules appear randomly oriented at the time of differentiation, they take on a net axial to shallow helix orientation as the root hair elongates (Van Bruaene et al., 2004). A similar

arrangement was observed by Ketelaar and colleagues (2002), prior to the treatment of *Arabidopsis* root hairs with 1 µM oryzalin. Oryzalin treatment depolymerized all microtubules and led to wavy root hairs without disrupting root hair elongation rate or nuclear positioning. The authors concluded that microtubules may guide the direction of anisotropic growth, while not being necessary for growth *per se* (Ketelaar et al., 2002). Similar results were previously observed when 5 µM oryzalin was applied to growing root hairs (Bibikova et al., 1999). In addition to altered directionality, these authors observed branching of root hairs when treated with a microtubule stabilizer, Taxol (5 µM). In contrast, both groups reported a reduction of elongation when actin was disrupted using either latrunculin A/B or cytochalasin D, indicating that actin-mediated cell expansion is responsible for tip growth in root hairs (Bibikova et al., 1999; Ketelaar et al., 2003). An increase in diameter was also observed in root hairs after actin disruption with either Latrunculin A or B. Treatment with cytochalasin D or latrunculin A led to isodiametric expansion at the apex of the growing root hair. Abolishing the actin and microtubule cytoskeleton, followed by allowing actin to recover, resulted in the resumption of growth in a new direction. These results support the concept of actin and microtubules working synergistically to specify the location of cell expansion (Ketelaar et al., 2003). Alternate concentrations of oryzalin (1 µM) or Taxol (10 µM) also caused swelling in *Arabidopsis* roots. The oryzalin treated root hairs were sometimes swollen or wavy, while root hairs exposed to Taxol grew straight and much longer than normal (Baskin et al., 1994). These results highlight the function of microtubules in maintaining the direction of elongation during root hair growth.

The cellulose microfibril arrangement in root hairs varies depending on the location. At the apex of the growing root hair, cellulose microfibrils are randomly oriented, but they become transversely oriented behind the apex (Akkerman et al., 2012). Some evidence supports that the apically localized cellulose present in the root hair is not deposited by canonical cellulose synthase proteins that are potentially associated with cortical microtubules. Primary cell wall cellulose synthase genes, CELLULOSE SYNTHASE 3 and 6 (CESA3; CESA6), do not localize to the apex of root hairs. Instead, CELLULOSE SYNTHASE-LIKE PROTEIN D3 (CSLD3/KOJAK), localizes to the apical periphery (Park et al., 2011). The root hairs of mutants in *Arabidopsis* CSLD3 (*atclsd3-1*) initiated just as in wild-type, but they were shorter and often leaked cytoplasm from the apex. This supports a disruption of the proposed apical localization of *At*CSLD3 (Wang et al., 2001). Treatment with a cellulose synthase inhibitor, 2,6-

dichlorobenzene (DCB), and with cellulase phenocopied the *AtCSLD3* mutation (Park et al., 2011).

Pollen tubes

Pollen tubes are essential to the sexual reproduction of flowering plants. The germinated pollen grain forms an extension that must undergo rapid and invasive anisotropic growth to deliver genetic material to an ovule. The cytoskeleton is critical to pollen tube morphogenesis. Recent reviews regarding the pollen tube cytoskeleton are available (Cai et al., 2015; Fu, 2015; Onelli et al., 2015).

When exploring the role of the cytoskeleton in *Papaver rhoeas* (poppy) pollen tube elongation, Gossot and Geitmann (2007) observed results similar to those seen in root hairs. Disruption of the actin cytoskeleton with low concentrations of latrunculin B (1-3 nM) reduced pollen tube germination and elongation rate. Actin destabilization also reduced the pollen tube's ability to penetrate obstacles, a necessary function of pollen tubes. However, abolishing microtubules using 1 µM oryzalin had no effect on germination, elongation, or obstacle penetration, but rather resulted in straighter pollen tubes when compared to the controls (Gossot & Geitmann, 2007). This demonstrates a role for microtubules in directional control of pollen tube growth, similar to the case with root hairs. When both antagonists were used in conjunction, germination only rarely occurred. Cytoskeletal visualization in fixed pollen tubes revealed axially oriented microtubules and actin filaments. Disrupting actin resulted in swollen apices, which is also similar to root hairs (Gossot & Geitmann, 2007). In living tobacco pollen tubes, axially oriented microtubules occurred cortically and medially throughout most of the cell, but they did not extend into the apex. This observation was possible due to the heterologous expression of an *Arabidopsis* GFP-tagged microtubule-associated protein, END BINDING 1 (EB1) (Cheung et al., 2008). In pollen tubes of *Picea abies*, exposure to oryzalin (100 µM) led to severely swollen pollen tubes that did not elongate normally, which is contrary to what was observed in poppy pollen tubes (Anderhag et al., 2000; Gossot & Geitmann, 2007). Treatment with colchicine (100 µM) resulted in swelling but also caused branching (Anderhag et al., 2000). Microtubules of tobacco pollen tubes (*Nicotiana sylvestris*) were abolished when treated with 25 µM colchicine, as demonstrated by immunofluorescence. Microtubule disruption in *N. sylvestris* resulted in a loss of directional growth control but no swelling was noted (Joos et al., 1994).

Live-cell imaging using a fluorescently tagged actin-binding protein domain focused on the highly dynamic actin cytoskeleton in lily pollen tubes (*Lilium formosanum*) (Rounds et al., 2014). This method clearly revealed an annular fringe of fine actin filaments just below the apex, as previously described by Lovy-Wheeler and colleagues when using immunofluorescence to visualize actin in cryo-fixed lily (*Lilium longiflorum*) and tobacco (*Nicotiana tabacum*) (Lovy-Wheeler et al., 2005). This unique structure is made up of short, non-bundled actin, and it is involved in maintaining the direction of pollen tube growth in lily. The actin fringe occurs just below the growing apical dome of the pollen tube and is responsible for localized cell expansion. Disruption of the actin fringe with latrunculin B leads to irregular pectin deposition near the apex (Rounds et al., 2014).

Another study showed that an increased amount of methyl-esterified pectin is secreted at the apex, relative to the rest of the pollen tube in tobacco (Bosch et al., 2005). Cellulose was shown to be evenly distributed throughout the pollen tube, while callose was shown to be absent from the apex. Crystalline cellulose was detected with Pontamine Fast Scarlet (S4B) and carbohydrate-binding module 3a (CBM3a), while callose was detected using either immunofluorescence or aniline blue. It was proposed that callose was another cell wall component used to solidify the cell wall distal from the apex (Biagini et al., 2014; Chebli et al., 2012). Microtubules were proposed to aid in callose distribution, as disruption of microtubules with oryzalin (1 μM) led to a change in callose distribution compared to the control in tobacco pollen tubes. It was noted that the secretion of pectins in the apex was not disrupted upon oryzalin treatment, suggesting that an actin-mediated control of this function was not altered (Biagini et al., 2014). This coincides with data from Sampathkumar et al. (2011), which showed that actin filaments are capable of some nucleation and polymerization at the cell's interior even after microtubules were abolished. Cellulose also plays a role in reinforcing the pollen tube shape. Treatment of pollen tubes from potato (*Solanum chacoense*) and lily (*Lilium orientalis*) with cellulase and a cellulose crystallization inhibitor, CGA (1-cyclohexyl-5-(2,3,4,5,6-pentafluorophenoxy)-1λ4,2,4,6-thiatriazin-3-amine), resulted in increased diametric expansion (Aouar et al., 2010).

Moss protonema

Mosses are non-vascular bryophytes that are evolutionarily ancestral to flowering plants. The moss, *Physcomitrella patens*, is a model organism for research on plant development and evolution. Growth in moss is accomplished through the extension of protonema; a filamentous, tip growing cell type. As they develop, protonema can differentiate into either chloronema or caulonema, both of which continue to elongate via tip growth while having different diameters. Chloronema contain many chloroplasts and elongate slowly relative to the alternative caulonema cells (Menand et al., 2007).

Recent work with *P. patens* showed that both microtubules and actin filaments terminated in interdependent clusters, or focal points, at the apex of moss protonema. Both actin filaments and microtubules form axial arrays parallel to the growing axis of the cell. A fluorescently tagged actin-binding protein (Lifeact; Vidali et al., 2009) revealed that an intense apical actin signal predicted the site of cell expansion. Microtubules were shown to co-localize with actin bundles in the apical domain (Wu & Bezanilla, 2018). Both formin (class II) and MYOSIN VIII also co-localized with the converging actin-microtubule clusters at the apex. Oryzalin (10 µM) treatment caused the disruption of both the formin and actin signal, suggesting that microtubules mediate formin localization to promote actin polymerization in a discrete apical cell region. Given that the disruption of either actin or microtubules disrupted the other array, the authors concluded that the actin-associated proteins may also interact with microtubules to stabilize the zone of cell expansion (Wu & Bezanilla, 2018).

Cellulose synthesis has recently been investigated in *P. patens* via live-cell particle tracking of fluorescently tagged CESA proteins. The investigators determined that CESA velocity in these tip growing cells was similar to what is observed in diffuse growing cells (Tran et al., 2018). Cellulose synthase tracks, however, did not indicate any alignment of cellulose deposition as would be expected in diffuse growing cells. Treatment with DCB (10 µM) and isoxaben (20 µM), both disruptors of cellulose synthesis, showed reduced CSC movement, similar to results reported for root hairs (Tran et al., 2018; Park et al., 2011). Cells treated with DCB tended to burst at the tip, while those treated with isoxaben showed reduced CSC motility, like DCB-treated cells, but no cell bursting was observed. No swelling of the protonema cells was reported with either treatment (Tran et al., 2018). The lack of a common cellulose-deficient phenotypes in moss, such as swelling, is similar to how root hairs responded to isoxaben

treatment. This implicated a potential role for CLSD3, which is thought to be responsible for CESA-independent cellulose synthesis at the root hair apex (Park et al., 2011).

Trichome branches

Arabidopsis leaf trichomes are a unicellular epidermal extensions with a short stalk and three pointed branches whose apical diameter shrinks as the branch elongates. Developing *Arabidopsis* trichomes exhibit transversely oriented microtubule arrays aligning just below the apex, similar to the arrangement in diffuse growing cells, (Yanagisawa et al., 2015). Early work looking at genetic mutants with abnormal trichome phenotypes established over 20 genes critical for proper trichome formation (Hulskamp et al., 1994). Some of these genes are now known to influence trichome branching, such as the kinesin motor protein, *ZWICHEL* (Oppenheimer et al., 1997). Other genes, like the *DISTORTED* family of genes, are important for normal trichome branch morphology (Schwab et al., 2003).

Later studies of other trichome mutants were able to distinguish between certain functions of the actin and microtubule cytoskeleton. Mutants in α-tubulin resulted in over-branched and twisted trichomes, while mutations in ARP3, part of the actin nucleating complex, resulted in twisted trichomes. In the tubulin mutant, *TORTIFOLIA2*, right-hand twisting was observed and may be attributed to the formation of microtubule bundles forming in ectopic locations during branching (Buschmann et al, 2009; Sambade et al., 2014). Taxol treatment revealed that *Arabidopsis* trichome branching is influenced by microtubule organization. Stabilization of microtubules in a the branchless mutant, *stichel*, resulted in directional changes indicative of branch formation. Branching was also increased in *zwichel* mutants that are usually deficient in branching (Mathur & Chua, 2000). *Arabidopsis* trichome branches treated with oryzalin (100 µM) prior to initiating elongation failed to develop branches at all (Szymanski et al., 1999)

Finite element modeling and live-cell imaging of *Arabidopsis* trichome branches indicated that spatially controlled cytoskeletal activity was critical to establishing, and maintaining, the branch shape. This was highlighted by the characterization of a microtubule depleted zone (MDZ) at the apex of the growing trichome branch (Yanagisawa et al., 2015, 2018). The authors documented a cell wall thickness gradient, in which the isotropic apex of the trichome branch was the thinnest, and the base of the trichome branch was the thickest. This

gradient was proposed to be essential to morphogenesis by contributing to increased cell strain at the apex in response to turgor pressure. The cell wall expanded most rapidly at the apex, relative to the distal zone of the branch tip, as demonstrated by bead labeling. Unfortunately, the finite element modeling did not mimic the empirical data indicating that some parameters of trichome morphogenesis are still not fully understood (Yanagisawa et al., 2015).

The isotropic nature of the apex is important for determining the overall shape of the cell. Expansion at the apex is coupled with the addition of cell wall material facilitated by the actin cytoskeleton. As the trichome branch begins to elongate distal from the apex, cortical microtubules, cellulose microfibrils, and cell wall remodeling reinforce the cell wall to prevent uncontrolled diametric expansion. Modeling indicated that the microfibril angle greatly influenced elongation. The transverse orientation of the cellulose microfibrils coincided with that of cortical microtubules. This was determined by imaging trichomes of transgenic *Arabidopsis* lines with fluorescent reporters fused to a microtubule-binding domain and CESA6 to observe microtubules and cellulose synthesis trajectories respectively (Yanagisawa et al., 2015). Pharmacological disruption of microtubules using oryzalin in transgenic *Arabidopsis* lines expressing markers for microtubules and actin showed that microtubules disruption resulted in altered localization of the apical actin signal. The apical actin activity, which is dependent upon membrane-bound proteins, was proposed to be physically sequestered to a discrete region at the apex by the transverse cortical microtubule array occurring in the sub-apical region (Yanagisawa et al., 2018). A similar arrangement of microtubules was inferred from live-cell imaging of 2 DPA transgenic cotton fibers expressing a fluorescent microtubule plus-end tracking protein (Yu et al., 2019).

Further investigation of the *Arabidopsis* trichome MDZ showed that the spatial regulation of microtubules was important for confining an actin polymerization signal to the apical domain. A guanine nucleotide exchange factor, SPIKE1, is responsible for recruiting activators of actin nucleation resulting in the generation of localized actin networks. SPIKE1 localizes to the plasma membrane at the apex of growing trichome branches, but it lost its apical localization when microtubules were disrupted with oryzalin (100 µM). SPIKE1 mutants also showed disrupted localization of ARP2/3 complex, supporting a role for SPIKE1 in influencing actin nucleation (Yanagisawa et al., 2018). The cortical microtubules closely associated with, and possibly bound to, the plasma membrane were proposed to moderate SPIKE1 localization by

acting as a physical barrier preventing displacement of membrane-bound proteins. A strong relationship between the shape of the apical dome and the MDZ was established using regression analysis of a plot of the apical radius of curvature versus the perimeter length of the MDZ (Yanagisawa et al., 2015). The authors later proposed that these mechanisms may be related to cotton fiber development. However, considering the different fates of these two cell types, the mechanisms regulating tip shape in trichome branches may or may not apply to cotton fibers, especially considering the diversity of cotton fiber tips.

Cotton fibers

As cotton fibers begin to expand, they protrude from the epidermis as an isodiametric bulge. Microtubules exhibit a random orientation when visualized via the time-lapse signal of a fluorescent microtubule plus end marker (Yu et al., 2019). Within the first 48 hours, cotton fibers transition into polar elongation while also refining the shape of the fiber apices (Stiff & Haigler, 2016; Yu et al., 2019). By 2 DPA, cortical microtubules have aligned into an array transverse to the longitudinal axis, similar to what is seen in diffuse growing cells. This has been shown by time-lapse, live-cell imaging of *G. hirsutum* fibers transformed with an EB1 microtubule plus-end marker (Yu et al., 2019). The cellulose microfibril angle is transverse, then helical, to the growing axis in older cotton fibers, corresponding with the changing microtubule angle over developmental time (Preuss et al., 2003; Seagull, 1986). The role of microtubules in older cotton fibers has also been probed using microtubule antagonists. Treatment with either 1 µM oryzalin, 10 µM Taxol, 100 µM colchicine in older cotton fiber (10-22 DPA) resulted in disruption of microtubule arrays and the Tinopal signal of stained cell wall components, indicating a connection between microtubules and cell wall patterning (Seagull, 1990).

The distribution of certain cell wall components has also been established in young cotton fibers. The first study that began to quantify differences in *G. hirsutum* and *G. barbadense* fibers measured the distribution of crystalline cellulose (S4B stain), methyl-esterified pectin (JIM7 antibody), less methyl-esterified pectin (JIM5 antibody), and xyloglucan (CCRCM1 antibody) along the first 55 µm of cotton fiber tips (Stiff & Haigler, 2016). The epitope abundance was measured relative to the apex of each fiber type, but the abundance of each epitope was not compared between fiber tip types. Even so, differential deposition patterns of

crystalline cellulose, xyloglucan, and pectin occurred between all three tip types that were analyzed (Stiff & Haigler, 2016).

Due to the large stature of cotton and its resistance to regeneration after transformation of callus, extensive infrastructure and time are needed to produce a sufficient number of stable transgenic cotton lines for reliable experimental conclusions. Therefore, most of the research so far on cytoskeletal ultrastructure, cellulose deposition, or protein localization in cotton fiber has relied upon imaging of birefringence in the polarizing microscope, immunofluorescence, or stains. Live cell imaging of stably transformed *G. hirsutum* fibers was recently published for the first time, although the methods for live-cell imaging were not provided and it was not established that cotton fibers were continuing to elongate at a normal rate during the observations (Yu et al., 2019). Also, the potential existence of two different tip morphologies was not mentioned. The authors used fluorescently tagged markers for an actin-binding protein and EB1 to track actin and microtubule dynamics respectively. Actin filaments were shown to extend into the apex of the fiber terminating in a loop structure at the apex. Vesicles were also tracked using FM4-64 and showed a bi-directional movement that aligned with the actin filaments (Yu et al., 2019). The pattern of EB1 also implicated a microtubule clear area at the apex analogous to the MDZ reported for *Arabidopsis* trichome branches (Yanagisawa et al., 2018; Yu et al., 2019).

Knowledge gaps addressed by my experiments

The experiments utilizing live-cell imaging of cotton fiber tips from Yu and colleagues (2019) did not: 1) recognize the occurrence of the two fiber phenotypes in *G. hirsutum*; 2) directly show the microtubule array structure; or 3) experimentally probe how the cytoskeleton was involved in the control of cotton fiber diameter. The results reported here address these deficiencies through applying microtubule antagonists to cultured cotton ovules at 1 DPA or 2 DPA following by analysis of changes in fiber tip shape 48 hours later on 3 or 4 DPA. Changes in the microtubule array over time and after treatment with microtubule antagonists were documented by immunofluorescence, and the data were used to test a potential similarity to the control of apical diameter in trichome branches. The data were synthesized to develop a comprehensive picture of how microtubules affect the development of fiber diameter in three tip types.

Table 1: Effects of perturbation of the cytoskeleton and cellulose synthesis on polar cell growth.

Growth Mode	Cell Type	Species	Antagonist/Mutation	Phenotype	Reference
Tip Growth	Root hair	*A. thaliana*	Oryzalin (1-5 µM)	Wavy	Ketelaar et al., 2002;
		A. thaliana	Oryzalin (0.17-1 µM)*	Wavy, reduced elongation, swelling	Baskin et al., 1994
		A. thaliana	Oryzalin (1-5 µM) Taxol (1-5 µM) Latrunculin B (0.05-0.5 µM)	Wavy Wavy; Branching Reduced elongation	Bibikova et al., 1999
		A. thaliana	Cytochalasin D (0.0.1 µM) Latrunculin A (1-10 nM)	Reduced elongation; Apical swelling	Ketelaar et al. 2003
		A. thaliana	*AtCSLD3-1*	Reduced elongation; swelling; Apical rupture	Wang et al., 2001
		A. thaliana	2,6-dichlorobenzene (DCB; 20 µM);	Reduced elongation; swelling; Apical rupture	Park et al., 2011
	Pollen tube	*P. rhoeas*	Oryzalin (1 µM) Latrunculin B (1-10 nM)	Straighter than control Reduced germination & elongation; Apical swelling	Gossot & Geitmann, 2007
		P. abies	Oryzalin (100 µM) Colchicine (100 µM) Cytochalasin B (1 µM) Cytochalasin D (0.5 µM)	Swelling; Reduced elongation; Branching Swelling; Branching	Anderhag et al., 2000
		N. sylvestris	Colchicine (25 µM)	Reduced directional control	Joos et al., 2004
		L. formosanum	Latrunculin B (2 nM)	Reduced elongation; Altered pectin distribution	Rounds et al., 2014
		N. tabacum	Oryzalin (1 µM)	Altered callose distribution	Biagini et al., 2014
		S. chacoense *L. orientalis*	1-cyclohexyl-5-(2,3,4,5,6-pentafluorophenoxy)-1λ4,2,4,6-thiatriazin-3-amine (CGA; 0.1-100 µM)	Swelling	Aouar et al., 2010
	Protonema	*P. patens*	Oryzalin (10 µM)	Disrupted actin localization; Ectopic elongation	Wu & Bezanilla, 2018
		P. patens	2,6-dichlorobenzene (DCB; 10 µM) Isoxaben (20 µM)	Reduced CSC movement; Apical rupture (DCB only)	Tran et al., 2019
Diffuse Growth	Trichome branch	*A. thaliana*	*ZWICHEL/KCBP*	Reduced branching	Oppenheimer et al., 1997
		A. thaliana	DISTORTED group (*DISTORTED1/2, CROOKED, SPIRRIG, ALIEN, KLUNKER, WURM, GNARLED*)	Reduced directional control; Swelling; Reduced branching	Schwab et al., 2003

Table 1 (continued)

	A. thaliana	*ARP3*	Twisting	Buschmann et al., 2009
	A. thaliana	*TORTIFOLIA2*	Twisting	Sambade et al., 2014
	A. thaliana	Oryzalin (100 µM)	Inhibits branching; Disrupts ARP2/3 and SPIKE1 localization	Szymanski et al., 1999; Yanagisawa et al., 2018
Cotton fiber	*G. hirsutum* (10-22 DPA)	Oryzalin (1 µM) Taxol (10 µM) Colchicine (100 µM)	Altered cell wall component distribution	Seagull, 1990

REFERENCES

Akkerman, M., Franssen-Verheijen, M. A. W., Immerzeel, P., Den Hollander, L., Schel, J. H. N., & Emons, A. M. C. (2012). Texture of cellulose microfibrils of root hair cell walls of *Arabidopsis thaliana*, *Medicago truncatula*, and *Vicia sativa*. *Journal of Microscopy*, *247*(1), 60–67. https://doi.org/10.1111/j.1365-2818.2012.03611.x

Anderhag, P., Hepler, P. K., & Lazzaro, M. D. (2000). Microtubules and microfilaments are both responsible for pollen tube elongation in the conifer *Picea abies* (Norway spruce). *Protoplasma*, *214*(3–4), 141–157. https://doi.org/10.1007/BF01279059

Aouar, L., Chebli, Y., & Geitmann, A. (2010). Morphogenesis of complex plant cell shapes: The mechanical role of crystalline cellulose in growing pollen tubes. *Sexual Plant Reproduction*, *23*(1), 15–27. https://doi.org/10.1007/s00497-009-0110-7

Avci, U., Pattathil, S., Singh, B., Brown, V. L., Hahn, M. G., & Haigler, C. H. (2013). Cotton Fiber Cell Walls of *Gossypium hirsutum* and *Gossypium barbadense* Have Differences Related to Loosely-Bound Xyloglucan. *PLoS ONE*, *8*(2). https://doi.org/10.1371/journal.pone.0056315

Bashline, L., Lei, L., Li, S., & Gu, Y. (2014). Cell Wall, Cytoskeleton, and Cell Expansion in Higher Plants. *Molecular Plant*, *7*(4), 586–600. https://doi.org/10.1093/mp/ssu018

Baskin, T I, Wilson, J. E., Cork, A., & Williamson, R. E. (1994). Morphology and microtubule organization in *Arabidopsis* roots exposed to oryzalin or taxol. *Plant & Cell Physiology*, *35*(6), 935–942. https://doi.org/10.1093/oxfordjournals.pcp.a078679

Baskin, T. I. (2005). Anisotropic Expansion of the Plant Cell Wall. *Annual Review of Cell and Developmental Biology*, *21*(1), 203–222. https://doi.org/10.1146/annurev.cellbio.20.082503.103053

Biagini, G., Faleri, C., Cresti, M., & Cai, G. (2014). Sucrose concentration in the growth medium affects the cell wall composition of tobacco pollen tubes. *Plant Reproduction*, *27*(3), 129–144. https://doi.org/10.1007/s00497-014-0246-y

Bibikova, T. N., Blancaflor, E. B., & Gilroy, S. (1999). Microtubules regulate tip growth and orientation in root hairs of *Arabidopsis thaliana*. *Plant Journal*, *17*(6), 657–665. https://doi.org/10.1046/j.1365-313X.1999.00415.x

Bidhendi, A. J., & Geitmann, A. (2016). Relating the mechanics of the primary plant cell wall to morphogenesis. *Journal of Experimental Botany*, *67*(2), 449–461. https://doi.org/10.1093/jxb/erv535

Blanchoin, L., Amann, K. J., Higgs, H. N., Marchand, J., Kaiser, D. A., & Pollard, T. D. (2000). Direct observation of dendritic actin complex and WASP/Scar proteins. *Nature*, *404(6781), 1007*. https://doi.org/10.1038/35010008

Blanchoin, L., Boujemaa-Paterski, R., Henty, J. L., Khurana, P., & Staiger, C. J. (2010). Actin

dynamics in plant cells: A team effort from multiple proteins orchestrates this very fast-paced game. *Current Opinion in Plant Biology*, *13*(6), 714–723. https://doi.org/10.1016/j.pbi.2010.09.013

Bosch, M., Cheung, A. Y., & Hepler, P. K. (2005). Pectin Methylesterase, a Regulator of Pollen Tube Growth. *Plant physiology, 138(3), 1334-1346.* https://doi.org/10.1104/pp.105.059865.nor

Buschmann, H., Hauptmann, M., Niessing, D., Lloyd, C. W., & Schäffner, A. R. (2009). Helical growth of the *Arabidopsis* mutant *tortifolia2* does not depend on cell division patterns but involves handed twisting of isolated cells. *The Plant Cell*, *21*(7), 2090–2106. https://doi.org/10.1105/tpc.108.061242

Cai, G., Parrotta, L., & Cresti, M. (2015). Organelle trafficking, the cytoskeleton, and pollen tube growth. *Journal of Integrative Plant Biology*, *57*(1), 63–78. https://doi.org/10.1111/jipb.12289

Chebli, Y., Kaneda, M., Zerzour, R., & Geitmann, A. (2012). The cell wall of the *Arabidopsis* pollen tube--spatial distribution, recycling, and network formation of polysaccharides. *Plant Physiology*, *160*(4), 1940–1955. https://doi.org/10.1104/pp.112.199729

Cheung, A. Y., Duan, Q. H., Costa, S. S., De Graaf, B. H. J., Di Stilio, V. S., Feijo, J., & Wu, H. M. (2008). The dynamic pollen tube cytoskeleton: Live cell studies using actin-binding and microtubule-binding reporter proteins. *Molecular Plant*, *1*(4), 686–702. https://doi.org/10.1093/mp/ssn026

Constable, G., Llewellyn, D., Walford, S. A., & Clement, J. D. (2015). Cotton breeding for fiber quality improvement. In V. M. V. Cruz & D. A. Dierig (Eds.), *Industrial Crops, handbook for plant breeding* (pp. 191–232). New York: Springer. https://doi.org/10.1007/978-1-4939-1447-0

Cosgrove, D. J. (2018). Diffuse Growth of Plant Cell Walls. *Plant Physiology*, *176*, 16–27. https://doi.org/10.1104/pp.17.01541

Crowell, E. F., Bischoff, V., Desprez, T., Rolland, A., Stierhof, Y. D., Schumacher, K., Gonneau, M., Hofte, H. Vernhettes, S. (2009). Pausing of Golgi Bodies on Microtubules Regulates Secretion of Cellulose Synthase Complexes in Arabidopsis. *The Plant Cell Online*, *21*(4), 1141–1154. https://doi.org/10.1105/tpc.108.065334

Crowell, E. F., Gonneau, M., Stierhof, Y. D., Höfte, H., & Vernhettes, S. (2010). Regulated trafficking of cellulose synthases. *Current Opinion in Plant Biology*, *13*(6), 700–705. https://doi.org/10.1016/j.pbi.2010.07.005

Elliott, A., & Shaw, S. L. (2018). Update: Plant Cortical Microtubule Arrays. *Plant Physiology*, *176*(1), 94–105. https://doi.org/10.1104/pp.17.01329

Eng, R. C., & Sampathkumar, A. (2018). Getting into shape: the mechanics behind plant morphogenesis. *Current opinion in plant biology*, *46*, 25-31.

https://doi.org/10.1016/j.pbi.2018.07.002

Fu, Y. (2015). The cytoskeleton in the pollen tube. *Current Opinion in Plant Biology*, *28*, 111–119. https://doi.org/10.1016/j.pbi.2015.10.004

Fujikura, U., Elsaesser, L., Breuninger, H., & Sa, C. (2014). Atkinesin-13A Modulates Cell-Wall Synthesis and Cell Expansion in *Arabidopsis thaliana* via the THESEUS1 Pathway. *PLoS genetics, 10(9), e1004627.* https://doi.org/10.1371/journal.pgen.1004627

Geitmann, A., & Ortega, J. K. E. (2009). Mechanics and modeling of plant cell growth. *Trends in Plant Science*, *14*(9), 467–478. https://doi.org/10.1016/j.tplants.2009.07.006

Goley, E. D., & Welch, M. D. (2006). The ARP2/3 complex: an actin nucleator comes of age. *Nature Reviews. Molecular Cell Biology*, *7*(10), 713–726. https://doi.org/10.1038/nrm2026

Gossot, O., & Geitmann, A. (2007). Pollen tube growth: Coping with mechanical obstacles involves the cytoskeleton. *Planta*, *226*(2), 405–416. https://doi.org/10.1007/s00425-007-0491-5

Grierson, C. S., Nielsen, E., Ketelaar, T., & Schiefelbein, J. W. (2014). Root hairs. *The Arabidopsis Book*, *12*(12), e0172. https://doi.org/10.1199/tab.0172

Gu, Y., Kaplinsky, N., Bringmann, M., Cobb, A., Carroll, A., Sampathkumar, A., Baskin, T. I. Persson, S., Somerville, C. R. (2010). Identification of a cellulose synthase-associated protein required for cellulose biosynthesis. *Proceedings of the National Academy of Sciences*, *107*(29), 12866–12871. https://doi.org/10.1073/pnas.1007092107

Guerriero, G., Hausman, J. F., & Cai, G. (2014). No stress! relax! mechanisms governing growth and shape in plant cells. *International Journal of Molecular Sciences*, *15*(3), 5094–5114. https://doi.org/10.3390/ijms15035094

Haigler, C. H., Betancur, L., Stiff, M. R., & Tuttle, J. R. (2012). Cotton fiber: a powerful single-cell model for cell wall and cellulose research. *Frontiers in Plant Science*, *3*(May), 104. https://doi.org/10.3389/fpls.2012.00104

Harries, P. A., Pan, A., & Quatrano, R. S. (2005). Actin-related protein2/3 complex component ARPC1 is required for proper cell morphogenesis and polarized cell growth in *Physcomitrella patens*. *The Plant Cell*, *17*(8), 2327–2339. https://doi.org/10.1105/tpc.105.033266

Hashimoto, T. (2015). Microtubules in Plants. *The Arabidopsis Book*, *13*, e0179. https://doi.org/10.1199/tab.0179

Havelková, L., Nanda, G., Martinek, J., Bellinvia, E., Sikorová, L., Seifertová, D., & Petrá˘, J. (2015). Arp2/3 complex subunit ARPC2 binds to microtubules. *Plant Science, 241, 96-108.* https://doi.org/10.1016/j.plantsci.2015.10.001

Helal, M. A., Khalifa, S., & Ahmed, S. (2013). Differential binding of latrunculins to G-actin: a

molecular dynamics study. *Journal of chemical information and modeling*, *53*(9), 2369-2375.

Henty-Ridilla, J. L., Li, J., Blanchoin, L., & Staiger, C. J. (2013). Actin dynamics in the cortical array of plant cells. *Current Opinion in Plant Biology*, *16*(6), 678–687. https://doi.org/10.1016/j.pbi.2013.10.012

Hulskamp, M., Misera, S., & Jurgens, G. (1994). Genetic Dissection of Trichome Cell Development in *Arabidopsis*. *Cell*, *76*, 555–566.

Joos, U., van Aken, J., & Kristen, U. (1994). Microtubules are involved in maintaining the cellular polarity in pollen tubes of *Nicotiana sylvestris*. *Protoplasma*, *179*(1–2), 5–15. https://doi.org/10.1007/BF01360732

Ketelaar, T. (2013). The actin cytoskeleton in root hairs: All is fine at the tip. *Current Opinion in Plant Biology*, *16*(6), 749–756. https://doi.org/10.1016/j.pbi.2013.10.003

Ketelaar, T., de Ruijter, N. C. A., & Emons, A. M. C. (2003). Unstable F-actin specifies the area and microtubule direction of cell expansion in *Arabidopsis* root hairs. *The Plant Cell*, *15*(1), 285–292. https://doi.org/10.1105/tpc.007039

Ketelaar, T., Faivre-Moskalenko, C., Esseling, J. J., de Ruijter, N. C. A., Grierson, C. S., Dogterom, M., & Emons, A. M. C. (2002). Positioning of nuclei in *Arabidopsis* root hairs: An actin-regulated process of tip growth. *The Plant Cell*, *14*(11), 2941–2955. https://doi.org/10.1105/tpc.005892

Kong, Z., Ioki, M., Braybrook, S., Li, S., Ye, Z. H., Lee, Y. R., Hotta, T., Chang, A., Tian, J., Wang, Guangda, Liu, B. (2015). Kinesin-4 Functions in Vesicular Transport on Cortical Microtubules and Regulates Cell Wall Mechanics during Cell Elongation in Plants. *Molecular Plant*, *8*(7), 1011–1023. https://doi.org/10.1016/j.molp.2015.01.004

Krtková, J., Benáková, M., & Schwarzerová, K. (2016). Multifunctional Microtubule-Associated Proteins in Plants. *Frontiers in Plant Science*, *7*(4), 1–13. https://doi.org/10.3389/fpls.2016.00474

Li, S., Lei, L., Somerville, C. R., & Gu, Y. (2012). Cellulose synthase interactive protein 1 (CSI1) links microtubules and cellulose synthase complexes. *Proceedings of the National Academy of Sciences*, *109*(1), 185–190. https://doi.org/10.1073/pnas.1118560109

Li, S., Lei, L., Yingling, Y. G., & Gu, Y. (2015). Microtubules and cellulose biosynthesis: The emergence of new players. *Current Opinion in Plant Biology*, *28*, 76–82. https://doi.org/10.1016/j.pbi.2015.09.002

Libault, M., Brechenmacher, L., Cheng, J., Xu, D., & Stacey, G. (2010). Root hair systems biology. *Trends in Plant Science*, *15*(11), 641–650. https://doi.org/10.1016/j.tplants.2010.08.010

Lovy-Wheeler, A., Wilsen, K. L., Baskin, T. I., & Hepler, P. K. (2005). Enhanced fixation

reveals the apical cortical fringe of actin filaments as a consistent feature of the pollen tube. *Planta*, *221*(1), 95-104.

Lu, L., Lee, Y. J., Pan, R., Maloof, J. N., & Liu, B. (2005). An Internal Motor Kinesin Is Associated with the Golgi Apparatus and Plays a Role in Trichome Morphogenesis in *Arabidopsis*. *Molecular Biology of the Cell*, *16*(2), 811–823. https://doi.org/10.1091/mbc.E04-05-0400

Mathur, J., & Chua, N. (2000). Microtubule Stabilization Leads to Growth Reorientation in *Arabidopsis* Trichomes. *The Plant Cell*, *12*(4), 465–477.

Menand, B., Calder, G., & Dolan, L. (2007). Both chloronemal and caulonemal cells expand by tip growth in the moss *Physcomitrella patens*. *Journal of experimental botany*, *58*(7), 1843–1849. https://doi.org/10.1093/jxb/erm047

Mendrinna, A., & Persson, S. (2015). Root hair growth: it's a one way street. *F1000Prime Reports*, *7*, 1–6. https://doi.org/10.12703/P7-23

Naylor, G. R., Stanton, J. H., & Speijers, J. (2014). Skin comfort of base layer wool garments. Part 2: Fiber diameter effects on fabric and garment prickle. *Textile Research Journal*, *84*(14), 1506–1514. https://doi.org/10.1177/0040517514523174

Onelli, E., Idilli, A. I., & Moscatelli, A. (2015). Emerging roles for microtubules in angiosperm pollen tube growth highlight new research cues. *Frontiers in Plant Science*, *6*(February), 51. https://doi.org/10.3389/fpls.2015.00051

Oppenheimer, D. G., Pollock, M. A., Vacik, J., Szymanski, D. B., Ericson, B., Feldmann, K., & Marks, D. (1997). Essential role of a kinesin-like protein in *Arabidopsis* trichome morphogenesis. *Proceedings of the National Academy of Science of the Uineted States of America*, *94*. https://doi.org/10.1073/pnas.94.12.6261

Paavilainen, V. O., Bertling, E., Falck, S., & Lappalainen, P. (2004). Regulation of cytoskeletal dynamics by actin-monomer-binding proteins. *Trends in cell biology*, *14*(7). https://doi.org/10.1016/j.tcb.2004.05.002

Palin, R., & Geitmann, A. (2012). The role of pectin in plant morphogenesis. *BioSystems*, *109*(3), 397–402. https://doi.org/10.1016/j.biosystems.2012.04.006

Paradez, A., Wright, A., & Ehrhardt, D. W. (2006). Microtubule cortical array organization and plant cell morphogenesis. *Current Opinion in Plant Biology*, *9*(6), 571–578. https://doi.org/10.1016/j.pbi.2006.09.005

Park, S., Szumlanski, A. L., Gu, F., Guo, F., & Nielsen, E. (2011). A role for CSLD3 during cell-wall synthesis in apical plasma membranes of tip-growing root-hair cells. *Nature Cell Biology*, *13*(8), 973–980. https://doi.org/10.1038/ncb2294

Park, Y. B., & Cosgrove, D. J. (2012). A Revised Architecture of Primary Cell Walls Based on Biomechanical Changes Induced by Substrate-Specific Endoglucanases. *Plant Physiology*,

158(4), 1933–1943. https://doi.org/10.1104/pp.111.192880

Paterson, A. H., Wendel, J. F., Gundlach, H., Guo, H., Jenkins, J., Jin, D., Llewellyn, D. J., Showmaker, K. C., Shu, S., Udall, J. A., Yoo, M., Byers, R., Chen, W., Doron-Faigenboim, A., Duke, M. V., Gong, L., Grimwood, J., Grover, C., Grupp, K., Hu, G., Lee, T., Li, J., Lin, L., Liu, T., Marler, B. S., Page, J. T., Roberts, A. W., Romanef, E., Sanders, W. S., Szadkowski, E., Tan, X., Tang, H., Xu, C., Wang, J., Wang, Z., Zhang, D., Zhang, L., Ashrafi, H., Bedon, F., Bowers, J. E., Brubaker, C. L., Chee, P. W., Das, S., Gingle, A. R., Haigler, C. H., Harker, D., Hoffmann, L. V., Hovav, R., Jones, D. C., Lemke, C., Mansoor, S., ur Rahman, M., Rainville, L. N., Rambani, A., Reddy, U. K., Rong, J., Sarmga, Y., Scheffler, B. E., Scheffler, J. A., Stelly, D. M., Triplett, B. A., Van Deynze, A., Vaslin, M. F. S., Waghmare, V. N., Walford, S. A., Wright, R. J., Zaki, E. A., Zhang, T., Dennis, E. S., Mayer, K. F. X., Peterson, D. G., Rokhsar, D. S., Wang, X., Schroutz, J. (2012). Repeated polyploidization of *Gossypium* genomes and the evolustion of spinnable cotton fibers. *Nature*, *492*(7429), 423–427. https://doi.org/10.1038/ nature11798

Preuss, M. L., Delmer, D. P., & Liu, B. (2003). The cotton kinesin-like calmodulin-binding protein associates with cortical microtubules in cotton fibers. *Plant Physiology*, *132*(5), 154–160. https://doi.org/10.1104/pp.103.020339.of

Reddy, A. S. N., & Day, I. S. (2001). Kinesins in the *Arabidopsis* genome: A comparative analysis among eukaryotes. *BMC Genomics*, *2*(1), 2. https://doi.org/10.1186/1471-2164-2-2

Rounds, C. M., Hepler, P. K., & Winship, L. J. (2014). The Apical Actin Fringe Contributes to Localized Cell Wall Deposition and Polarized Growth in the Lily Pollen Tube. *Plant Physiology*, *166*(1), 139–151. https://doi.org/10.1104/pp.114.242974

Sagot, I., Rodal, A. A., Moseley, J., Goode, B. L., & Pellman, D. (2002). An actin nucleation mechanism mediated by Bni1 and Profilin. *Nature cell biology*, *4*(8), 1–6. https://doi.org/10.1038/ncb834

Sambade, A., Findlay, K., Schäffner, A. R., Lloyd, C. W., & Buschmann, H. (2014). Actin-Dependent and Independent Functions of Cortical Microtubules in the Differentiation of *Arabidopsis* Leaf Trichomes. *The Plant Cell*, *26*(4), 1629–1644. https://doi.org/10.1105/tpc.113.118273

Sampathkumar, A., Lindeboom, J. J., Debolt, S., Gutierrez, R., Ehrhardt, D. W., Ketelaar, T., & Persson, S. (2011). Live cell imaging reveals structural associations between the actin and microtubule cytoskeleton in *Arabidopsis*. *The Plant Cell*, *23*(6), 2302–2313. https://doi.org/10.1105/tpc.111.087940

Scherlach, K., Boettger, D., Remme, N., & Hertweck, C. (2010). The chemistry and biology of cytochalasans. *Natural product reports*, *27*(6), 869-886. https://doi.org/10.1039/b903913a

Schwab, B., Mathur, J., Saedler, R., Schwarz, H., Frey, B., Scheidegger, C., & Hulskamp, M. (2003). Regulation of cell expansion by the DISTORTED genes in *Arabidopsis thaliana*: actin controls the spatial organization of microtubules, *Molecular Genetics and Genomics*, *269*(3), 350-360. https://doi.org/10.1007/s00438-003-0843-1

Seagull, R. W. (1986). Changes in Microtubule Organization and Wall Microfibril Orientation during *In vitro* Cotton Fiber Development - an Immunofluorescent Study. *Canadian Journal of Botany-Revue Canadienne De Botanique*, *64*(7), 1373–1381.

Seagull, R. W. (1990). The effects of microtubule and microfilament disrupting agents on cytoskeletal arrays and wall deposition in developing cotton fibers. *Protoplasma*, *159*(1), 44–59. https://doi.org/10.1007/BF01326634

Stiff , M. R., & Haigler, C. H. (2016). Cotton fiber tips have diverse morphologies and show evidence of apical cell wall synthesis. *Scientific Reports*, *6*, 27883. https://doi.org/10.1038/srep27883

Stiff, M. R., & Haigler, C. H. (2012). Recent Advances in Cotton Fiber Development. *Flowering and Fruiting in Cotton*, 163–192.

Szymanski, D. B., Marks, M. D., & Wick, S. M. (1999). Organized F-actin is essential for normal trichome morphogenesis in *Arabidopsis*. *The Plant Cell*, *11*(12), 2331–2347. https://doi.org/10.1105/tpc.11.12.2331

Szymanski, D., & Staiger, C. J. (2018). The Actin Cytoskeleton: Functional Arrays for Cytoplasmic Organization and Cell Shape Control. *Plant physiology*, *176*(1), 106-118. https://doi.org/10.1104/pp.17.01519

Tran, M. L., Mccarthy, T. W., Sun, H., Wu, S., Norris, J. H., Bezanilla, M., Vidali, L., Anderson, C. T., Roberts, A. W. (2018). Direct observation of the effects of cellulose synthesis inhibitors using live cell imaging of Cellulose Synthase (CESA) in *Physcomitrella patens*. *Scientific reports, 8(1), 735.* https://doi.org/10.1038/s41598-017-18994-4

Van Bruaene, N., Joss, G., & Van Oostveldt, P. (2004). Reorganization and *in vivo* dynamics of microtubules during *Arabidopsis* root hair development. *Plant Physiology*, *136*(4), 3905–3919. https://doi.org/10.1104/pp.103.031591

Vidali, L., & Bezanilla, M. (2012). *Physcomitrella patens*: A model for tip cell growth and differentiation. *Current Opinion in Plant Biology*, *15*(6), 625–631. https://doi.org/10.1016/j.pbi.2012.09.008

Vidali, L., Mckenna, S. T., & Hepler, P. K. (2001). Actin Polymerization Is Essential for Pollen Tube Growth. *Molecular Biology of the Cell*, *12*(8), 2534-2545.

Vidali, L., Rounds, C. M., Hepler, P. K., & Bezanilla, M. (2009). Lifeact-mEGFP reveals a dynamic apical F-actin network in tip growing plant cells. *PLoS ONE*, *4*(5). https://doi.org/10.1371/journal.pone.0005744

Vidali, L., van Gisbergen, P. a C., Guérin, C., Franco, P., Li, M., Burkart, G. M., Augustine, R. C., Blanchoin, L., Bezanilla, M. (2009). Rapid formin-mediated actin-filament elongation is essential for polarized plant cell growth. *Proceedings of the National Academy of Sciences of the United States of America*, *106*(32), 13341–13346. https://doi.org/10.1073/pnas.0901170106

Wang, X., Cnops, G., Vanderhaeghen, R., De Block, S., Van Montagu, M., & Van Lijsebettens, M. (2001). AtCSLD3, a cellulose synthase-like gene important for root hair growth in arabidopsis. *Plant Physiology*, *126*(2), 575–586. https://doi.org/10.1104/pp.126.2.575

Whittington, A. T., Vugrek, O., Wei, K. J., Hasenbein, N. G., Sugimoto, K., Rashbrooke, M. C., & Wasteneys, G. O. (2001). MOR1 is essential for organizing cortical microtubules in plants. *Nature*, *411*(6837), 610–613. https://doi.org/10.1038/35079128

Wu, S. Z., & Bezanilla, M. (2018). Actin and microtubule cross talk mediates persistent polarized growth. *Journal of Cell Biology*, *217*(10), 3531-3544.

Xiao, C., Zhang, T., Zheng, Y., Cosgrove, D. J., & Anderson, C. T. (2016). Xyloglucan Deficiency Disrupts Microtubule Stability and Cellulose Biosynthesis in Arabidopsis, Altering Cell Growth and Morphogenesis. *Plant Physiology*, *170*(1), 234–249. https://doi.org/10.1104/pp.15.01395

Yanagisawa, M., Alonso, J. M., & Szymanski, D. B. (2018). Microtubule-Dependent Confinement of a Cell Signaling and Actin Polymerization Control Module Regulates Polarized Cell Growth. *Current Biology*, *28*(15), 2459-2466.e4. https://doi.org/10.1016/j.cub.2018.05.076

Yanagisawa, M., Desyatova, A. S., Belteton, S. A., Mallery, E. L., Turner, J. A., & Szymanski, D. B. (2015). Patterning mechanisms of cytoskeletal and cell wall systems during leaf trichome morphogenesis. *Nature Plants*, *1*(3), 15014. https://doi.org/10.1038/nplants.2015.14

Yu, Y., Wu, S., Nowak, J., Wang, G., Han, L., Feng, Z., Mendrinna, A., Ma, Y., Wang, H., Zhang, X., Tian, J., Dong, L., Nikoloski, Z., Persson, S., Kong, Z. (2019). Live-cell imaging of the cytoskeleton in elongating cotton fibres. *Nature Plants*, *5*(5), 498–504. https://doi.org/10.1038/s41477-019-0418-8

Zhang, R., Alushin, G. M., Nogales, E., Zhang, R., Alushin, G. M., Brown, A., & Nogales, E. (2015). Mechanistic Origin of Microtubule Dynamic Instability and Its Modulation by EB Proteins Article Mechanistic Origin of Microtubule Dynamic Instability and Its Modulation by EB Proteins. *Cell*, *162*(4), 849–859. https://doi.org/10.1016/j.cell.2015.07.012

Zhang, Y., Nikolovski, N., Sorieul, M., Vellosillo, T., Mcfarlane, H. E., Dupree, R., Driemeier, C., Lathe, R., Lampugnani, E., Yu, X., Kesten, C., Ivakov, A., Doblin, M. S., Mortimer, J. C., Brown, S. P., Persson, S., Dupree, P. (2016). Golgi-localized STELLO proteins regulate the assembly and trafficking of cellulose synthase complexes in *Arabidopsis*. *Nature communications*, *7*, 11656. https://doi.org/10.1038/ncomms11656

Zhu, C., Ganguly, A., Baskin, T. I., McClosky, D. D., Anderson, C. T., Foster, C., Meunier, K. A., Okamoto, R., Berg, H., Dixit, R. (2015). The fragile Fiber1 kinesin contributes to cortical microtubule-mediated trafficking of cell wall components. *Plant Physiology*, *167*(3), 780–792. https://doi.org/10.1104/pp.114.251462

CHAPTER 2

Cultures of *Gossypium barbadense* cotton ovules offer insights into the microtubule-mediated control of fiber cell expansion

Ethan T. Pierce[1,2], Benjamin P. Graham[2], Michael R. Stiff[1], Jason A. Osborne[3], and Candace H. Haigler[1,2]

[1]Department of Crop and Soil Sciences, North Carolina State University, Raleigh, North Carolina 27695 U.S.A.

[2]Department of Plant and Microbial Biology, North Carolina State University, Raleigh, North Carolina 27695 U.S.A.

[3]Department of Statistics, North Carolina State University, Raleigh, North Carolina 27695 U.S.A.

Published in Planta (2019) 249:1551-1563

Contribution Statement

My contribution to this study is reflected in Table 1, Figures 5, 6, and 7, and supplementary Figures S6, S7, and S8. I carried out the experiments leading to the fiber measurements, generated a protocol for reproducible and non-biased measurements, and mentored an undergraduate student (Robin Grant Moore) and Ethan Pierce in making the measurements, as well as making measurements myself. I carried out the initial statistical analysis of the fiber diameter data and trained Ethan Pierce in these methods, then consulted with a statistician (Dr. Jason Osborne) to generate the published statistical analysis. I performed the immunofluorescence experiments, collected and processed images, and generated the figure.

Planta (2019) 249:1551–1563
https://doi.org/10.1007/s00425-019-03106-5

ORIGINAL ARTICLE

Cultures of *Gossypium barbadense* cotton ovules offer insights into the microtubule-mediated control of fiber cell expansion

Ethan T. Pierce[1,2] · Benjamin P. Graham[2] · Michael R. Stiff[1,4] · Jason A. Osborne[3] · Candace H. Haigler[1,2]

Received: 14 November 2018 / Accepted: 31 January 2019 / Published online: 7 February 2019

Abstract

Main conclusion **A novel method for culturing ovules of *Gossypium barbadense* allowed in vitro comparisons with *Gossypium hirsutum* and revealed variable roles of microtubules in controlling cotton fiber cell expansion.**

Cotton fibers undergo extensive elongation and secondary wall thickening as they develop into our most important renewable textile material. These single cells elongate at the apex as well as elongating and expanding in diameter behind the apex. These multiple growth modes represent an interesting difference compared to classical tip-growing cells that needs to be explored further. In vitro ovule culture enables experimental analysis of the controls of cotton fiber development in commonly grown *Gossypium hirsutum* cotton, but, previously, there was no equivalent system for *G. barbadense*, which produces higher quality cotton fiber. Here, we describe: (a) how to culture the ovules of *G. barbadense* successfully, and (b) the results of an in vitro experiment comparing the role of microtubules in controlling cell expansion in different zones near the apex of three types of cotton fiber tips. Adding the common herbicide fluridone, 1-Methyl-3-phenyl-5-[3-(trifluoromethyl)phenyl]-4(1H)-pyridinone, to the medium supported *G. barbadense* ovule culture, with positive impacts on the number of useful ovules and fiber length. The effect is potentially mediated through inhibited synthesis of abscisic acid, which antagonized the positive effects of fluridone. Fiber development was perturbed by adding colchicine, a microtubule antagonist, to ovules of *G. barbadense* and *G. hirsutum* cultured 2 days after flowering. The results supported the zonal control of cell expansion in one type of *G. hirsutum* fiber tip and highlighted differences in the role of microtubules in modulating cell expansion between three types of cotton fiber tips.

Keywords Colchicine · Cotton fiber · Cytoskeleton · Fluridone · Ovule culture · Plant cell growth

Ethan T. Pierce and Benjamin P. Graham have contributed equally to this work.

Electronic supplementary material The online version of this article (https://doi.org/10.1007/s00425-019-03106-5) contains supplementary material, which is available to authorized users.

✉ Candace H. Haigler
candace_haigler@ncsu.edu

[1] Department of Crop and Soil Sciences, North Carolina State University, Raleigh, NC 27695, USA

[2] Department of Plant and Microbial Biology, North Carolina State University, Raleigh, NC 27695, USA

[3] Department of Statistics, North Carolina State University, Raleigh, NC 27695, USA

[4] Present Address: Department of Biology, Lenoir-Rhyne University, Hickory, NC 28601, USA

Abbreviations

ABA	Abscisic acid
ANOVA	Analysis of variance
DPA	Days post-anthesis
DMSO	Dimethyl sulfoxide
Gb	*Gossypium barbadense*
Gh	*Gossypium hirsutum*
HSD	Honestly significant difference

Introduction

The cotton fiber is a highly elongated, single cell extending from the seed epidermis. At maturity after secondary wall deposition has concluded, many fibers are about 3 cm long and composed of about 95% cellulose (Haigler et al. 2012). Cotton fibers are used worldwide in the manufacture of renewable textiles and many other products, and their

cellular morphogenesis determines the quality parameters of importance to industry. However, the mechanisms linking the biology and utility of this important cell are only beginning to be understood. Further progress is needed to increase the quality of the fiber on commonly grown *Gossypium hirsutum* (hereafter called *Gh*), which would increase the competitiveness of renewable cotton with synthetic fibers. This goal appears to be achievable, because another species of commercial cotton, *G. barbadense* or Pima cotton (*Gb*), produces longer, stronger, and smaller diameter fibers. However, this species can be grown only in limited locations with lower yield, making the highest quality cotton textiles expensive.

For 45 years, research on cotton fiber development has been aided by a *Gh* ovule culture system where fibers elongate and mature on the surface of floating ovules (Beasley and Ting 1973). The ovules are dissected from the ovary shortly after flowering (or anthesis) and floated on a tissue culture medium that typically contains auxin and gibberellic acid. The subsequent development of the ovules and their epidermal fibers is described temporally as days post-anthesis (DPA), because fibers initiate on the day that the flower opens. *Gh* fibers differentiating in vitro typically elongate and thicken their cell walls to a lesser extent than observed in planta, but the overall developmental progression and cell wall composition are quite similar in the two conditions (Meinert and Delmer 1977). Previously, there was no effective in vitro culture system for *Gb* ovules, which limited experiments on this important commercial cultivar as well as experiments comparing fiber morphogenesis in the two species.

Here, we report the development of an ovule culture system for *Gb* cv. Phytogen 800 and compare its outcomes to those for *Gh* cv. Deltapine 90. Each of these cultivars is an elite non-transgenic commercial tetraploid cotton that was in use in the early 1990s. Following a lead from a brief report on the positive impact of 5 mg/l (7.6 µM) fluridone on *G. arboreum* ovule culture (Nayyar et al. 1989), we showed that adding this herbicide, 1-Methyl-3-phenyl-5-[3-(trifluoromethyl)phenyl]-4(1H)-pyridinone, to the culture medium increased the percentage of useful ovules and fiber length in *Gb* cultures. Fluridone is a commonly used herbicide that inhibits phytoene desaturase activity in synthesizing β-carotene and its downstream derivatives such as strigolactone, xanthoxin, and abscisic acid (ABA) (Kitahata and Asami 2011). Interestingly, it can selectively hinder grass and broadleaf weed germination in cotton cropping systems (Waldrep and Taylor 1976), which correlates with its non-lethal effects in cotton ovule culture observed previously (Nayyar et al. 1989) and in the current research.

We then used the optimized system for *Gb* ovule culture to gain insight into the role of microtubules in regulating cell expansion in three types of cotton fiber tips. Two types of fiber tips exist during the early *Gh* fiber elongation, *tapered* narrow tips and broad *hemisphere* tips, whereas only one narrow tip type occurs in *Gb* cotton fiber. Results from pulse-labeling of cell walls and treatment with cell wall-degrading enzymes supported fiber cell expansion at the apex and selected distal regions (Stiff and Haigler 2016), reflecting a 'mixed mode' of plant cell growth different from classical tip-growing cells that expand only at the apex (Qin and Zhu 2011; Guerriero et al. 2014). This 'mixed mode' of cotton fiber expansion is able to regulate both anisotropic cell elongation and increase in diameter behind the apex, which does not occur in classical tip-growing cells such as pollen tubes and root hairs.

Microtubules play variable roles in different modes of anisotropic plant cell expansion through helping to control the synthesis of cellulose and/or the deposition of cell wall matrix components (Geitmann and Ortega 2009). In anisotropic diffuse growth, new cell wall is synthesized over a broad area, while microtubules are transverse to the longitudinal cell axis, as occurs in older, rapidly elongating, cotton fibers (Seagull 1993). In this growth mode, perturbing microtubule activity either pharmacologically or through mutations typically causes cells to swell (Baskin 2005; Sedbrook and Kaloriti 2008). Alternatively, classical tip-growing cells often have microtubules aligned with the longitudinal cell axis. The microtubules help to control the monoaxial directionality of tip growth, given that wavy or branched cells have been observed after treatment with microtubule antagonists (Bibikova et al. 1999; Geitmann 2011). These different roles of microtubules are related to variations in the role of actin and cell wall chemistry and structure between the cell types as reviewed previously (Baskin 2005; Geitmann and Ortega 2009; Geitmann 2011; Rounds and Bezanilla 2013).

We perturbed microtubules to test the hypothesis that growth control mechanisms differed zonally in one cotton fiber tip and between different tip types. We cultured 2 DPA *Gh* and *Gb* ovules with or without colchicine, an alkaloid that hinders microtubule polymerization at low concentrations or causes de-polymerization at high concentrations through binding at the interface between the α- and β-tubulin monomers (Stanton et al. 2011). Fiber tip diameter at 4 DPA was measured at the apex and 40 µm and 200 µm behind it. These locations were chosen because: (a) cell wall composition changes in all three types of fiber tips through 55 µm back from the apex; (b) zonal cell wall synthesis occurred in *Gh hemisphere* and *Gh tapered* tips through 85 µm; (c) diametric expansion increases from the apex through 200 µm in all three tip types (Stiff and Haigler 2016) (Table 1). The results provided further evidence that growth processes in cotton fiber tips can be under zonal control, with further variation between tip types. The data also demonstrate the

Table 1 Median and mean diameters at three locations for three types of control (−Col) or colchicine-treated (+Col) fiber tips

Tip types	Apex			40 µm			200 µm		
	−Col	+Col (µm)	% change	−Col (µm)	+Col (µm)	% change	−Col (µm)	+Col (µm)	% change
Gb									
Median	4.30	4.87	13.26	7.14	7.91	10.78	11.86	13.07	10.20
Mean	4.48	5.41[c]	20.76	7.26	8.37[c]	15.29	12.06	13.70[c]	13.60
STD	1.00	2.36		1.05	2.36		2.62	4.01	
Gh tapered									
Median	5.16	4.59	− 11.05	8.70	9.29	6.78	15.70	17.71	12.80
Mean	5.28	4.82[a]	− 8.71	8.81	10.08[a]	14.42	15.66	20.56[c]	31.29
STD	1.31	1.22		1.52	3.76		3.87	8.79	
Gh hemisphere									
Median	12.61	12.61	0	17.30	18.19	5.14	21.53	22.37	3.90
Mean	12.17	14.32[b]	17.66	16.58	19.52[c]	17.73	21.78	23.76	9.09
STD	2.02	5.91		2.86	6.46		3.37	6.90	

50 µm colchicine was added at 2 DPA and measurements were made at 4 DPA. The % changes in the presence of colchicine and standard deviations of the means (STD) are shown.

Replication of controls: for apex and 40 µm, $n = 95–260$ fibers from a minimum of 8 replications over 5 trials; and for 200 µm, $n = 52–137$ fibers from a minimum of 7 replications over 3 trials. Replication of colchicine treatments; the number of fibers measured within the same trials was: for the apex and 40 µm, $n = 99–257$ fibers and for 200 µm, $n = 62–146$

Superscript letters indicate significant differences between the means for +Col compared to −Col for that fiber tip type and location: [a] $p \leq 0.05$

[b] $p \leq 0.01$

[c] $p \leq 0.001$ (determined as described in "Materials and methods", with Bonferroni adjustment for multiplicity of comparisons)

utility of the newly developed *Gb* ovule/fiber culture system in comparative experiments with *Gh* ovule cultures.

Materials and methods

Plant growth

Seeds of *G. barbadense* cv. Phytogen 800 and *G. hirsutum* cv. Deltapine 90 were hand-ginned to remove fiber and either germinated in soil or on a wet paper towel (30 °C, dark) prior to transplanting. Young plants were grown in 4.5-L pots in a 1:2 (v/v) mixture of Redi-earth Plug and Seedling Mix (# F1153; Sun Gro Horticulture, Canada) and gravel (#16, construction grade). Plants were grown to 4–6 weeks old in a growth chamber with 26/22 °C day/night cycle (12 h/12 h) with 290-µmol m^{-2} s^{-1} light intensity (near the middle of the plant) from fluorescent bulbs. Then, they were transferred to a greenhouse with the same temperature cycle and grown to maturity. In the greenhouse during the winter, day length was supplemented to approximately 12 h with 1000 W metal halide lights. The frequency of watering with Hoagland's solution (https://phytotron.ncsu.edu/procedural-manual/) changed with the age of the plants: three times a week for the first 4 weeks, then daily for 2 weeks, and then twice daily after 6 weeks.

Cotton ovule culture

Flowers were tagged on the day of anthesis to facilitate harvest of 2 DPA bolls for culture. Bolls were surface sterilized in 12.5% bleach (Clorox) containing 0.01% (v/v) Triton X-100. Dissected ovules were floated on cotton ovule culture medium (Beasley and Ting 1973) with the modification of 120-mM glucose used as the sole carbon source (Singh et al. 2009). Hormones (0.5-µM gibberellic acid and 5-µM indole acetic acid) were added to autoclaved media (stored dark, RT, no more than 2 weeks) from filter-sterilized stocks immediately before use.

Short-term experiments (up to 16 DPA) were set up in 6-well tissue culture plates (#353046, Corning, Inc., Corning, NY) with 10-ml medium and six ovules per well. The longer term experiment (8–37 DPA) was set up in 30 ml medium with 11–15 ovules in 100 ml, parafilm-wrapped, lidded vessels (#8630 and #B8648, Sigma-Aldrich, St. Louis, MO). The treatments and the control always had the same number of ovules. Each well or vessel contained randomized ovules from at least two bolls and typically three or more bolls. Cultures were incubated at 30 °C in the dark, and an entire vessel or well was harvested at each assay time.

The stocks of fluridone (30.36 mM, 10 mg/ml; #A1049, Sigma-Aldrich; CAS Number 59756-60-4) and ABA (66 mM; #45511, Sigma-Aldrich; CAS Number 14375-45-2) were dissolved in dimethyl sulfoxide (DMSO). The fluridone st ock was made weekly and stored at 4 °C. Colchicine was added from a 100-mM filter-sterilized aqueous stock, stored at − 20 °C. The controls contained the maximum amount of DMSO that was in any treatment for each experiment.

Ovule scoring and analysis of fiber morphology

Whole cultures were photographed and individual ovules were scored as 'useful' if they appeared to have at least 80% of the vigor of an optimum cultured ovule of the same age. A standard of less than 100% was set to reflect the approximate nature of visual scoring and to allow rapid scoring. Among the useful ovules, three from each replicate that appeared to have the most abundant white and lustrous fibers were used for length measurements.

For length measurements, the fiber of 3–7 DPA ovules fixed in Histochoice (AMRESCO Inc, Solon, OH) was relaxed by warming in 1% (v/v) Nonidet-40 (80 °C, 20 min; #N3500, US Biological, Swampscott, MA). Cooled ovules were placed on a slide and the attached fiber was gently combed away from the chalazal end with an angled metal probe to form a straight cone, which was imaged in a dissecting microscope. The straight line tool in Fiji (Schindelin et al. 2012) was used to measure the length of the cone, representing the majority of the fibers. To relax the 8–23 DPA fiber, ovules were vigorously shaken (1 min) in 5 ml 0.025 N HCl (80 °C). To relax the older 30–37 DPA fiber, ovules were pulse heated (8–10 s) in a microwave with 0.025 N HCl. The chalazal fiber (or the most prominent fiber, if it was sporadic on treated ovules) was straightened by a gentle stream of water on a glass slide and measured with a millimeter ruler at the place the main fiber halo ended.

Using digital images of chalazal fibers, Fiji was used to measure tip diameters at three locations. The diameter of curvature, or the diameter of the circle fitting within the apical dome, provided the apical diameter, and diameters at 40 µm and 200 µm back from the apex were measured perpendicularly to the fiber axis using the straight line tool. For *Gh* tips, the apical diameters were used as a main classifier of tip type, with 9 µm as the demarcator between *Gh tapered* and *Gh hemisphere* tips before and after treatment. In addition, all tips were classified visually, in terms of pointed versus blunt apices, and seven treated tips with 7–8 µm apical diameters were re-classified as *Gh hemisphere* prior to graphing and statistical analysis.

Fibers were analyzed microscopically for the onset of secondary cell wall synthesis. Attached fibers that had been fixed and stored in HistoChoice were removed from the chalazal end of the ovule, and observed with polarization and differential interference contrast optics (Olympus BH-2

microscope; http://www.olympus-lifescience.com/en/). Images of birefringence were captured from fibers oriented similarly in the field of view under the same optical conditions and the same exposure time (75 ms), except at 30 DPA, images were captured with 25 ms exposure time due to the strong birefringence from increased amounts of secondary wall cellulose.

Graphs were produced using Kaleidagraph software (www.synergy.com). For box plots, empty circles represent outliers that were automatically identified as lying outside an acceptable range, and an 'x' denotes the mean value. Analysis of significant differences between means was performed using pairwise (one-tailed *T* tests or Mann–Whitney *U* tests) or groupwise (ANOVA or Kruskal–Wallis tests) methods by use of Kaleidagraph or the Real Statistics Resource Pack for Excel (http://www.real-statistics.com/) (Zaiontz 2015). The parametric *T* test or ANOVA was used when the data were normally distributed with similar variance, as assessed by the Shapiro–Wilk or Levene's tests, respectively. If not, the non-parametric Mann–Whitney U or Kruskal–Wallis tests were used. All pairwise comparisons among means were carried out using Tukey's Honestly Significant Difference (HSD) or Dunn's test to control the experiment-wise type I error rate, as noted in the figure legends.

Analysis of colchicine effects on fiber tips

For indirect immunofluorescence of microtubules, the 4 DPA cultured fibers (with and without colchicine treatment at the time of culture on 2 DPA) were fixed (1% v/v glutaraldehyde in microtubule stabilizing buffer) while still attached to ovules by the adaptation of methods previously used for older fibers (Seagull 1990). After fixation, all steps prior to mounting occurred under gyratory agitation with three ovules contained in a permeable holder (#62327-10, Electron Microscopy Sciences, Hatfield, PA) and 4 ml solution in each well of a 6-well tissue culture plate. A mouse monoclonal anti-tubulin primary antibody (1:1000, 1 h, RT; #T9026, Sigma-Aldrich) and an AlexaFluor 488-conjugated goat-anti-mouse secondary antibody (1:200, 4 °C, overnight; #A11001, Thermo Fisher Scientific, Waltham, MA) were used. Dissected chalazal pieces of the ovule with fiber attached were mounted on slides with an anti-fade reagent (#P36930, Thermo Fisher Scientific) and allowed to cure (24 h, RT, dark). Coverslips were then sealed with nail polish, and slides were either stored indefinitely at − 20 °C or at 4 °C (for a maximum of 2 weeks) prior to imaging. Microtubules were imaged in multiple Z-planes (0.46 µm) across the diameter of the entire tip by laser scanning confocal microscopy (LSM 880; 40× water immersion objective; 488 nm excitation with 490 nm barrier; 570 nm emission filters; Zen 2.3 image capture and processing software; Carl Zeiss Microscopy, Jena, Germany). After image normalization by background subtraction for each fiber, maximum intensity Z-stacks were generated for display.

For statistical analysis of the effects of colchicine on diameter at three locations in three tip types, we used a linear mixed model appropriate to the three-factor completely randomized split-plot design (using the language of factorial experiments) (SAS software, https://www.sas.com). There were two crossed whole-plot factors, tip type (three levels) and colchicine treatment (two levels), and one split-plot factor, distance from the apex (three levels). The experimental units were 773 total fiber tips, each measured at three separate locations, or distances relative to the apex. Diagnostic residual plots from models fit to the raw diameter measurements indicated that variability in the response increased with the mean, violating the homogeneity of variance assumption underlying ANOVA. Specifically, if *i*, *j*, *k*, and *l* index tip type, colchicine, distance, and tip unit, respectively, then the statistical model may be written as follows:

$$Y_{ijkl} = \mu + \alpha_i + \beta_j + \delta_k + (\alpha\beta)_{ij} + (\alpha\delta)_{ik} + (\beta\delta)_{jk} + (\alpha\beta\delta)_{ijk} + F_{l(ij)} + E_{ijkl}.$$

In this model, *F* and *E* denote random fiber effects and experimental errors, respectively. Fiber effects are nested within the combination of tip type and colchicine. Plots of residuals computed from this model conformed to the assumptions of normally distributed data with roughly constant variance. Three types of comparisons were made: (a) effects of colchicine for nine combinations of tip type and distance; (b) the effect of colchicine across tip types at each fixed distance; (c) the effect of colchicine across distance for each fixed tip type. Comparisons among means were interpreted as significantly different if $p \leq 0.05$ after Bonferroni adjustment for the multiplicity of comparisons.

Results

Adding fluridone increased the percentage of useful *Gb* ovules and *Gb* fiber length

In the culture medium commonly used for *Gh* ovules (Beasley and Ting 1973), *Gb* ovules cultured at 2 DPA often developed extensive callus or the initiated fiber failed to elongate (Fig. 1a; Suppl. Fig. S1). These ovules were not useful for experiments on fiber development, the most frequent use of cultured cotton ovules. Useful cultured ovules should produce abundant long fiber, similar to healthy *Gh* or *Gb* ovules in planta and *Gh* ovules cultured in the standard medium (Fig. 1c). Commonly, cultured cotton ovules are assessed visually prior to more time-consuming analyses.

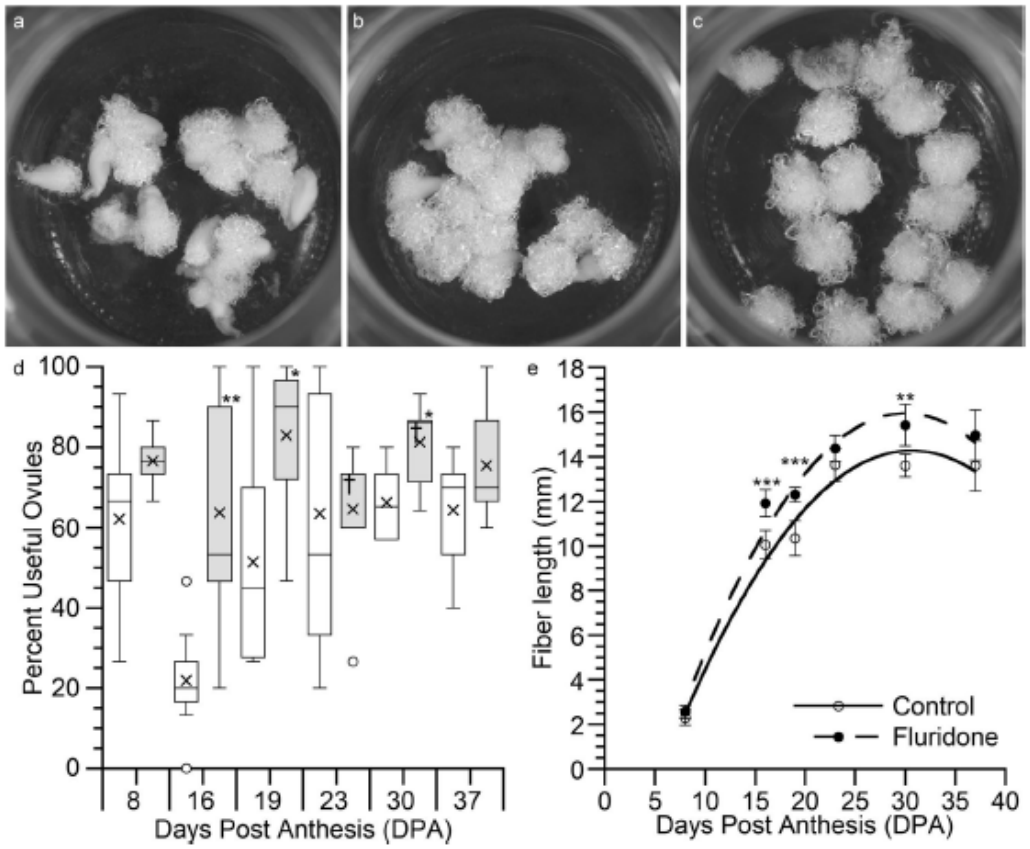

Fig. 1 Fluridone (15.2 µM) had positive effects on the performance and fiber length on *Gb* cultured ovules. **a–c** Photographs of 16 DPA *Gb* or *Gh* ovule cultures, selected to show percent useful ovules near each median value. **a** 50% useful ovules in a *Gb* culture without fluridone. **b** 83.3% useful ovules in a *Gb* culture with fluridone. **c** 86.6% useful ovules in a *Gh* culture without fluridone. **d** Quantitation of the percent useful ovules in cultures with and without fluridone (gray and white boxes, respectively). A significant increase in the percent useful ovules in the presence of fluridone was observed at 16, 19, and 30 DPA. An 'x' denotes the mean, empty circles denote outliers, and a dagger symbol denotes the location of the median value when it overlapped with one of the quartile boundaries. **e** Analysis over a time-course showed that fluridone enhanced fiber elongation on useful *Gb* ovules. The Kruskal–Wallis test indicated differences between all the means in **a** ($p=0.006$) and **b** ($p<0.001$). In **a** and **b**, the means at each DPA were compared with the Mann–Whitney *U* test, with asterisks indicating significant differences: $*p\leq0.05$; $**p\leq0.01$; and $***p\leq0.001$. For each treatment in **a**, $n=6$–13 vessels, typically containing 14–15 ovules each, within 2–7 trials; in total, the data reflect the results of 19 trials. For each treatment in **b**, fiber was measured on $n=17$–39 ovules from the same samples. Error bars in **b** are 95% confidence intervals. All cultures contained 0.05% (v/v) DMSO

In this study, we scored an ovule as useful if it appeared to have at least 80% of the vigor of an optimum ovule of the same age. The overall response of cultured *Gb* ovules was highly variable in the standard medium: they performed well in some trials and failed entirely in others, as shown by multiple trials within 1 week (Suppl. Fig. S1). The addition of 15.2 µM (10 mg/l) fluridone increased the average percent of useful ovules in these closely spaced trials (Suppl. Fig. S1) and in other prior tests of a 3.8–30.4 µM (2.5–20 mg/l) range of fluridone concentrations (Suppl. Fig. S2).

Fluridone was added at 15.2 µM final concentration in all subsequent experiments, with a notable positive effect on the vigor of cultured *Gb* ovules (Fig. 1b). When the percent useful ovules were assessed at 6 days between 8 and 37 DPA, the controls had an overall mean of 55% useful ovules as compared to 75% in cultures with fluridone. The mean percent useful ovules was significantly greater at 16, 19, and 30 DPA (Fig. 1d). A time-course experiment showed that fluridone also enhanced fiber length on *Gb* cultured ovules (Fig. 1e), confirming the other tests at 16 DPA only (Suppl. Fig. S2). The data in Fig. 1e were collected in 19 trials, which were set up in 7 months over 2 years and then graphed collectively, implying that the results are representative. *Gb* fiber length was similar through 8 DPA with and without fluridone, but fibers were typically longer

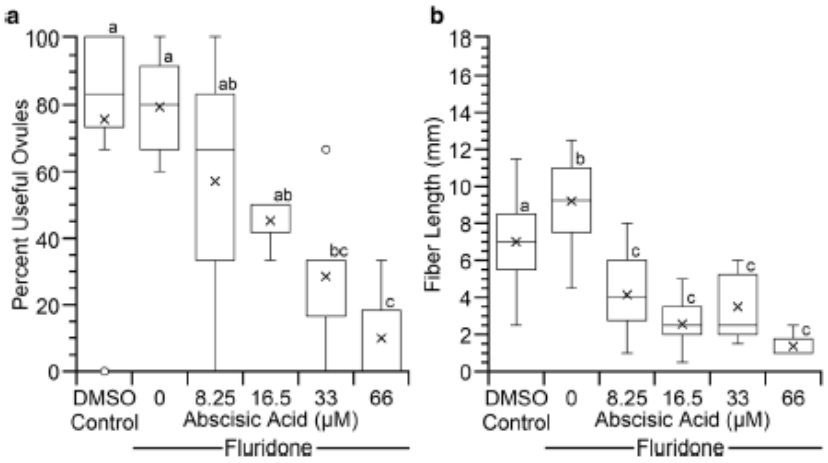

Fig. 2 Exogenous abscisic acid antagonized the performance and fiber length of 16 DPA *Gb* ovules cultured with fluridone. The ABA concentrations are shown, and cultures denoted by the line also contained 15.2 μM fluridone. **a** The percent useful ovules was significantly decreased when 33 μM or 66 μM ABA was present. **b** Average fiber length was significantly decreased by 8.25 to 66 μM ABA as compared to two controls: DMSO alone or fluridone added in DMSO. In **a** and **b**, box plot labeling is like Fig. 1, and the Kruskal–Wallis test indicated differences between all the means ($p<0.001$). Means with a common letter do not differ significantly, as determined by Dunn's test. For **a**, $n=7$ wells, containing 6 ovules each, within 5 trials, and for **b** fibers were measured on $n=4$–33 ovules from the same samples, with only 4 ovules having measureable fiber in the presence of 66 μM ABA. All cultures contained 0.1% (v/v) DMSO

in the fluridone treatments as compared to the controls at later DPA (Fig. 1e). For example, the fluridone-treated fibers were 19% longer on 19 DPA ovules. Note that these are conservative measurements of fiber length: longer fibers were usually present, but not measured, because they extended beyond the cone established by the majority of the fibers. The growth of *Gb* ovules was not affected by fluridone, and ovule size did not correlate with fiber length (Suppl. Fig. S3). Therefore, fluridone mainly affects fiber elongation on *Gb* cultured ovules. This helps to explain why the visual assessment of percent useful ovules did not consistently reveal differences at later DPA (Fig. 1d). When high-rate elongation was occurring at 16 and 19 DPA (Fig. 1e), the longer fiber in the presence of fluridone likely enhanced the perception of good performance in the intact ovule/fiber system. At later DPA, when fiber elongation was slowing or stopped, the differences were likely less perceptible until the fiber length was measured.

Positive effects of fluridone on *Gb* ovule culture were antagonized by exogenous ABA

Since fluridone is an upstream inhibitor of ABA biosynthesis, we tested the ability of ABA to antagonize ovule performance and fiber elongation (Fig. 2). In this set of trials, the percent useful ovules was similar in fluridone-treated cultures and controls, although, in one trial, the DMSO control cultures failed entirely. Compared to the DMSO control and fluridone-treated cultures, ABA added together with fluridone inhibited ovule performance in a concentration-dependent manner. Both 33 μM and 66 μM ABA causing a significant reduction in the percent of useful ovules (Fig. 2a). In the same cultures, 8.25–66 μM ABA added together with fluridone decreased fiber length as compared to both controls (Fig. 2b). In addition, these independent experiments (different data as compared to Fig. 1e and Suppl. Fig. S2) confirmed the positive effects of fluridone on fiber length, with 31% longer fiber occurring on 16 DPA fluridone-treated *Gb* ovules as compared to the DMSO controls ($p=0.023$).

The onset of secondary wall deposition is delayed in fluridone-treated *Gb* fibers

These observations included control *Gb* ovules that produced fiber in the absence of fluridone. The onset of secondary cell wall synthesis was monitored in two ways by previously established methods (Singh et al. 2009). First, polarized light microscopy revealed the white birefringence of organized crystalline cellulose only when the quantity of cellulose began to increase in the transition stage between primary and secondary cell wall syntheses, with the intensity of birefringence increasing as secondary wall synthesis continued (Fig. 3a). Second, differential interference contrast optics revealed the orientation of cellulose microfibrils, which shifts to helical at the transition stage (Fig. 3b; reviewed in Haigler et al. 2012). Both methods showed that the addition of fluridone delayed

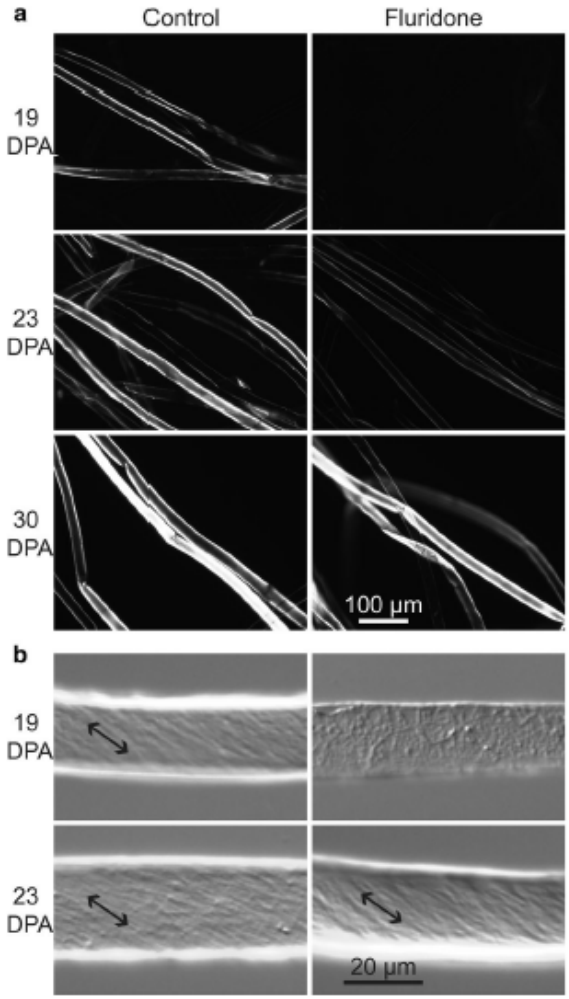

Fig. 3 Microscopic analysis of time of onset of secondary wall synthesis in *Gb* fibers with and without fluridone. **a** In polarization microscopy, only the control fibers showed white birefringence of secondary wall cellulose at 19 DPA. Fluridone-treated fibers were dimly birefringent at 23 DPA, consistent with an early stage of cell wall thickening. Both treated and untreated fibers were highly birefringent at 30 DPA, due to continuing cellulose deposition. The 30 DPA images were taken with one-third of the exposure time used for 19 and 23 DPA. **b** Differential interference contrast optics revealed the orientation of the helical cellulose microfibrils (highlighted by the double arrow) typical of secondary walls at 19 DPA in the control. To the contrary, helical microfibrils were not observed until 23 DPA in fluridone-treated *Gb* fibers. Images are representative of two independent trials. The 100 µm or 20 µm scale bars apply to all the images in panel **a** or **b**, respectively

the onset of secondary wall synthesis in cultured *Gb* fibers. In the DMSO control, both signs of secondary wall thickening were apparent by 19 DPA, whereas they were not apparent until 23 DPA in fluridone-treated fibers. The dim birefringence of 23 DPA fluridone-treated fibers is consistent with this being near the time of onset of cell wall thickening.

Comparative effects of fluridone on *Gb* and *Gh* ovule cultures

In the presence of fluridone, the elongation of *Gb* fibers after 8 DPA was broadly similarly to control (untreated) *Gh* fibers (Fig. 4a), with some differences as discussed below. These represent the best conditions for ovule culture in the two species, because fluridone hindered *Gh* ovule success without changing *Gh* fiber length (Fig. 4b, Suppl. Fig. S4). The *Gh* control fibers were longer than the *Gb* fluridone-treated fibers at 8 DPA ($p < 0.001$), but there was inconsistency in the comparison at 16 and 19 DPA due to experimental variation and the compilation of data from multiple trials into one graph (Fig. 4a). Since fiber elongation was approaching its endpoint around 23 DPA on both *Gh* and *Gb* cultured ovules and exact quantitative outcomes sometimes varied between trials, we collectively considered the 23, 30, and 37 DPA data to compare final fiber lengths (Fig. 4b). This led to the estimate of 7.2% longer fibers on fluridone-treated *Gb* ovules as compared to untreated (most useful) *Gh* ovules ($p = 0.031$). Comparing the fitted curves (Fig. 4a) supports the possibility that the fluridone-treated *Gb* fibers finally become longer than untreated *Gh* fibers due to a prolonged elongation period that is specific to *Gb*, as observed in planta for these two cultivars grown in parallel (Avci et al. 2013). In contrast, the cultured *Gb* and *Gh* fibers showed a similar response to fluridone in the delayed onset of secondary cell wall synthesis (compare Fig. 3 and Suppl. Fig. S5).

Early fiber elongation and tip morphology on *Gh* and *Gb* cultured ovules

The *Gh* and *Gb* fiber elongated relatively slowly between 2 and 4 DPA (Fig. 5a) when the colchicine experiments were conducted. During this time, anisotropic cell expansion is transforming the initially spherical fiber initials into the fiber morphology (Haigler et al. 2012). The rate of elongation had increased by 5 DPA in both species (with a larger change in the cultured *Gh* fiber) as a precursor to the prolonged phase of fast elongation that occurs later in culture (Fig. 4a) and in planta (Avci et al. 2013). During the early period of fiber morphogenesis, additional measurements added precision to our understanding of the three distinct fiber tip types: two in *Gh* and one in *Gb* (Stiff and Haigler 2016). As measured at 4 DPA, the diameter of each tip type progressively increased from the apex to 200 µm back, and each tip type had a different diameter at each measured location (Fig. 5b, Table 1). The *Gh hemisphere* tips were widest, and the narrow *Gh tapered* tips were 29.8% wider than the *Gb* tips at 200 µm.

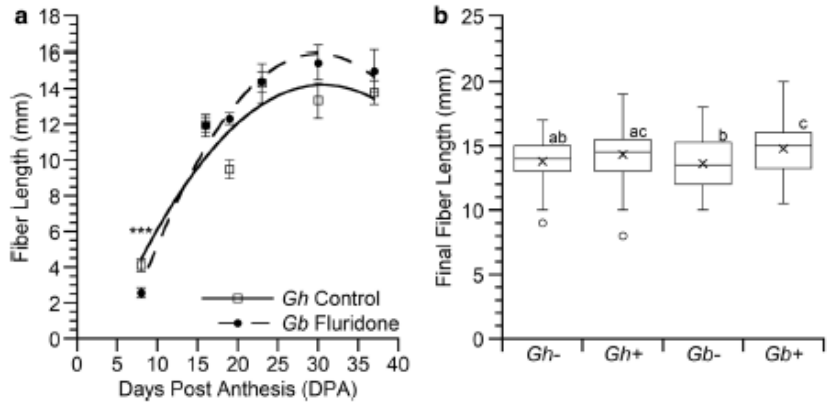

Fig. 4 Comparative effects of fluridone on fiber length in *Gh* and *Gb* ovule culture. **a** Fiber lengths are shown over the time-course for cultures grown under the best conditions for each species: with or without fluridone for *Gb or Gh* ovules, respectively. At 8 DPA, the *Gb* fibers were shorter than those on *Gh* ovules ($p<0.001$; Mann–Whitney *U* test). After 8 DPA, a similar rate of fiber elongation occurred for both species through 23 DPA. The data are replotted from Fig. 1e (*Gb*) and Suppl. Fig. S4 (*Gh*), and error bars are 95% confidence intervals. **b** Analysis of final fiber length with (+) and without (–) fluridone in *Gh* and *Gb* cultures. Given that the mean fiber lengths were near maximal and similar for both species at 23 DPA in **a**, all the data were combined for 23, 30, and 37 DPA in each case. Kruskal–Wallis indicated a difference between all the means ($p=0.007$), and the *Gb*+ fibers were 8.4% longer than those in *Gb*– ($p=0.001$) and 7.2% longer than those in *Gh*– ($p=0.031$). Box plot labeling is like Fig. 1, and means with a common letter do not differ significantly, as determined by Dunn's test. Replication information is in Fig. 1 and Suppl. Fig. S4, which also shows no effect of fluridone on *Gh* fiber length as measured over a time-course, even though the percent of useful *Gh* ovules was reduced

Effect of colchicine on microtubules, fiber length, and tip diameter

To help select a concentration for further use, we initially tested the effect of 25, 50, 100, and 200 µM colchicine on chalazal fiber length in comparison to controls. Surprisingly, between 2 and 4 DPA, only 200 µM colchicine significantly reduced the mean length of *Gh* chalazal fibers by 16.9%, whereas it had no effect on the length of *Gb* fibers (Suppl. Fig. S6). Although 50 µM colchicine did not affect the mean fiber length in either species, we chose this concentration for further work because no microtubules or greatly altered microtubules were typically observed in treated tips in contrast to well-organized microtubule arrays in untreated tips (Fig. 6). Only a minority of fibers (e.g., < 7% in one experiment) retained an apparently normal microtubule array after colchicine treatment. Furthermore, 50 µM colchicine caused changes in the diameter of all the tip types in two or three measured locations (Table 1, Suppl. Fig. S7). The only exception was for *Gh hemisphere* fibers at 200 µm, where a 9% increase in diameter was not statistically significant after Bonferroni adjustment for multiplicity of comparisons.

Colchicine induced a maximum increase in mean tip diameter of 31.29% at 200 µm in *Gh tapered* tips. Other significantly different increases in mean diameter ranged from 13.6% (*Gb* tips at 200 µm) to 20.76% (at the *Gb* tip apex). These changes in average diameter occurred within populations of fiber that retained bimodal or unimodal distributions, for *Gh* and *Gb,* respectively, similar to the controls. Colchicine-treated *Gh* tips retained the bimodal apical diameter distribution as found in control tips (Suppl. Fig. S8a, b), with 60% *tapered* and 40% *hemisphere* in controls versus 52% *tapered* and 48% *hemisphere* in treated tips. The apical diameters of colchicine-treated *Gb* tips remained unimodal like controls (Suppl. Fig. S8c, d).

Linear mixed models were used to contrast the magnitude of the effects of colchicine on tip diameter as measured at three locations within each of the three tip types (Fig. 7). The *Gh tapered* tips uniquely shrank at the apex when microtubules were perturbed by colchicine ($p<0.001$) (Fig. 7). To the contrary, colchicine induced swelling of the *Gh tapered* tips at 40 and 200 µm and the *Gh hemisphere* and *Gb* tips at all three measured locations. The *Gh tapered* tips swelled more at 200 µm as compared to 40 µm ($p=0.018$), whereas the *Gb* and *Gh hemisphere* tips swelled to a similar degree at all three measured locations when compared both within and between these two tip types ($p=1.0$ in all cases after Bonferroni adjustment for multiplicity of comparisons) (Table 1; Fig. 7). Without Bonferroni adjustment, the colchicine effect at 200 µm for *Gh tapered* tips was different from *Gb* ($p=0.028$) and *Gh hemisphere* tips ($p=0.01$). The most similar and a relatively low magnitude of swelling occurred at 40 µm (14.42–17.73% increase) for all three tip types.

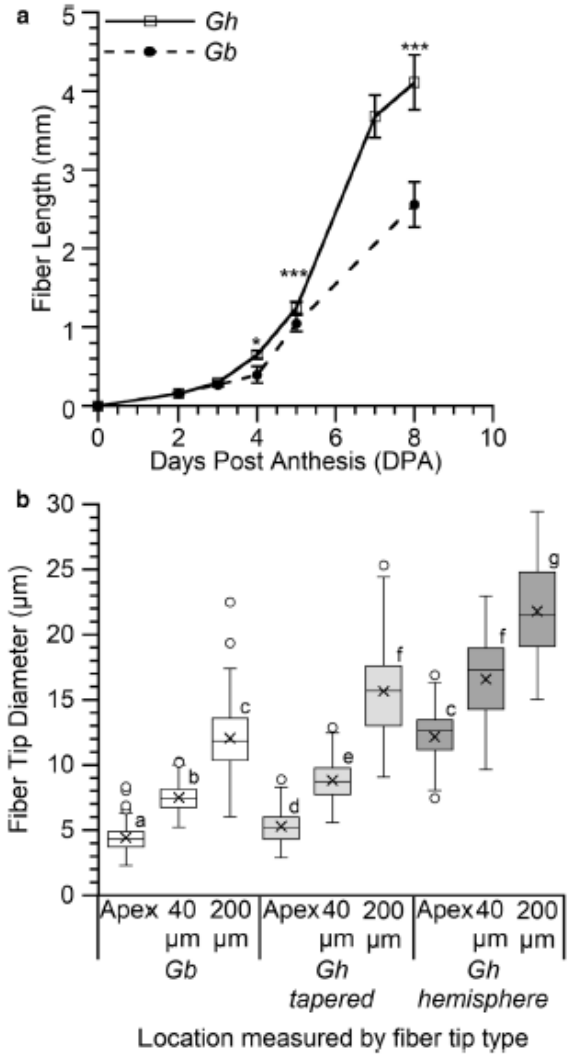

Fig. 5 Length and tip diameter of non-colchicine-treated fibers during early elongation when experiments with colchicine were conducted. For **a** and **b**, data for cultured fibers derive from cultures run under the best conditions for each species: with or without fluridone for *Gb or Gh* ovules, respectively. **a** Length of *Gh* and *Gb* fibers until 8 DPA after initiation on 0 DPA and culturing on 2 DPA. An early slow elongation phase ended near 4 DPA in both species, and then, *Gb* fibers elongated less than in *Gh* between 4 and 8 DPA. **b** Tip diameter at the apex and 40 µm and 200 µm behind the apex in three types of cultured fibers at 4 DPA. Each tip type increased in diameter behind its apex and had a distinct tip size [$p < 0.0001$; ANOVA, $F_{(8,1097)} = 710.79$]. Means with a common letter do not differ significantly, as determined by Tukey's HSD test. Box plot labeling is like Fig. 1, and replication is in Table 1. For **a**, the zero value at 0 DPA reflects fiber initiation; then, the 2 DPA lengths were measured for fiber on boll-grown ovules used to start the cultures (for each species, $n = 30$ individual fibers on 6 ovules from 3 bolls of 3 plants), and the 8 DPA are replotted from Fig. 4a. For lengths of cultured fibers on 3–8 DPA, the cone of chalazal fiber was measured on $n = 18$–32 ovules from 4–6 replications within 2–3 trials. Kruskal–Wallis showed a difference between all the means ($p < 0.001$), and significant differences between paired means (determined by the Mann–Whitney *U*test) are indicated by asterisks as in Fig. 1. Error bars are 95% Confidence Intervals, which are sometimes within the marker space

Discussion

The *Gh* ovule culture system has been a powerful research aid for decades, but an effective analogous method was not previously available for *Gb* cultures. Here, we showed that addition of fluridone, an inhibitor of ABA biosynthesis, resulted in a useful culture system for 2 DPA *Gb* ovules. A modern elite cultivar of Pima cotton, *Gb* cv Phytogen 800, was used as the exemplar and compared to a modern elite example of Upland cotton, *Gh* cv Deltapine 90. The *Gh* cultured ovules behaved as expected on the commonly used medium (Singh et al. 2009), and the addition of fluridone promoted *Gb* ovule success and fiber elongation in culture. With fluridone, the inherent variability in *Gb* ovule performance in culture was reduced, resulting in an average across all DPA analyzed of 75% of ovules being perceived as useful versus 55% in controls. The continuing variability in the response of *Gb* ovules to culture can be compensated by selecting useful ovules visually for downstream analysis, making sure that standardized selection criteria are used for any treatments to be compared. Fluridone caused an opposite effect on the performance of *Gh* ovules, with 63% or 91% useful ovules occurring with or without fluridone, respectively (Suppl. Fig. S4). This difference is likely related to the complex hormonal network operating within young cotton ovules/fibers (Chen et al. 1997; Liao et al. 2010), inclusive of varying ABA levels between species, and even the cultivars of one species (Dasani and Thaker 2006). The fiber on fluridone-treated *Gb* ovules finally became 8.4% longer than on untreated *Gb* controls and 7.2% longer than on untreated *Gh* ovules. These results were consistent with prior work on short-fibered *G. arboreum*, which had high levels of endogenous ABA and performed better in culture when fluridone was added (Nayyar et al. 1989).

ABA likely influences the performance of *Gb* ovules in culture, as inferred from its ability to reverse the positive effects of fluridone. Exogenous ABA also inhibits *Gh* fiber elongation in culture (Beasley and Ting 1973; Dhindsa et al. 1976; Kosmidou-Dimitropoulou 1986; Dasani and Thaker 2006), and endogenous ABA may inhibit the performance of *Gb* cultured ovules, so that fluridone has a positive effect. *Gb* ovule size was similar with and without fluridone and ovule size and fiber length were not correlated (Suppl. Fig. S3). Therefore, fluridone primarily impacted fiber elongation specifically in the *Gb* cultured ovule system. Why the fiber on all ovules cultured from healthy bolls did not respond equally to fluridone will be worthwhile to explore in future experiments. In general, the cotton ovule culture systems should be used with caution when investigating the hormonal controls of fiber development, given that exogenous auxin and gibberellic acid are added for both species, even variation of the type of auxin affects the temporal and

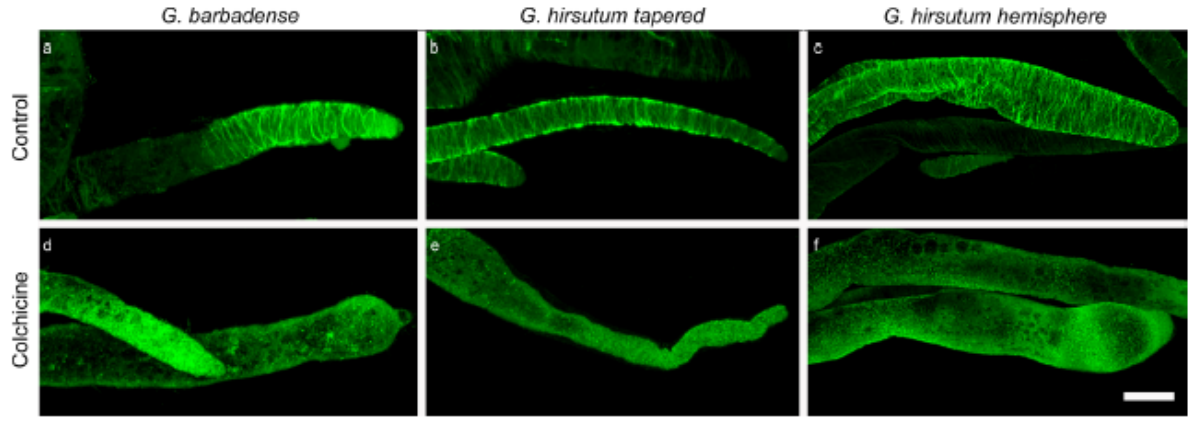

Fig. 6 Immunofluorescence of microtubules in 4 DPA cultured cotton fibers with and without 50 µM colchicine treatment at 2 DPA. Three fiber tip types are represented within two cotton species: (**a**, **d**) *Gb*; (**b**, **e**) *Gh tapered*; and (**c**, **f**) *Gh hemisphere*. Transverse microtubules occurred in untreated fiber tips (**a**–**c**), whereas microtubules were typically not present in the treated fiber tips (**d**–**f**). Scale bar = 10 µm for all images

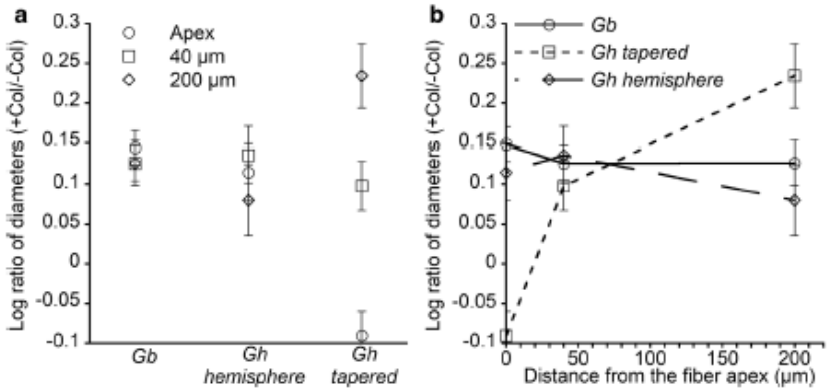

Fig. 7 Contrasts of the effects on tip diameter of colchicine as compared to untreated controls within and between tip types. **a** Contrasts are plotted within each of three tip types across three measured locations (the apex, 40 µm, and 200 µm). Only *Gh tapered* tips showed a statistically different response across locations. **b** Contrasts are plotted for each of three measured locations across tip types. The only significantly different effects across tip types occurred at the apex, as judged after Bonferroni adjustment for multiplicity of comparisons. See the text for further details of statistical analysis. Standard error bars are shown

quantitative aspects of *Gh* fiber development in vitro (Singh et al. 2009), and, unlike *Gb*, the *Gh* ovule/fiber culture was not improved by the addition of fluridone. Nonetheless, a common response to fluridone for the two species was observed in the delay of onset of fiber secondary cell wall synthesis. This is consistent with the positive role of ABA in initiating secondary wall synthesis in diverse cell types (Didi et al. 2015). If researchers compare the fibers at later stages on *Gb* and *Gh* ovules cultured with or without fluridone (the optimal condition for each species), it would be important to remember the delay in secondary cell wall synthesis that would occur only in *Gb* fibers.

The *Gb* ovule culture system run in parallel with the *Gh* ovule culture system allowed us to test the hypothesis that growth control mechanisms differed zonally within one cotton fiber tip and between tip types. Zonal control of microtubule-mediated cell expansion was demonstrated for the *Gh tapered* tips, which uniquely shrank at the apex in the presence of colchicine. Affirming a difference between tip types, the *Gh tapered* tips also swelled more at 200 µm than at 40 µm, whereas the *Gh hemisphere* and *Gb tips* swelled to a similar degree at all three measured locations. This shows that a broad and a narrow tip type in two different species responded similarly to colchicine, whereas a narrow tip type responded differently than a broad tip type in the same

species. Therefore, the microtubule-mediated control of cotton fiber expansion near the tip is not correlated with tip diameter or species. These results parallel the similar distributions of cell wall polymers near the tips of *Gh hemisphere* and *Gb* tips, whereas *Gh tapered* tips were more distinct (Stiff and Haigler 2016).

Although 50 µM colchicine typically greatly disturbed or removed the microtubule array in fiber tips, it had little or no effect on the early fiber elongation in either species. This observation is consistent with apical cell wall synthesis occurring in cotton fibers (Stiff and Haigler 2016), as also occurs in a microtubule-independent manner in most classical tip-growing cells (Rounds and Bezanilla 2013). However, when microtubules were perturbed at 2 DPA, the cotton fibers did not become branched or wavy, which has been observed in classical tip-growing cells that do not expand behind the apex (Bibikova et al. 1999; Geitmann 2011). This difference may relate to the predominantly transverse microtubule array near the cotton fiber tip, which generates the ability to control diametric expansion behind the apex. The three tip types each showed a similar degree of colchicine-induced swelling at 40 µm (14.42–17.73%). This location is within a zone of cell wall synthesis that began about 30 µm back from the apex in *Gh hemisphere* and *tapered* tips (with *Gb* tips not able to be similarly analyzed in pulse-chase experiments). All three fiber tip types showed changed amounts of high-methyl-esterified homogalacturonan, fucosylated xyloglucan, and crystalline cellulose at 35–45 µm as compared to the apex or nearby sub-apical regions (Stiff and Haigler 2016), with the results cumulatively suggesting that the region between 30 and 45 µm reflects the transition to diffuse growth in young cotton fibers. Distinct cell wall-based mechanisms have been predicted to regulate expansion along the length versus the width of anisotropically growing cells (Baskin 2005). All three of the control tip types had a transverse microtubule array behind the apex, consistent with the need to control diametric expansion during diffuse growth.

The data showed that median tip diameters were most often changed less than means by colchicine treatment, corresponding to 'outliers' often being automatically identified in box plots of the treated data sets. Strong responses of a few fibers after treatment at 2 DPA are consistent with the possibility that there may be a relatively transient developmental stage in which microtubules are essential for establishment of cotton fiber tip shape, which is then maintained through the unique combinations of features that control classical tip and diffuse growth in separate cells. After tip shape is initially established, the other cellular components such as actin and cell wall polymers may exert stronger control as tip diameter and overall fiber diameter are maintained during the additional 2–3 week period of cotton fiber elongation.

In addition to providing new information about different modes of growth control at the tips of cotton fibers, our results show that the newly developed *Gb* ovule culture system enables in vitro experiments on fiber development in this high value commercial cotton species. It also enables experimental comparisons of the cellular controls of fiber development in *Gh* and *Gb*, keeping in mind possible direct effects of potentially different levels of ABA (or other molecules with synthesis dependent on the desaturation of phytoene) if fluridone is added only to *Gb* cultures.

Author contribution statement MRS and CHH designed research; ETP, BPG, and JAO conducted experiments and/or statistical analysis; and ETP, BPG, and CHH wrote the paper with contributions from the other authors.

Acknowledgements For research support, we thank Cotton Incorporated, Cary, NC. For assistance with fiber tip measurements, we thank Robin Grant Moore and Anne Pajerski. For assistance with laser scanning confocal microscopy, we thank Dr. Eva Johannes in the Cellular and Molecular Imaging Facility of North Carolina State University.

Compliance with ethical standards

Conflicts of Interest The authors state that they have no conflict of interest.

References

Avci U, Pattathil S, Singh B, Brown VL, Hahn MG, Haigler CH (2013) Cotton fiber cell walls of *Gossypium hirsutum* and *Gossypium barbadense* have differences related to loosely-bound xyloglucan. PLoS One 8:e56315. https://doi.org/10.1371/journal.pone.0056315

Baskin TI (2005) Anisotropic expansion of the plant cell wall. Annu Rev Cell Dev Biol 21:203–222. https://doi.org/10.1146/annurev.cellbio.20.082503.103053

Beasley CA, Ting IP (1973) The effects of plant growth substances on in vitro fiber development from fertilized cotton ovules. Am J Bot 60:130–139. https://doi.org/10.1002/j.1537-2197.1973.tb10209.x

Bibikova TN, Blancaflor EB, Gilroy S (1999) Microtubules regulate tip growth and orientation in root hairs of *Arabidopsis thaliana*. Plant J 17:657–665. https://doi.org/10.1046/j.1365-313X.1999.00415.x

Chen J-G, Du X-M, Zhou X, Zhao H-Y (1997) Levels of cytokinins in the ovules of cotton mutants with altered fiber development. J Plant Growth Reg 16:181–185. https://doi.org/10.1007/pl00006994

Dasani SH, Thaker VS (2006) Role of abscisic acid in cotton fiber development. Russ J Plant Physiol 53:62–67. https://doi.org/10.1134/s1021443706010080

Dhindsa RS, Beasley CA, Ting IP (1976) Effects of abscisic acid on in vitro growth of cotton fiber. Planta 130:197–201. https://doi.org/10.1007/bf00384420

Didi V, Jackson P, Hejátko J (2015) Hormonal regulation of secondary cell wall formation. J Expt Bot 66:5015–5027. https://doi.org/10.1093/jxb/erv222

Geitmann A (2011) Generating a cellular protuberance: mechanics of tip growth. In: Wojtaszek P (ed) Mechanical integration of

plant cells and plants. Springer, Berlin, pp 117–132. https://doi.org/10.1007/978-3-642-19091-9_5
Geitmann A, Ortega JKE (2009) Mechanics and modeling of plant cell growth. Trends Plant Sci 14:467–478. https://doi.org/10.1016/j.tplants.2009.07.006
Guerriero G, Hausman J-F, Cai G (2014) No stress! relax! mechanisms governing growth and shape in plant cells. Int J Mol Sci 15:5094–5114. https://doi.org/10.3390/ijms15035094
Haigler C, Betancur L, Stiff M, Tuttle J (2012) Cotton fiber: a powerful single-cell model for cell wall and cellulose research. Front Plant Sci 3:104. https://doi.org/10.3389/fpls.2012.00104
Kitahata N, Asami T (2011) Chemical biology of abscisic acid. J Plant Res 124:549–557. https://doi.org/10.1007/s10265-011-0415-0
Kosmidou-Dimitropoulou K (1986) Hormonal influences on fiber development. In: Mauney JR, Stewart JMCD (eds) Cotton physiology. The Cotton Foundation, Memphis, pp 361–373
Liao W, Zhang J, Xu N, Peng M (2010) The role of phytohormones in cotton fiber development. Russ J Plant Phyisol 57:462–468. https://doi.org/10.1134/s1021443710040023
Meinert MC, Delmer DP (1977) Changes in the biochemical composition of the cell wall of the cotton fiber during development. Plant Physiol 59:1088–1097
Nayyar H, Kaur K, Basra AS, Malik CP (1989) Hormonal regulation of cotton fibre elongation in *Gossypium arboreum* L. in vitro and in vivo. Biochem Physiol Pflanz 185:415–421. https://doi.org/10.1016/S0015-3796(89)80065-4
Qin Y-M, Zhu Y-X (2011) How cotton fibers elongate: a tale of linear cell-growth mode. Curr Opin Plant Biol 14:106–111. https://doi.org/10.1016/j.pbi.2010.09.010
Rounds CM, Bezanilla M (2013) Growth mechanisms in tip-growing plant cells. Annu Rev Plant Biol 64:243–265. https://doi.org/10.1146/annurev-arplant-050312-120150
Schindelin J, Arganda-Carreras I, Frise E, Kaynig V, Longair M, Pietzsch T, Preibisch S, Rueden C, Saalfeld S, Schmid B, Tinevez J-Y, White DJ, Hartenstein V, Eliceiri K, Tomancak P, Cardona A (2012) Fiji: an open-source platform for biological-image analysis. Nat Methods 9:676. https://doi.org/10.1038/nmeth.2019
Seagull RW (1990) The effects of microtubule and microfilament disrupting agents on cytoskeletal arrays and wall deposition in developing cotton fibers. Protoplasma 159:44–59. https://doi.org/10.1007/BF01326634
Seagull RW (1993) Cytoskeletal involvement in cotton fiber growth and development. Micron 24:643–660. https://doi.org/10.1016/0968-4328(93)90042-Y
Sedbrook JC, Kaloriti D (2008) Microtubules, MAPs and plant directional cell expansion. Trends Plant Sci 13:303–310. https://doi.org/10.1016/j.tplants.2008.04.002
Singh B, Cheek HD, Haigler CH (2009) A synthetic auxin (NAA) suppresses secondary wall cellulose synthesis and enhances elongation in cultured cotton fiber. Plant Cell Rep 28:1023–1032. https://doi.org/10.1007/s00299-009-0714-2
Stanton RA, Gernert KM, Nettles JH, Aneja R (2011) Drugs that target dynamic microtubules: a new molecular perspective. Med Res Rev 31:443–481. https://doi.org/10.1002/med.20242
Stiff MR, Haigler CH (2016) Cotton fiber tips have diverse morphologies and show evidence of apical cell wall synthesis. Sci Rep 6:27883. https://doi.org/10.1038/srep27883
Waldrep TW, Taylor HM (1976) 1-Methyl-3-phenyl-5-[3-(trifluoromethyl)phenyl]-4(1H)-pyridinone, a new herbicide. J Agric Food Chem 24:1250–1251. https://doi.org/10.1021/jf60208a047
Zaiontz C (2015) Real statistics using excel. www.real-statistics.com. Accessed Oct 2015

Supplementary Material

Cultures of *Gossypium barbadense* cotton ovules offer insights into the microtubule-mediated control of fiber cell expansion

Ethan T. Pierce, Benjamin P. Graham, Michael R. Stiff, Jason A. Osborne, and Candace H. Haigler

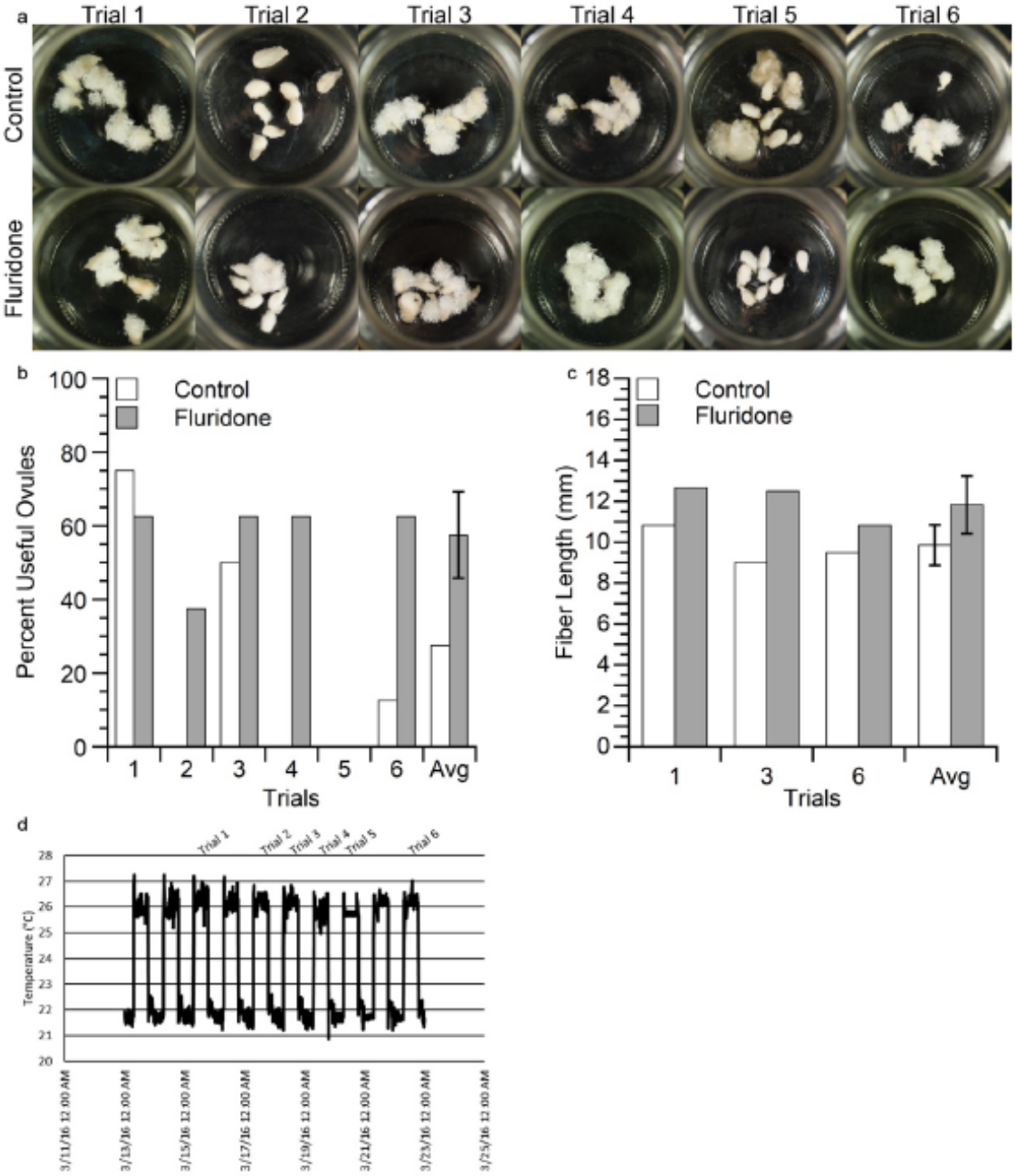

Supplementary Fig. S1 Outcomes of six trials of *Gb* ovule culture over eight consecutive days with and without 15.2 μM fluridone. The ovules of one boll were mainly used to set up each trial, but 3-4 ovules from a second boll were used for trials 1, 2, 4, and 5. **a** Photographs of control or fluridone-treated cultures at 16 DPA in six trials. **b** Percentage of ovules scored as useful ($\geq$ 80% visual vigor relative to an optimal *in planta* or *in vitro Gh* ovule). In four of six trials, fluridone rescued or improved ovule performance as compared to the control. Trial 5 was initiated on a rainy/cloudy day, and it failed entirely and is not included in the average. However, zero values for the controls in Trials 2 and 4 are included in the average. Overall, fluridone improved ovule performance (p=0.047, T-test of average values). **c** Fiber length on 1-3 useful ovules per treatment was measured for trials 1, 3, and 6 and averaged (n=7-9 per treatment; only one trial 6 control ovule was within 80% of optimal). The average fiber length increased 21.7% with fluridone (p = 0.016; T-test of average values). Error bars for the average values represent 95% confidence intervals for **b** and **c**, although no bar is shown for the control value in **b** due to the inclusion of zero values. **d** The daily temperature cycle in the greenhouse while the trials were conducted

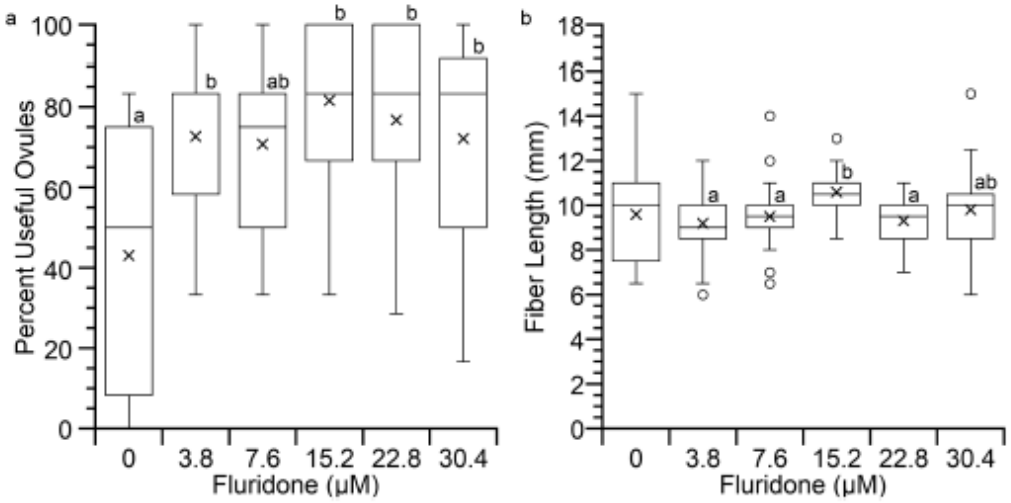

Supplementary Fig. S2 The addition of fluridone positively affected the performance of cultured *Gb* ovules analyzed at 16 DPA. **a** The percent useful ovules in control cultures compared to treated cultures with 3.8 to 30.4 μM fluridone added. All the fluridone concentrations enhanced the median percentage of useful ovules (75 - 83.3%) as compared to the control (50%). There were differences between the means (p=0.049), and means with a common letter do not differ significantly (Kruskal Wallis followed by Dunn's test). **b** Fiber length in the same cultures. Among the concentrations tested, 15.2 μM fluridone slightly increased *Gb* fiber length at 16 DPA if only the fluridone-treated cultures were statistically analyzed together [p=0.005; ANOVA, $F_{(4,138)}$= 3.8]. Due to the long fiber sometimes observed in controls in this set of experiments, there were no significant differences if the control data were included in the group-wise test. Means with a common letter do not differ significantly as determined by Tukey's HSD test. In the boxplots, '**x**' denotes the mean and empty circles denote outliers. For each treatment in **a**, n=12 wells, containing 6 ovules each, within 8 trials. For each treatment in **b**, n=22-23 ovules from 10 wells within 6 trials. All cultures contained 0.1% (v/v) DMSO

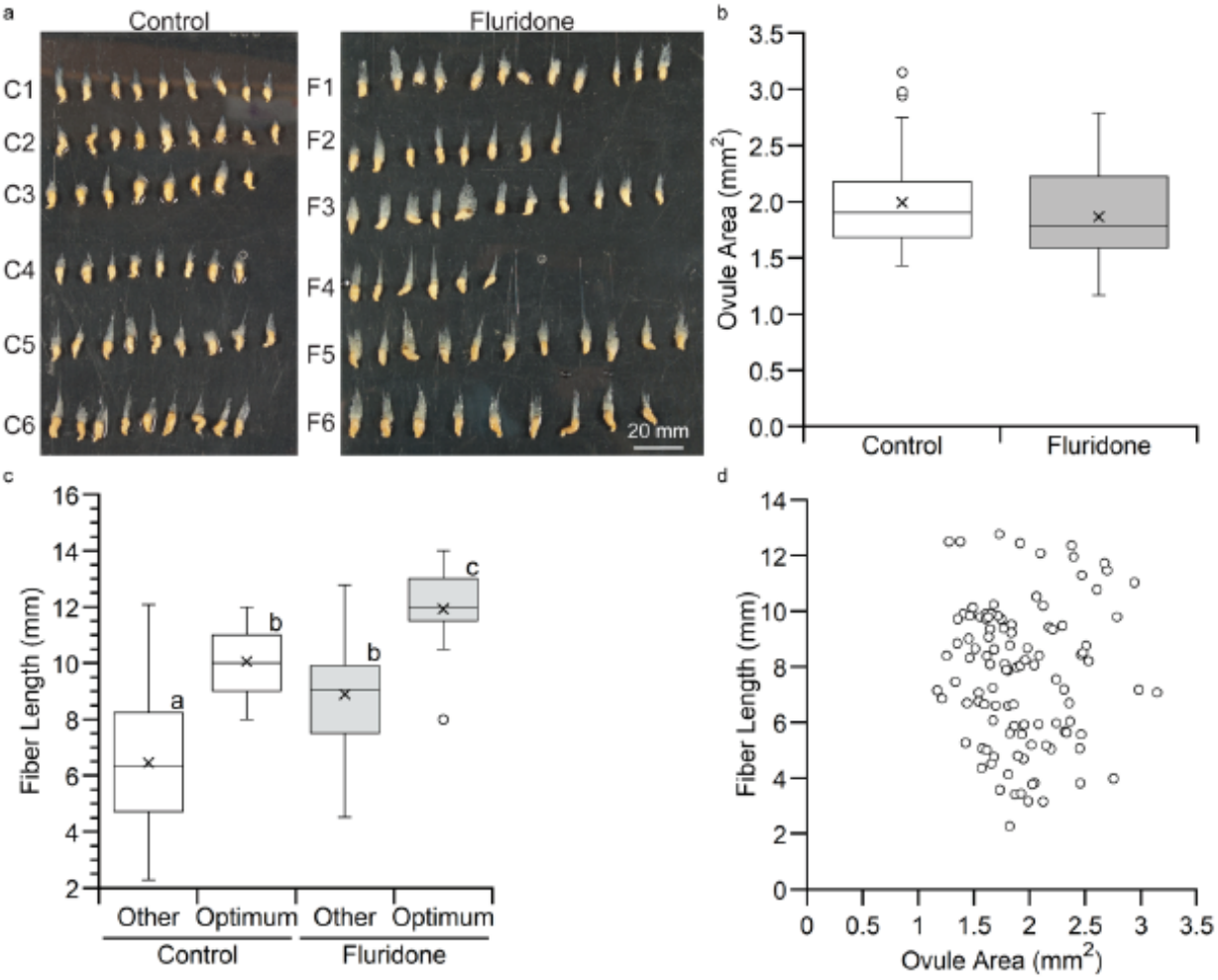

Supplementary Fig S3 Analysis of the effect of 15.2 μm fluridone on *Gb* ovule growth versus fiber length at 16 DPA. **a** Photographs of the control and fluridone-treated *Gb* ovules that were analyzed. These were the non-callused ones that remained after three optimum ovules were removed to measure fiber length (data in **c** and Fig. 1e). The fiber on the fixed ovules was relaxed (see the main text) and laid down extended away from the ovule so that both fiber length and ovule cross-sectional area could be measured on the photographs with Fiji. The 'C' and 'F' labels indicate 6 replicates of control and fluridone treatments from 3 trials, not including the optimum ovules measured previously for Fig. 1e. The 20 mm scale bar applies to both panels. **b** Ovule cross-sectional area in control and fluridone-treated cultures showed no significant difference (p=0.059; Mann-Whitney test). **c** Comparison of fiber length with and without fluridone for the optimum ovules (data from Fig. 1e) and others as shown in **a.** Fluridone increased fiber length on the optimum and the other ovules compared to their counterparts in the control cultures. Kruskal Wallis showed a significant difference among all the means ($p < 0.001$), but means with the same letter do not differ significantly (Dunn's test). **d** No relationship was observed between fiber length and ovule area when all the data in **a** were analyzed together. Similarly, no relationship was found when control and fluridone data were analyzed separately in the same way (data not shown)

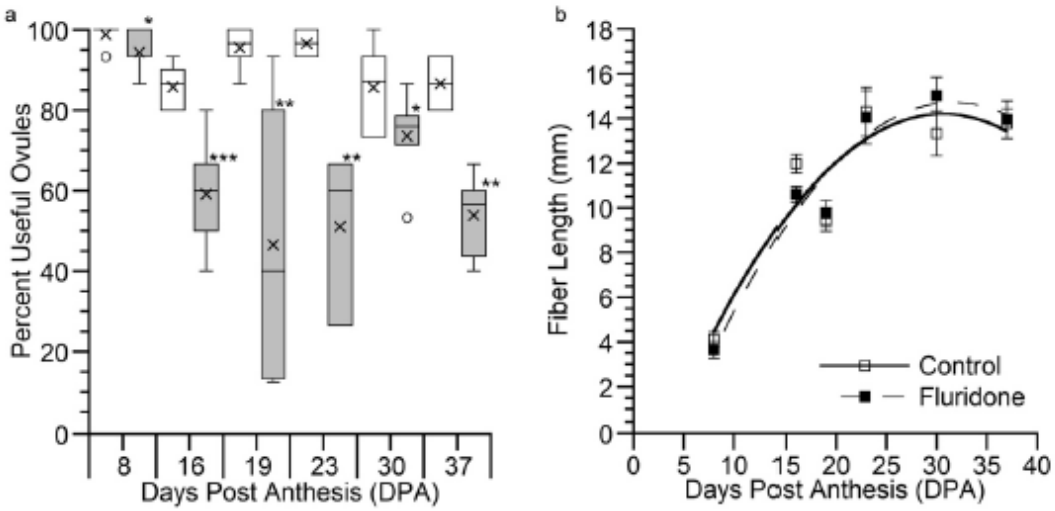

Supplementary Fig. S4 Fluridone had a negative effect on the performance of *Gh* cultured ovules, but no effect on final fiber length on the best-performing ovules in each replicate. **a** On every day analyzed, the percent of useful *Gh* ovules, as assayed visually, was significantly decreased by the addition of 15.2 μM fluridone (grey plots) as compared to untreated controls (white plots). This was correlated with frequent and extensive browning of *Gh* ovules in fluridone (data not shown), which was not commonly observed for *Gb* ovules. **b** Fiber length on optimal control and fluridone-treated *Gh* ovules between 8 - 37 DPA. In **a**, '**x**' denotes the mean and empty circles denote outliers. Each treatment in **a** reflects n= 6-8 vessels (with 14-16 ovules each) from 2-4 trials. The Kruskal Wallis test showed significant differences among the means ($p=0.003$), and the Mann-Whitney U test revealed significantly different means at each DPA: *, $p \leq 0.05$; **, $p \leq 0.01$; and ***, $p \leq 0.001$. In **b**, fiber was measured on each DPA for n=16-56 ovules from the same samples, with the three most vigorous ovules selected from each replicate. Error bars are 95% Confidence Intervals. See Fig. 4 in the main text for statistical analysis of final fiber length in the control. All cultures contained 0.05% (v/v) DMSO

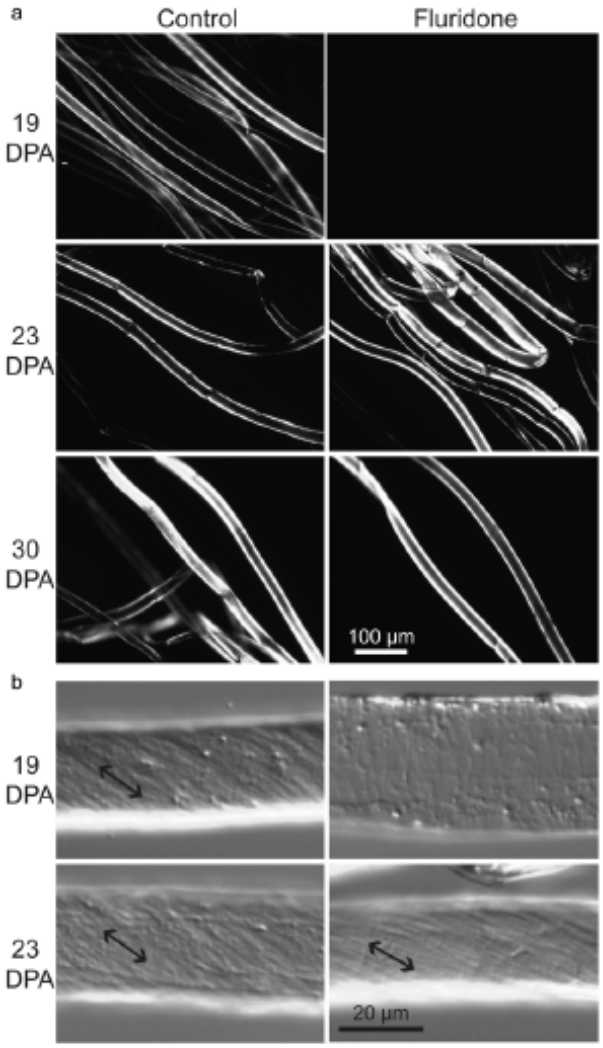

Supplementary Fig. S5 Microscopic analysis of time of onset of secondary wall synthesis in *Gh* fibers cultured without and with fluridone. **a** In polarization microscopy, only the control fibers showed white birefringence of secondary wall cellulose at 19 DPA. Fluridone-treated fibers were birefringent at 23 DPA. Both treated and untreated fibers were highly birefringent at 30 DPA, due to continuing cellulose deposition. (The 30 DPA images were taken with one third of the exposure time used for 19 and 23 DPA.) **b** Differential interference contrast optics revealed the orientation of the helical cellulose microfibrils (highlighted by the double arrow) typical of secondary walls at 19 DPA in the control. To the contrary, helical microfibrils were not observed until 23 DPA in fluridone-treated *Gh* fibers. Images are representative of two independent trials. The 100 μm or 20 μm scale bars apply to all the images in panel **a** or **b**, respectively

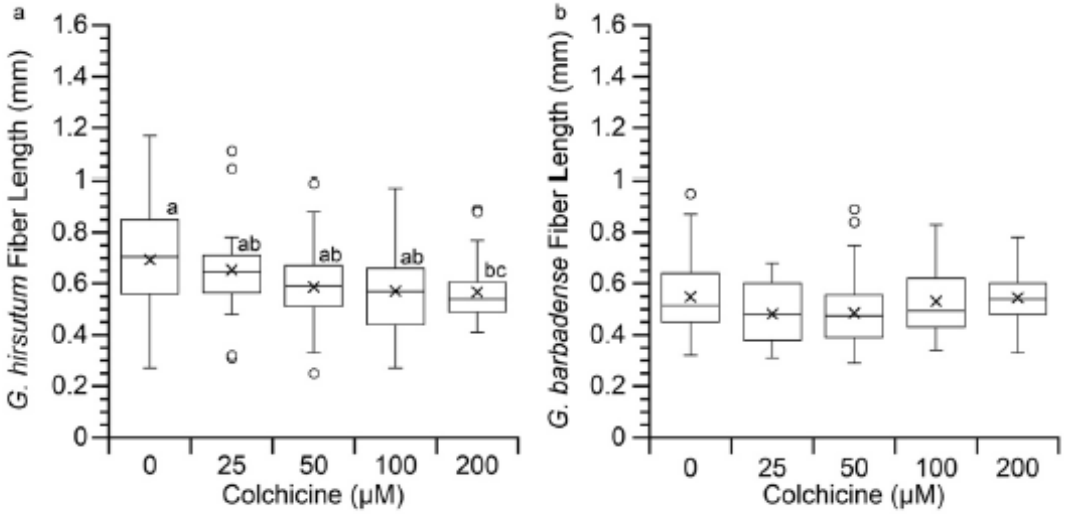

Supplementary Fig. S6 Comparison of *Gh* and *Gb* fiber length at 4 DPA with and without colchicine treatment at 2 DPA. In **a**, treatment with 200 μM colchicine caused a 16.9% decrease in *Gh* fiber length compared to the control [p=0.01; ANOVA, $F_{(4,160)}$=3.28]. In **b**, no significant differences were observed in the length of *Gb* fibers. Box plot labeling is like Suppl. Fig. S2. In **a**, means with common letter do not differ significantly, as determined by Tukey's HSD test. The chalazal fiber length was measured on different ovules, n=16-51 or n=18-42 for *Gh* or *Gb*, respectively, collected from 6-13 repetitions within 3-6 trials. The control and 50 μM treatment were most extensively replicated

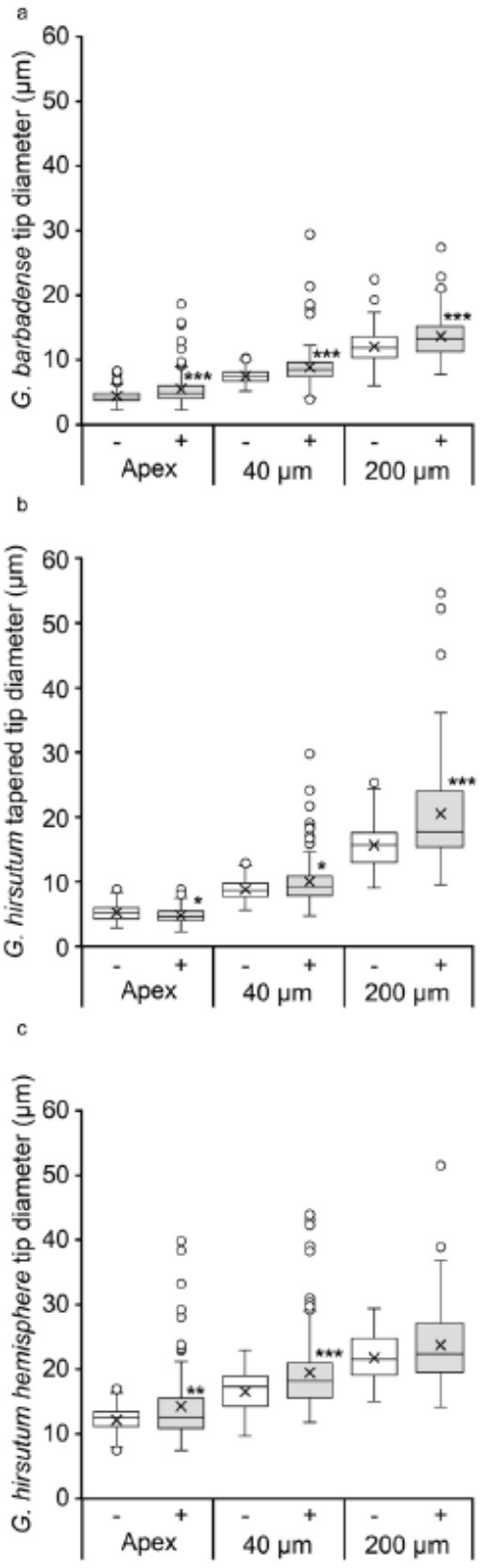

Supplementary Fig. S7 The effect of colchicine on three different cotton fiber tip types. These box plots illustrate the data in main text Table 1, and the control values (white plots) are also graphed together in Fig. 5b of the main text. Ovules were cultured at 2 DPA and optionally treated with 50 μm colchicine (grey plots), then measured at 4 DPA. For each tip type, pairwise comparisons of control and treated tip diameters were made for three measurement locations: the apex and 40 μm and 200 μm back from the apex. Apical diameter was defined by its diameter of curvature, or the diameter of the circle fitting within the apex. **a** *Gb* fiber tips: Colchicine-treated fibers are swollen at each location, with the greatest increase occurring at the apex (20.76% increase in mean apical diameter). **b** *Gh tapered* fiber tips: Colchicine-treated fibers are changed at each location, with the greatest (31.29%) increase in diameter occurring at 200 μm and uniquely decreasing diameter at the apex (8.71% decrease in mean apical diameter). **c** *Gh hemisphere* fiber tips: Colchicine-treated fibers swelled at the apex (17.66% increase in mean apical diameter) and at 40 μm (17.73% increase in mean diameter). Box plot labeling is like Suppl. Fig. S2. Replication information is in main text Table 1. Asterisks indicate significant differences for pairwise comparisons at each measured location, as shown in Suppl. Fig. S4. See Materials and Methods in the main text for details of statistical analysis

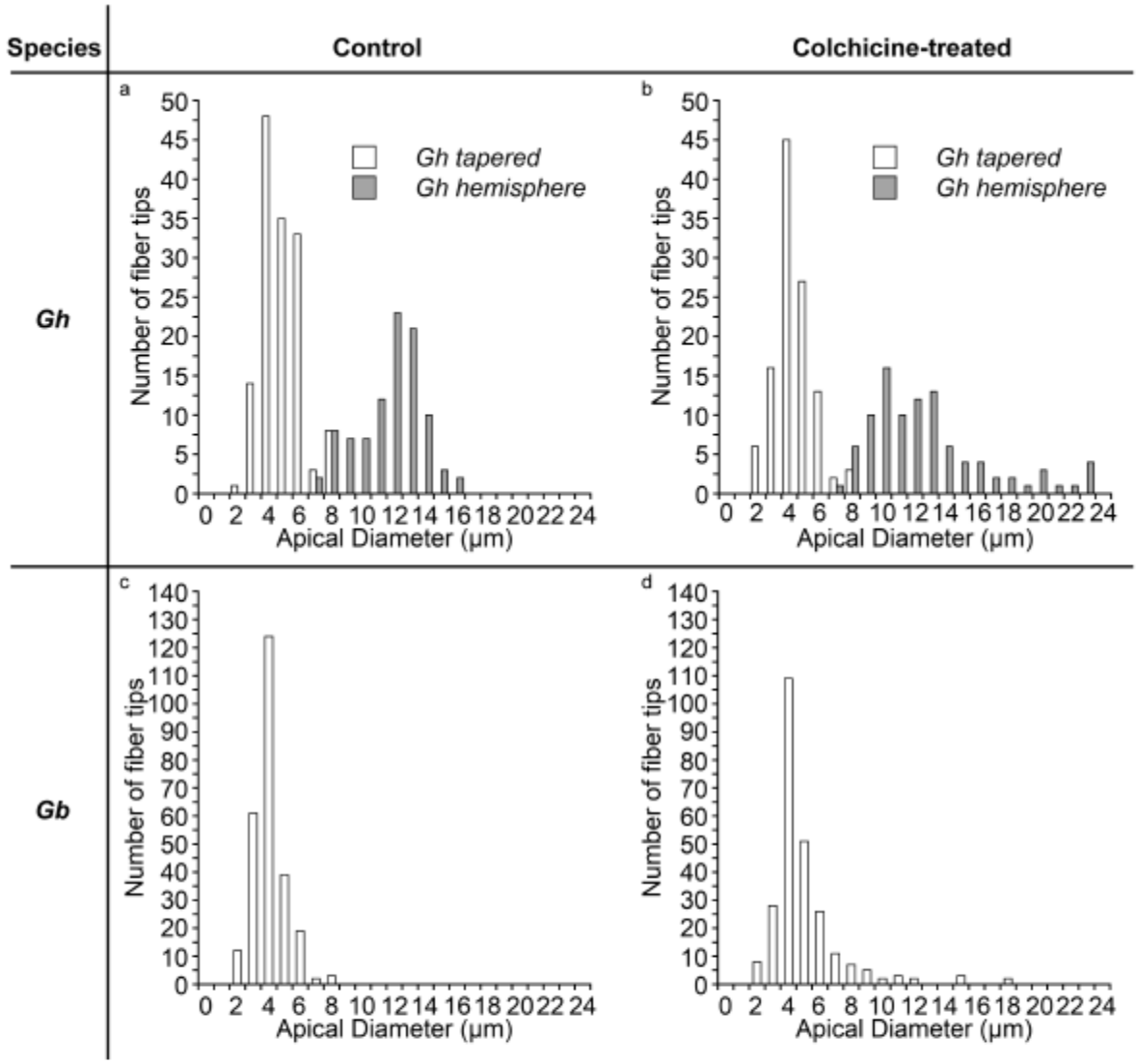

Supplementary Figure S8. Distribution of apical diameters in 4 DPA *G. hirsutum* (*Gh*) and *G. barbadense* (*Gb*) fiber tips with and without 50 µm colchicine added at 2 DPA. The diameter of the apex was defined by its diameter of curvature. **a, b** *Gh* data. **a** Control *Gh* fiber tips had a biomodal distribution reflecting *tapered* and *hemisphere* tip types, confirming prior results. **b** In colchicine, the two sub-populations persisted, but the peak around 12 µm in *Gh hemisphere* tips disappeared. Some colchicine-treated tips had larger apical diameters as compared to controls. (Values for five even larger *Gh hemisphere* tips are not shown.) **c, d** *Gb* data. (**c**) As before, control *Gb* fiber tips were in a single class with 4-5 µm peak apical diameter. **d** Colchicine increased the number of larger-diameter *Gb* tips. Replication information: **a** *Gh* control, 3 trials, 6 replications, n=240 (145 *tapered*, 95 *hemisphere*); **b** *Gh* colchicine-treated, 3 trials, 6 replications, n=213 (112 *tapered*, 101 *hemisphere*); **c** *Gb* control, 3 trials, 7 replications, n=260; and **d** *Gb* colchicine-treated, 3 trials, 7 replications, n=257

CHAPTER 3

Cotton Fiber Tip Shape is Dependent upon Temporal and Spatial Regulation of Microtubules

This chapter is written in the style of a journal paper, but data displays will be reduced before submission. I collected or supervised the collection of all the data in this chapter, then performed the statistical analysis, graphing, and preparation of images and diagrams. I mentored two undergraduate students who assisted with data collection and/or analysis (Anne Pajerski and Robin Grant Moore). JJ Shen assisted in refinement of the microtubule immunofluorescence protocol.

Abstract

Cotton fibers are single cells that elongate from the seed epidermis of *Gossypium* species. The details of cellular morphogenesis determine the fiber quality traits that affect the value and uses of the fiber, such as length, strength, and diameter. Lower and more consistent diameter would increase the competitiveness of cotton fiber with synthetic fiber, but we do not know how this trait is controlled. We showed that the fiber tip is a region of both control and variability in diameter, which differs between three tip types in the two commercially grown cotton species. To further understand the control of cotton fiber diameter, we used ovule cultures, morphology measurements, and immunofluorescence of microtubules to observe the effects of microtubule antagonists (colchicine, oryzalin, and Taxol) on fiber shape and diameter within 80 µm of the apex. The treatments were applied for 48 hours, beginning at either 1 or 2 days post-anthesis (DPA), reflecting different stages in early fiber development. Our results show that inhibiting the presence and/or dynamic activity of microtubules typically causes larger diameter tips to form, with greater effects most often observed with earlier treatment. Nuanced differences in the responses of three tip types, considering the apex and the distal regions, reflect fine control of mechanisms of cell expansion in closely spaced regions of one cell without correlation with tip diameter or species. How temporally and spatially controlled dynamic microtubule arrays impact tip shape and diameter during early cotton fiber morphogenesis will be discussed.

Introduction

The cotton fiber is a unique and commercially valuable plant cell that is cultivated worldwide for the production of renewable textiles. *Gossypium hirsutum* (*Gh*) and *G. barbadense* (*Gb*) are responsible for nearly 95% of the cotton fiber cultivated today. *Gossypium hirsutum* grows well in more locations and has a higher yield, resulting in its use for ~90% of the worldwide cotton fiber, while *Gb* is responsible for ~6% even though it produces higher quality fiber that is valued for the production of premium textiles (Constable et al., 2015). Cotton fibers initiate their development as isodiametric protrusions from the ovule surface on or near the day of anthesis. Within 24 hours anisotropic growth ensues and the earliest stage of elongation begins (Stewart, 1975). Elongation and primary cell wall synthesis can continue for several weeks. Between 16-20 DPA (days post anthesis) fiber cells transition from elongation to secondary cell wall synthesis. The thickening of the cell wall will continue until maturity is reached, when the cell dies and collapses, around 50 DPA (Stiff & Haigler, 2012).

Complexity in our understanding of fiber diameter was revealed by the characterization of two fiber tip types in *Gh* cv Deltapine90, termed *Gh tapered* (narrow, pointed) and *Gh hemisphere* (broad, blunt) tips, whereas only narrow one tip type exists in *Gb* cv. Phytogen 800. These two tip types in *Gh* were initially characterized based on morphological appearance and apical diameter at 10 µm behind the apex (Stiff & Haigler, 2016) and later shown to be mainly discriminated by the diameter of curvature of the apex (DOC) (Pierce et al., 2019). The average apical diameter of *Gb* at 4 DPA is 4.2 µm which is similar to *Gh tapered* fibers (5.5 µm). However, *Gh hemisphere* fibers, which comprise about half the fibers on an ovule, have a mean apical diameter of 11.8 µm. The mature *Gh* fiber finally has a larger average diameter (16.8 µm) than the mature *Gb* fiber (14.8 µm) (Avci et al., 2013), with the narrower (finer) fiber being preferred for high-quality textiles (Naylor et al., 2014). Despite the potential benefits of reducing *Gh* fiber diameter, this trait has not yet been improved by breeding (Dr. Kater Hake, personal communication).

To support the future production of more economical high-quality *Gh* cotton fiber, we need to understand the cellular controls of fiber diameter. Curiously, how fiber diameter is set in any plant cell is relatively unknown. The pointed tips of *Arabidopsis* trichome branches are best characterized so far, as previously discussed in Chapter 1. The cause of the differences in cotton fiber diameter, within and between the *Gh* and *Gb* species, is unknown. Moreover, recent work

showed that cotton fibers develop in a manner that is not yet well characterized and warrants further investigation. Tinopal staining of young cotton fiber showed that new cell wall material was being synthesized at the apex of 5 DPA cotton fibers (Stiff & Haigler, 2016). Seagull (1995) observed high concentrations of secretory vesicles and cellulose microfibril deposition within 3 µm of the fiber apex consistent with apical cell wall synthesis. Other researchers have found evidence of tip focused calcium gradients in cotton fiber, a feature associated with tip growth (Huang et al., 2008). A microtubule-depleted zone (MDZ), characterized as important for apically-biased diffuse growth in *Arabidopsis* trichome branches, has also been reported in young cotton fiber (US 2016/0230180 A1, 2016; Yanagisawa et al., 2018; Yu et al., 2019). Combined, these observations indicate that cotton fibers may elongate in a manner not completely consistent with diffuse growth.

Our prior work, with the addition of colchicine at 2 DPA followed by measurement at 4 DPA, showed that tip shape was dependent on microtubules, but differences were observed in the response between the tip types and between locations measured (apex, 40µm, and 200 µm) within a tip type. The results also were consistent with microtubule-dependent tip shaping occurring earlier than 2 DPA (Pierce et al., 2019). Here we further explore the temporal and cellular controls of *Gh* and *Gb* cotton fiber diameter. Changes in the shape of the cotton fiber tips were determined after another microtubule inhibitor (oryzalin) and a microtubule stabilizer (Taxol) were added to cultured cotton ovules at 1 and 2 DPA. Indirect immunofluorescence was used to reveal the organization of the microtubule array in young cotton fibers between 1 and 4 DPA, to further characterize a potential MDZ, and to analyze the potential relationship between its perimeter and the size of the apex. The results demonstrate a stronger role of a dynamic microtubule array in controlling tip shape and fiber diameter early in cotton fiber morphogenesis and a strong, yet transient, relationship between the MDZ and apex shape in *Gh tapered* fibers.

Results

Early cotton fiber diameter

To investigate the control of cotton fiber diameter, we first expanded our understanding of the morphology of the cotton fiber tip early in development. The size of the fiber apex was quantified by measuring the diameter of curvature (DOC), or the diameter of a perfect circle that fits within the apex. The apical diameter was used as an indicator of *Gh* fiber tip type.

Histograms of the *Gh* apical DOCs showed a bimodal distribution corresponding to *tapered* and *hemisphere* tips. The two distributions are separated by a minimum of 9 µm, which was used as a demarcator between the two *Gh* fiber tip types. Overlaying the DOC distribution of *Gb* fiber tips shows that they most resemble the *Gh tapered* tips (Fig. 1a). Although both *Gb* and *Gh tapered* tips are narrow relative to *Gh hemisphere* tips, all three tip types had different shapes (Fig. 1b).

The rate of fiber elongation increases daily, from ~5 µm/hr at 2 DPA to ~30 µm/hr by 5 DPA, in both species (Fig. 2). During this time, cotton fibers elongate to around 1 mm in length while refining the shape of the apex in both species (Fig. 3). By 1 DPA, a transverse microtubule array has formed in fibers exhibiting a variety of morphological differences, likely representing developmental stages. Distal from the chalazal end of the ovule, short fiber cells resembling fiber initials are present in both *Gb* and *Gh* (Fig. 4a & 4d). As the fibers begin to elongate more rapidly, the apical diameter is also reduced. This results in substantial tip tapering in some fibers of *Gh* (Fig. 4b). Other fibers of *Gh*, and all fibers of *Gb*, do not undergo as much tapering at this time (Fig. 4b & 4e). At 1 DPA, the most developed *Gh tapered* fibers have established the characteristic taper associated with later time points (Fig. 4c). Substantial tapering was not observed in fibers of *Gb* at 1 DPA (Fig. 4f) even though they achieve a large reduction in apical diameter by 2 DPA (Fig. 3b). In *Gb*, the apical diameter increases slightly between 3 and 4 DPA while the apical diameter is stable in both *Gh* fiber tip types during the same time period (Fig. 5). Between 1 and 2 DPA, the narrowing of the fiber apex occurs, resulting in the appearance of the two dissimilar tip types in *Gh*. While *Gh hemisphere* fibers do undergo a reduction in the size of their apex, *Gh tapered* and *Gb* fibers exhibit a much sharper decline in apical diameter by 2 DPA (Fig. 5).

Importance of the state of the microtubule array during elongation differs by species

The microtubule antagonist, colchicine, has been shown to disrupt fiber elongation when treated during initiation, resulting in spherical fiber initials (Tiwari & Wilkins, 1995). When treated with colchicine (200 µM) or oryzalin (1.5 µM) after elongation has begun at 2 DPA, fibers of *Gh* were reduced in length by 17% and 40% respectively. Inhibitor concentrations that resulted in fiber swelling, but did not completely inhibit elongation were chosen for further examination. (Fig. 6d & 6e). Stabilization of microtubules with Taxol (10 µM) did not reduce fiber length in *Gh*, but did in *Gb* fibers by 28% (Fig. 6c). The microtubule inhibitors had no

effect on *Gb* fiber length indicating a mechanism of elongation that does not depend on microtubules, similar to observations from tip growing cells (Fig 6a & 6b).

The microtubule array at the cotton fiber tip

By 2 DPA, the fibers of *Gh* refine their apices to achieve a mixed population of *tapered* and *hemisphere* fibers (Fig. 7b & 7c). During this time, the transverse microtubule array was apparent in all tip types; although, many microtubules were observed at variable angles and lengths. By 3 DPA, the microtubule array consisted of primarily transversely oriented cortical microtubules (Fig. 7d -7f). The arrangement of microtubules within the first 80 µm from the apex was examined at 4 DPA to establish a baseline for comparisons to fiber cells treated with microtubule antagonists (Fig. 7g - 7i).

Using immunofluorescence, changes in the microtubule patterning of cotton fibers, treated at 2 DPA with microtubule antagonists for 48 hours, were documented to establish a link between changes in microtubule organization and cell morphology. In the majority of colchicine treated cells no microtubules were visible, while a small disorganized population of microtubules remained after oryzalin treatment (Fig. 7j -7o). Taxol treatment resulted in fiber cells with regions of closely aligned microtubules that often differed in overall orientation from adjacent regions of aligned microtubules within the same cell. Discrete increases in cell diameter often coincided with regions of microtubules aligned at varying angles relative to the longitudinal axis of the fiber (Fig. 7p -7r). Cell morphology changes resulting from the three treatments were considered to be a result of an absence of microtubules (colchicine), a weak microtubule network (oryzalin), or a present but static and misaligned microtubule network (Taxol).

Proximity of the microtubule array to the fiber apex varies over time

The apex of the elongating fiber cells often had a small region within the apical dome where microtubules could not be detected. The microtubule-free area at the apex of 4 DPA cotton fibers appeared transient since randomly oriented microtubules could be observed traversing the apical dome of *Gb* and *Gh hemisphere* tips (Fig. 8). An extreme example of this is seen in 4 DPA *Gh tapered* fibers, where the transverse microtubule array was observed at 20 µm from the apex.

The discrete microtubule zonation observed in cotton fibers sometimes appears similar to the MDZ described for leaf trichome branches. This special region is maintained throughout branch development, and its perimeter correlates with apical dome size (Yanagisawa et al., 2015). A patent application also suggested that a similar process may occur in cotton fiber, as evidenced by an immunofluorescence image of microtubules that highlighted a MDZ in one cotton fiber tip at 1 DPA (Szymanski DB, US 2016/0230180 A1, 2016). Although a MDZ was clearly observed in similar 1 DPA *Gh* and *Gb* fibers (about 10 µm DOC) in the research reported here, no strong relationship between the apical dome size and MDZ perimeter was detected during this early stage of polar elongation (Fig. 9). However, in the earliest stages of tip tapering in 1 DPA *Gh* fibers, there was a strong relationship between the two parameters ($R^2 = 0.73$). A much weaker relationship was observed in 1 DPA fibers of *Gb* ($R^2 = 0.33$), which did not appear to taper as much as *Gh* fibers during the same time frame (Fig. 10). At this developmental stage, either 88% or 68% of the *Gb* or *Gh tapered* fiber tips, respectively, exhibited a clear MDZ at the apex. Both apical diameter and MDZ perimeter in *Gh tapered* tips often clustered around 4-6 µm, but about a third of the tips measured exhibited either a larger MDZ, DOC, or both (Fig.10d). When analyzed alone, the 4-6 µm cluster produced a weaker relationship ($R^2 = 0.57$; not shown), indicating that the overall variability in *Gh tapered* fiber tip size contributes to the relationship between MDZ perimeter size and apical diameter. On *Gh* ovules, many fibers did not show any signs of tapering at 1 DPA. These could be fibers that had not reached that developmental stage or, more likely, *Gh hemisphere* fibers, as many of them were similar in length to the *tapered* fiber tips that were measured. The untapered 1 DPA *Gh* fiber tips typically had microtubules traversing the apical dome in multiple directions with only 7% of those imaged exhibiting a clear MDZ, which resulted in their exclusion from the quantitative analysis at 1 DPA. The relationship between MDZ perimeter and apical diameter was transient as based on low R^2 values for 2 DPA *Gb* ($R^2 = 0.06$) and *Gh tapered* ($R^2 = 0.08$) fiber tips (Fig. 11).

Microtubules are involved in tip tapering in Gh

Treatment with each of the microtubule antagonists at 1 DPA caused a marked increase in the percentage of *Gh hemisphere* tips at 3 DPA (62-67% versus 38% in controls; Fig 12a). To the contrary, the percentage of *hemisphere* tips remained similar after treatment (41-46%) as compared to the controls (45%) following treatment at 2 DPA (Fig. 12b). The distribution of

apical diameters typically used to identify different tip types was also disrupted when treated with microtubule antagonists at 1 DPA. Treatment of *Gb* with colchicine and Taxol resulted in shifting of the center of the distribution of apical diameters towards a larger diameter (Fig. 13a & 13d). Treating at 2 DPA did not have as large an impact on the overall distribution in *Gb*, but did cause it to skew towards larger apical diameters (Fig. 14a & 14d). No major shifts in the distribution of apical diameters were observed in *Gh tapered* fibers regardless of treatment time or type (Fig. 13d - 13f; Fig. 14d - 14f). The apical diameter of *Gh hemisphere* fibers was most effected by colchicine and Taxol treatment. While Taxol tended to shift the overall distribution towards a larger apical diameter, colchicine treatment caused strong skewing of the distribution towards larger diameters at both time points (Fig 13g - 13i; Fig. 14g - 14i). This was due to exceptionally large apical diameters being observed in colchicine treated *Gh hemisphere* fibers with some reaching 38-40 µm wide when treated at either 1 or 2 DPA (Fig. 13g; Fig 14g). Swelling and/or bulging was clearly evident in some fibers after colchicine and Taxol treatments, whereas visual effects of oryzalin were often relatively less apparent (Fig. 15).

Zonal and temporal regulation by microtubules by tip type and species

Due to the amount of morphology data collected, and the many potential comparisons that could be made, the same data are represented in three different ways to highlight different aspects of the effects observed. The most detailed representation is shown in tabular form (Tables 1-6) which provides mean, median, and percent change results for all three fiber tip types after treatment with microtubule antagonists at 1 and 2 DPA. The percent change in fiber diameter after 48 hour microtubule antagonist treatment was also overlaid on to-scale diagrams of the fiber tips to make the differential effects of the drug treatment, tip type, and time point more readily apparent (Fig. 16 & 18). Boxplots of the data were also prepared to better illustrate the range of fiber diameters observed before and after microtubule disruption (Fig. 17 & 19).

After colchicine or Taxol treatment, cotton fiber tip diameters showed a larger range compared to the controls, inclusive of more frequent outliers, particularly in the distal regions. The greatest (+77%) percent increase in diameter occurred at the apex of Taxol treated *Gb* tips. Their apical diameter also increased substantially in colchicine (+39%) when treated at 1 DPA (Tables 1 & 3; Fig. 16). In contrast, the *Gh tapered* tips were less dependent on microtubules, as illustrated by the lack of effect on apical diameter after colchicine treatment at 3 and 4 DPA

(Tables 1 & 4; Fig. 16 & 18; Fig. 17d & 19d). Interestingly, *Gh tapered* tips actually shrank in Taxol by either -9 or -14% when measured at 3 and 4 DPA respectively (Tables 3 & 6). At 3 DPA, *Gh hemisphere* tips showed colchicine-induced swelling at the apex (+28%) and in the distal regions up through 80 µm (+43%), with only +20-23% increase in diameter observed at all locations in Taxol (Fig. 17g & 17i; Tables 1 & 3).

For colchicine treatment, the least swelling that was still significant was observed at 40 µm and 80 µm in 3 DPA *Gb* tips (+11%; Table 2). For Taxol treatment, the least swelling that was still significant was observed at 20 µm in 3 DPA *Gh tapered* tips (+18%; Table 3). In summary, at 3 DPA, *Gb* relies strongly on dynamic microtubules to limit the diameter of the apex and distal regions. The apical diameter of *Gh tapered* tips is less dependent on microtubules, whereas their distal diameters are limited by microtubules. *Gh hemisphere* tips show a consistent dependence on microtubules throughout their length at 3 DPA.

Oryzalin had no effect on the diameter of *Gb* fiber tips, but caused diametric expansion at 80 µm from the apex in both *Gh* fiber tip types at 3 DPA (Table 2; Fig. 17b, 17e, & 17h). This effect was similar to that of colchicine for *Gh tapered* tip types, but not for *Gh hemisphere* tips. Oryzalin can often leave a smaller disorganized population of microtubules intact within the fiber cell while colchicine typically removes all traces of microtubules. This difference may be the cause for the different response from *Gh hemisphere* fiber tips to the two drugs. This would suggest that even a disrupted microtubule array may be sufficient for maintaining the tip diameter of *Gh hemisphere* cells, while complete abolishment with colchicine or stabilization with Taxol, results in reduced control of diametric expansion. The analysis also showed that Taxol treatment caused the largest percent increases in diametric expansion behind the apex in all three tip types at 3 DPA (Table 3; Fig. 16; Fig. 17c, 17f, & 17i).

At 4 DPA, *Gb* fiber tips did not exhibit any apical expansion after Taxol treatment, although all locations behind the apex showed expansion ranging from 28-42% (Table 6; Fig. 18; Fig 19c). At the same time point, the apex of *Gh tapered* fiber tips shrank nearly 15% while expanding behind the apex to +40-45% of their original size (Table 6; Fig. 18; Fig 19f). Taxol resulted in significant ($p<0.01$) swelling in *Gh hemisphere* fibers at 40 and 80 µm form the apex (Table 6; Fig. 18; Fig. 19i).

Dynamic role of microtubules over time

To provide insight into how or if the role of microtubules changed during early cotton fiber development, changes in diameter resulting from microtubule antagonist treatment were analyzed as percent changes. These values were used for assessing the magnitude of the drug-dependent effect in 3 DPA fiber tips. The magnitude of the changes in 3 DPA fiber was then compared to the magnitude of change in 4 DPA fiber tips, using percent change for each fiber tip type and location.

In *Gb* fiber tips, a significantly larger increase of apical diameter was observed for both colchicine ($p<0.05$) and Taxol ($p<0.001$) treated groups at 3 DPA compared to 4 DPA (Fig. 20a & 20c). The trend of colchicine-induced diametric expansion behind the apex was similar when comparing the two time points. Taxol caused more swelling at all measured locations in *Gb* tips when compared to 4 DPA. The most dramatic difference between the two time points was at the apex, where no increase was seen at 4 DPA but a large increase was observed at 3 DPA (Fig. 20c). The larger increase in diameter in 3 DPA *Gb* fiber tips, as a result of Taxol treatment, suggests that the rearrangement of the microtubule array is critical for controlling tip shape and diameter at this stage of *Gb* fiber development. Oryzalin treatment did not result in increased diameter at either time point in *Gb* fiber tips (Fig. 17b, 19b, & 20b). The large Taxol-induced swelling observed at the apex of *Gb* tips treated at 1 DPA, not observed after treatment at 2 DPA, is consistent with a lesser requirement for dynamic microtubules at the apex by 2 DPA.

The *Gh tapered* apex showed a similar response to microtubule antagonists added at either 1 or 2 DPA, either not changing or shrinking slightly in both colchicine and Taxol. Behind the apex, more swelling was observed upon treatment with colchicine at 1 DPA for *Gh tapered* tips, whereas the most swelling was induced by treatment with Taxol at 2 DPA (Fig. 20d & 20f). Disruption of microtubules resulted in a smaller apical diameter for each drug treatment and DPA with the exception of oryzalin treatment in 3 DPA fiber tips which exhibited only a minimal increase. Oryzalin-treated *Gh tapered* tips showed similar trends of swelling behind the apex at 3 and 4 DPA, with the impact on fiber diameter being significantly ($p<0.001$) greater at 3 DPA at the apex (Fig. 20e).

The *Gh hemisphere* fibers exhibited substantial swelling behind the apex when treated with colchicine at either 1 or 2 DPA. However, the swelling was significantly greater at 40 and 80 μm ($p<0.001$) in fibers treated at 1 DPA (Fig. 20g). This indicates that microtubules may be

more important for constraining fiber diameter distal from the apex earlier on in development. The magnitude of the oryzalin effect in 4 DPA *Gh hemisphere* fiber tips increased with distance from the apex. The effect of oryzalin was similar at 3 and 4 DPA at all locations.

Interestingly, with the exception of the apical diameter of *Gh hemisphere* fibers, Taxol caused greater diametric expansion at 4 DPA of both fiber tip types of *Gh*. With the exception of the apical diameter of *Gh tapered* fiber tips, colchicine caused a greater increase in diameter at all locations in both *Gh* fiber tip types at 3 DPA. The *Gh tapered* tip apex did follow the same trend at 3 and 4 DPA after colchicine treatment, with the DOC decreasing slightly at 4 DPA.

Discussion

The recent advent of the culture system for *Gb* ovules is an ideal tool for direct comparisons between two economically important crop species. Initial comparisons using colchicine provided insight into the differences in shape regulation of three fiber tip types found in the two species (Pierce et al., 2019). Here, I firmly established that each fiber tip type has a distinct shape that is highly related to the mature fiber diameter. I also demonstrated that the microtubule regulation of tip shape and fiber diameter in young cotton fibers varies by tips type, species, and time of development. All three tip types possessed transverse microtubule arrays indicative of anisotropic diffuse growth. However, the varying distance of the microtubule array from the apex of *Gh tapered* tips indicates some variation in how apical diameter is regulated between two tip types found adjacent to one another on ovules of *Gh*. I demonstrated that microtubule inhibition did not disrupt fiber elongation in *Gb*. This result is consistent with what has been reported in root hairs and pollen tubes, both of which are tip growing cells (Park et al., 2011; Wu & Bezanilla, 2018). This supports the idea that cotton fibers develop using a mixed growth mode including diffuse and apically-biased cell wall synthesis, at least early in development.

This idea is further supported when comparing how the different pharmacological antagonists affected the different fiber tip types. It should be noted that single fibers were not measured over time, meaning conclusions regarding morphological changes are inferred from the average shape of independent samples collected for each time period. Colchicine treatment resulted in swollen fibers in *Gb* at 3 and 4 DPA with the largest percent increases being at the apex. This suggests that microtubules are playing a critical role in modulating the tip shape of

young *Gb* fibers. This observation is in stark contrast to the lack of colchicine-induced swelling in *Gh tapered* tip apices at either time point (Tables 1 & 4). This supports different methods of apical cell wall synthesis between fiber tip types that are the most similar morphologically, *Gb* and *Gh tapered*. Part of the difference between *Gb* and *Gh* fiber tip types may be due to the use of different α-tubulin orthologues. Oryzalin resistance can be conferred by alternate amino acid residues present in the oryzalin binding domain of α-tubulin (Ma et al., 2007). It is not known if this is the case with *Gb* fiber cells, but it is one plausible factor.

The lack of swelling at the *Gh tapered* apex at both time points may also indicate a shifting of zonal importance with regard to microtubule-mediated cell wall reinforcement. This shows that, at least in *Gh tapered* tips, microtubules may primarily contribute to diffuse growth behind the apex while tip refinement relies on another mechanism, such as actin-mediated secretion. This differs in *Gh hemisphere* tips, where each location swelled by 3 DPA when treated with colchicine or Taxol (Fig. 16; Fig. 17g & 17i) but only the 20 and 40 µm locations swelled at 4 DPA (Fig. 18; Fig. 19g & 19i). This supports a shifting role for microtubules over time, where tip shape relies more on microtubules earlier in development, but then shifts to a primary role behind the apex.

Differences in 3 and 4 DPA apical diameter were also observed in oryzalin treated *Gh tapered* fiber tips (Fig. 20e). The oryzalin effect was greater at 80 µm for 4 DPA fibers than in 3 DPA fibers. No differences were detected in the intermediate 20 and 40 µm locations. When treated with Taxol, the effect at the apex was similar for both time points with minor shrinking occurring (Fig. 20f). However, behind the apex, the 4 DPA treated tips swelled significantly more than the 3 DPA fiber tips, an opposite effect when compared to the microtubule destabilizer colchicine (Fig. 20d).

Taxol treatment often led to the greatest increase in diameter (Tables 3 & 6). This indicates that microtubule rearrangement may be more necessary as the fiber transitions from early tip remodeling and polar elongation (1-3 DPA) to a higher rate of elongation with limited tip refinement (2-4 DPA). Taken together, these data indicate that microtubules play a role in apical remodeling in the 1-3 DPA time frame, but they are likely to contribute relatively less to this role later in time.

The apical diameter of *Gh hemisphere* fiber tips is affected by disruption of the microtubules when treated with colchicine or Taxol, which suggests that tip development is

much more microtubule-dependent than in *Gh tapered* fibers. Microtubule disruption with colchicine in *Gh hemisphere* fiber tips had a greater effect when treated at 1 DPA compared to 2 DPA (Fig. 20g). In *Gh hemisphere* fibers, microtubule antagonist treatment caused similar trends at both time points. The effect of colchicine was greater behind the apex at 3 DPA, but the trend was similar. Taxol and oryzalin treated fibers showed very similar increases in diameter at all locations at both time points. This supports a growth mode in *Gh hemisphere* fibers where spatial regulation of development is more consistent over time than in the other two fiber tip types (Fig. 20).

These comparisons of the diameter control of three tip types from two *Gossypium* species have shown that cotton fiber tip diameter is influenced by variable microtubule regulation. Both *Gb* and *Gh hemisphere* fiber tips have transverse microtubule arrays that can consistently be observed within 5 µm of the apex at 4 DPA. This apical population of microtubules may play a critical role in stabilizing the diameter through cell wall modifications as new wall material is deposited at the apex. The colchicine-induced expansion in *Gh tapered* fibers behind the apex is consistent with the larger distance from the apex within which the intact transverse microtubule array may occur in this tip type. This indicates that cell wall modification, or deposition, is independent of the microtubule array close to the apex in *Gh tapered* tips.

A microtubule organization similar to what was observed here in cotton fibers has been previously described in *Arabidopsis* trichome branches. The authors identified a linear relationship between the shape of the apex and the perimeter of the MDZ in developing trichome branches and suggested that a similar relationship may exist in cotton fiber tips (Yanagisawa et al., 2015, 2018). This same assertion was made in a patent outlining potential methods for influencing cell wall properties by modifying actin-mediated processes involved in cell shape control (US 2016/0230180 A1, 2016). The patent used an image of a 1 DPA *Gh* cotton fiber with a transverse microtubule array and a clearly defined MDZ as the basis for the claim that cotton fibers and trichome branches may develop in a similar fashion. This conception was further supported when Yu and colleagues (2019) showed an MDZ at the apex of 2 DPA *G. hirsutum* fibers, which appeared to be the *tapered* type with a small DOC around 5 µm. In both instances, the cotton fibers were examined without considering more than one fiber tip morphology in *Gh* and no comparison was made to *Gb*.

These prior results prompted our investigation into any relationship between the tip geometry and microtubule zonation in cotton fiber. To interpret the results, keep in mind the asynchrony of fiber development on one ovule: at any one time, fibers may be in different developmental stages and the stages must be interpreted by morphology and not time alone. At the early stage of polar elongation, I observed a MDZ in 1 DPA *Gh* and *Gb* tips, but there was no quantitative relationship between its perimeter and the apical diameter. I found a strong linear relationship between these two parameters in more developed 1 DPA *Gh tapered* tips. A much weaker relationship was observed in 1 DPA *Gb* fiber tips at the onset of tip tapering, which began at a later time than what occurred in *Gh*. Future experiments can address whether *Gb* tips show a stronger relationship in the middle of the night prior to the morning of 2 DPA. After the tip shape was established (by 2 DPA), there was again no strong relationship between the two parameters.

In summary, there is a short window of time during the tip tapering process in *Gh* when a linear relationship between the MDZ perimeter and apical diameter exists, similarly to what has been reported for *Arabidopsis* trichome branches observed with live cell imaging. Interestingly, the *Gh tapered* tips with the strongest relationship had values for MDZ and apical diameter in the 3 – 12 µm range (median values around 4.8 µm), whereas the *Arabidopsis* trichome branches had a 1 – 12 µm range (median values around 3 µm). Note that these cotton fiber diameters are likely underestimated by about 30% due to the shrinking that occurred during immunofluorescence processing. The lower values in the trichome branches reflect them ultimately becoming pointed and sharp, whereas cotton fibers tips do not narrow that extensively. These parallels are important because, although the fates of trichome branches and cotton fibers are very different, they may share some regulatory processes critical for shape determination. Differences in microtubule organization influence the shape and therefore, the usefulness of the cotton fiber. Understanding what causes the differences between the patterning of the microtubule array in cotton fibers and other associated cellular players will potentially lead to a greater ability to produce more versatile textile products from a renewable resource as well as further our understanding of plant cell morphogenesis.

Materials and Methods

Plant growth, ovule culture, and fiber measurements

Plants were grown and ovules were cultured as described previously, including the addition of 15.2 µm fluridone to improve fiber elongation on *Gb* cultured ovules (Pierce et al., 2019). The drug stocks included 2 mM oryzalin in DMSO, 100 mM colchicine in water, and 2 mM paclitaxel (Taxol) in DMSO. After testing a concentration series in each case, the concentrations used for most experiments were 50 µM colchicine, 1.5 µM oryzalin, or 2.5 µM Taxol. The length of chalazal fibers on whole ovules imaged under a dissecting scope was measured. As described before (Pierce et al., 2019), the FIJI image processing package (Schindelin et al. 2012) was used to measure the DOC of the apex and the tip diameter at 20 µm, 40 µm and 80 µm behind the apex. Only the most well-developed fibers from the chalazal end of the ovule were selected for imaging and subsequent measuring. Less developed fibers nearer the micropylar end sometimes swelled more extensively, but were not measured (data not shown). Control and treated *Gh* fibers with < 6 µm or > 10 µm apical diameter were classified as *tapered* or *hemisphere*, respectively, which was consistent with a visual inspection. Between these values, *Gh* tips were visually inspected and most were consistent with the assignment using a 9 µm demarcator between tips types: a few others were reassigned to the alternative tip type before final data analysis. Treated fibers with substantially swollen apices but no visual tip tapering were classified as *hemisphere* type. A few treated *Gh* fibers were not measured because they had such aberrant apical morphology that it was impossible to classify their tip type. However, there were <3 of these in any data set presented (i.e. for any one tip type x treatment x location).

Immunofluorescence observations were made on control or treated chalazal fibers harvested and fixed between 9 – 10 am for each DPA examined. The one exception was for the tapering *Gb* tips in Fig. 9, these were harvested and fixed the evening of 1 DPA, at 9-10 pm, to try and find *Gb* fibers that more closely matched the degree of tapering observed in the *Gh* fibers. The DOC was measured as previously described. The MDZ perimeter was measured using the freehand line tool in FIJI as described for Arabidopsis trichome branches (Yanagisawa et al., 2015). The outline of the fiber apex was traced from the first point where microtubule signal was detected on one side of the cell to the equivalent point on the opposite side. Fibers were measured at several time-points in order to capture distinct morphological changes between 1 and 2 DPA. About 30% shrinkage of fiber tips was observed after processing for

immunofluorescence (compare mean apical diameters in Fig. 3 to those in Figs. 9, 10, 11). Therefore, the numerical demarcator was not used to classify tip types in immunofluorescence images. Instead, *Gh tapered* tips were visually identified by an isodiametric zone at the apex with a diameter smaller than occurred below the apex, with others classed as *hemisphere*. *Gb* tips were measured similarly even though they did not show obvious signs of tip tapering at the same time. The shrinking effect prevents direct comparisons of diameter values of fibers fixed for light microscope imaging and those prepared for immunofluorescence.

Microtubule Immunofluorescence

Microtubule detection via indirect immunofluorescence was performed mainly as previously described (Pierce et al., 2019) with some modifications. The fiber penetration with antibody was enhanced by performing the pectinase step at a lower pH (5.0). The microtubule stabilization buffer was amended to include MES instead of PIPES buffer to maintain the lower pH. Pectinase activity and microtubule staining were also improved by incubating at 30°C as opposed to room temperature. Fibers at 1 and 2 DPA produced more intense cytoplasmic background signal when fixed with only 1% glutaraldehyde. To overcome this, 4% formaldehyde with 0.1% glutaraldehyde was used as a fixative. Fixation with either glutaraldehyde exclusively, or a mix of formaldehyde and glutaraldehyde, did not produce any noticeable difference in microtubule structural preservation.

Confocal microscopy

Fibers were imaged by laser scanning confocal microscopy (488 nm excitation; 490 nm barrier; 570 nm emission) or with Airyscan (420-480 nm excitation; 495-550 nm emission) (Zeiss 880; C-Apochromatic 40x/1.2 W Korr FCS M27 objective). Zen 2.3 software was used for image capture and processing. Z-stacks were captured with 0.22 or 0.46 µm step size, for standard or Airyscan imaging, respectively, then displayed as maximum Z-projections. Signal detection was optimized through manipulation of laser power and/or exposure time, and fluorescence intensity was normalized by background subtraction for each image.

Graphing and statistical analysis

Graphs were made in KaleidaGraph (Synergy Software, Reading, PA). In box plots, any outliers (empty circles) were automatically identified by the software. Statistical analysis was done with Excel supplemented with the Real Statistics Resource Pack software (Zaiontz, 2019). When diameter measurements showed a normal distribution and equal variance, means were compared using ANOVA with Bonferroni correction followed by Tukey's HSD test to assign groups. When these assumptions were not met, the diameter measurements were log-transformed (LOG10) and tested via the non-parametric group-wise Welch's test with Bonferroni correction (McDonald, 2014). Pairwise comparisons were carried out using the Games-Howell test. Significant differences were then associated with the corresponding untransformed data depicted in the figures.

Table 1. Median and mean diameters at three locations for three types of control (-Col) or colchicine-treated (+Col) fiber tips at 3 DPA.

Tip types		apex			20 µm			40 µm			80 µm		
		-Col (µm)	+Col (µm)	% change	-Col (µm)	+Col (µm)	% change	-Col (µm)	+Col (µm)	% change	-Col (µm)	+Col (µm)	% change
Gb	Median	2.87	4.30	50	6.94	7.77	12	8.50	8.89	5	10.87	11.31	4
	Mean	2.97	4.14 [c]	39	6.99	8.51 [c]	22	8.58	9.51 [b]	11	10.90	12.06 [a]	11
	STD	1.06	1.65		0.93	2.94		1.24	2.75		1.61	3.80	
Gh tapered	Median	5.73	5.73	0	9.07	13.06	44	10.98	13.62	24	14.11	17.54	24
	Mean	5.65	5.72	1	9.11	15.16 [c]	66	11.03	16.14 [c]	46	14.01	20.29 [c]	45
	STD	1.50	1.29		1.52	7.58		1.89	7.55		2.80	7.93	
Gh hemis-phere	Median	12.04	13.47	12	15.82	21.53	36	17.86	23.59	32	20.20	26.83	33
	Mean	12.21	15.67 [c]	28	15.81	22.97 [c]	45	17.92	25.96 [c]	45	20.56	29.49 [c]	43
	STD	2.49	7.00		2.52	7.97		2.85	9.17		3.02	10.45	

Superscript letters indicate significant differences between the means (with standard deviation, STD) for +Col compared to -Col for each tip type and location: [a], $p \leq 0.05$; [b], $p \leq 0.01$; and [c], $p \leq 0.001$. Measurements were taken from fibers cultured in 6 replications over 3 trials for *Gh* and 4 replications over 2 trials for *Gb*. The number of fibers measured within the same trials were: for *Gh tapered* and *Gh hemisphere*, n=77-148; and for *Gb*, n=140-210.

Table 2. Median and mean diameters at three locations for three types of control (-Ory) or oryzalin-treated (+Ory) fiber tips at 3 DPA.

Tip types		apex			20 µm			40 µm			80 µm		
		-Ory (µm)	+Ory (µm)	% change	-Ory (µm)	+Ory (µm)	% change	-Ory (µm)	+Ory (µm)	% change	-Ory (µm)	+Ory (µm)	% change
Gb	Median	2.87	2.58	-10	6.94	6.83	-2	8.50	8.31	-2	10.87	10.53	-3
	Mean	2.97	2.84	-5	6.99	6.97	0	8.58	8.55	0	10.90	10.70	-2
	STD	1.06	0.86		0.93	0.98		1.24	1.34		1.61	1.61	
Gh tapered	Median	5.73	6.02	5	9.07	9.35	3	10.98	11.06	1	14.11	15.72	11
	Mean	5.65	6.28 [a]	11	9.11	9.72	7	11.03	11.70	6	14.01	16.27 [b]	16
	STD	1.50	1.42		1.52	1.73		1.89	2.30		2.80	5.82	
Gh Hemis-phere	Median	12.04	12.32	2	15.82	16.65	5	17.86	19.25	8	20.20	23.58	17
	Mean	12.21	12.85	5	15.81	16.73	6	17.92	19.65	10	20.56	24.24 [c]	18
	STD	2.49	3.15		2.52	3.96		2.85	4.77		3.02	7.43	

Superscript letters indicate significant differences between the means (with standard deviation, STD) for +Ory compared to -Ory for each tip type and location: [a], $p \leq 0.05$; [b], $p \leq 0.01$; and [c], $p \leq 0.001$. Measurements were taken from fibers cultured in 6 replications over 3 trials for *Gh* and 4 replications over 2 trials for *Gb*. The number of fibers measured within the same trials were: for *Gh tapered* and *Gh hemisphere*, n=91-148; and for *Gb*, n=160-210.

Table 3. Median and mean diameters at three locations for three types of control (-Tax) or Taxol-treated (+Tax) fiber tips at 3 DPA.

Tip types		apex			20 µm			40 µm			80 µm		
		-Tax (µm)	+Tax (µm)	% change	-Tax (µm)	+Tax (µm)	% change	-Tax (µm)	+Tax (µm)	% change	-Tax (µm)	+Tax (µm)	% change
Gb	Median	2.87	5.16	80	6.94	9.86	42	8.50	12.32	45	10.87	15.28	41
	Mean	2.97	5.26 [c]	77	6.99	11.06 [c]	58	8.58	13.64 [c]	59	10.90	17.08 [c]	57
	STD	1.06	2.09		0.93	3.49		1.24	4.85		1.61	6.00	
Gh tapered	Median	5.73	5.02	-12	9.07	10.13	12	10.98	11.99	9	14.11	16.26	15
	Mean	5.65	5.12	-9	9.11	10.74 [b]	18	11.03	13.28 [c]	20	14.01	17.44 [c]	24
	STD	1.50	1.59		1.52	3.63		1.89	4.67		2.80	5.34	
Gh Hemis-phere	Median	12.04	14.90	24	15.82	18.98	20	17.86	20.79	16	20.20	23.51	16
	Mean	12.21	14.93 [c]	22	15.81	19.37 [c]	23	17.92	21.69 [c]	21	20.56	24.57 [c]	20
	STD	2.49	3.49		2.52	4.29		2.85	5.60		3.02	5.62	

Superscript letters indicate significant differences between the means (with standard deviation, STD) for +Tax compared to -Tax for each tip type and location: [a], $p \leq 0.05$; [b], $p \leq 0.01$; and [c], $p \leq 0.001$. Measurements were taken from fibers cultured in 6 replications over 3 trials for *Gh* and 4 replications over 2 trials for *Gb*. The number of fibers measured within the same trials were: for *Gh tapered* and *Gh hemisphere*, n=78-152; and for *Gb*, n=129-210.

Table 4. Median and mean diameters at three locations for three types of control (-Col) or colchicine-treated (+Col) fiber tips at 4 DPA.

		apex			20 µm			40 µm			80 µm		
Tip type		-Col (µm)	+Col (µm)	% change	-Col (µm)	+Col (µm)	% change	-Col (µm)	+Col (µm)	% change	-Col (µm)	+Col (µm)	% change
Gb	Median	4.30	4.87	13.26	6.35	7.22	13.70	7.14	7.91	10.78	8.61	9.80	13.82
	Mean	4.48	5.41 [c]	20.76	6.46	7.88 [c]	21.96	7.26	8.37 [c]	15.29	8.87	10.20 [c]	14.96
	STD	1.00	2.36		0.82	2.90		1.05	2.36		1.62	3.11	
Gh tapered	Median	5.16	4.59	-11.05	7.47	7.68	2.74	8.70	9.29	6.78	11.08	11.49	3.66
	Mean	5.28	4.82	-8.71	7.52	8.40	11.73	8.81	10.08	14.42	11.01	12.64 [b]	14.74
	STD	1.31	1.22		1.33	3.60		1.52	3.76		2.14	4.03	
Gh hemi-sphere	Median	12.61	12.61	0	15.29	17.54	14.72	17.30	18.19	5.14	18.72	19.49	4.11
	Mean	12.17	14.32	17.66	14.75	19.22 [c]	30.25	16.58	19.52 [b]	17.73	18.54	20.44	10.24
	STD	2.02	5.91		2.42	6.91		2.86	6.46		3.10	5.37	

Superscript letters indicate significant differences between the means (with standard deviation, STD) for +Col compared to -Col for each tip type and location: [a], $p \leq 0.05$; [b], $p \leq 0.01$; and [c], $p \leq 0.001$. The n values for each mean were: 257-260 for *Gb*; 114-145 for *Gh tapered*; and 95-99 for *Gh hemisphere*, as sampled from 7 replicates within 3 trials.

Table 5. Median and mean diameters at three locations for three types of control (-Ory) or oryzalin-treated (+Ory) fiber tips at 4 DPA.

		apex			20 µm			40 µm			80 µm		
Tip type		- Ory (µm)	+ Ory (µm)	% change	- Ory (µm)	+ Ory (µm)	% change	- Ory (µm)	+ Ory (µm)	% change	- Ory (µm)	+ Ory (µm)	% change
Gb	Median	4.30	4.01	-6.74	7.23	7.47	3.39	8.87	9.02	1.75	11.12	11.41	2.56
	Mean	4.29	4.08	-4.97	7.37	7.54	2.33	8.95	9.02	0.80	11.23	11.29	0.49
	STD	0.83	0.96		0.73	1.03		1.09	1.40		1.66	2.26	
Gh tapered	Median	6.02	5.73	-4.82	9.08	8.94	-1.54	10.45	11.16	6.79	12.40	14.81	19.36
	Mean	6.09	5.65	-7.22	9.19	9.63	4.76	10.57	12.05 [b]	14.00	12.56	16.64 [c]	32.53
	STD	1.53	1.49		1.55	2.95		1.81	3.61		2.25	8.04	
Gh hemi-sphere	Median	11.75	11.46	-2.47	14.57	15.51	6.42	15.92	18.05	13.38	18.52	21.83	17.87
	Mean	11.75	11.56	-1.61	14.62	15.84 [a]	8.37	16.21	18.67 [c]	15.18	18.52	22.81 [c]	23.50
	STD	2.11	2.60		2.67	2.95		2.99	4.81		3.36	7.91	

Superscript letters indicate significant differences between the means (with standard deviation, STD) for +Ory compared to -Ory for each tip type and location: [a], $p \leq 0.05$; [b], $p \leq 0.01$; and [c], $p \leq 0.001$. The n values for each mean were: 120 for *Gb*; 106-142 for *Gh tapered*; and 98-134 for *Gh hemisphere*, as sampled from 3 (for *Gb*) to 6 replicates within 3 trials.

Table 6. Median and mean diameters at three locations for three types of control (-Tax) or Taxol-treated (+Tax) fiber tips at 4 DPA.

		apex			20 µm			40 µm			80 µm		
Tip type		- Tax (µm)	+ Tax (µm)	% change	- Tax (µm)	+ Tax (µm)	% change	- Tax (µm)	+ Tax (µm)	% change	- Tax (µm)	+ Tax (µm)	% change
Gb	Median	3.73	3.73	0	6.36	8.02	27.67	7.58	10.01	23.06	9.39	11.24	19.70
	Mean	3.81	3.86	1.40	6.40	8.90 [c]	38.89	7.67	10.94 [c]	42.74	9.49	12.17 [c]	28.25
	STD	0.89	1.32		0.89	2.78		1.10	3.66		1.51	3.73	
Gh tapered	Median	5.16	4.30	-16.67	6.91	8.62	24.75	8.29	11.25	35.79	10.21	13.20	27.35
	Mean	5.36	4.57 [c]	-14.69	7.33	10.22 [c]	39.50	8.49	12.39 [c]	45.87	10.29	14.70 [c]	42.85
	STD	1.46	1.38		1.59	5.02		1.89	5.10		2.27	6.16	
Gh hemi-sphere	Median	11.18	13.18	17.89	13.58	17.08	25.77	14.84	18.51	24.73	16.88	19.67	16.53
	Mean	11.46	13.52	17.80	13.77	17.50 [c]	27.05	15.12	19.40 [b]	28.31	17.18	21.15	23.09
	STD	1.93	4.12		2.18	4.97		2.63	6.60		2.82	7.70	

Superscript letters indicate significant differences between the means (with standard deviation, STD) for +Tax compared to -Tax for each tip type and location: [a], $p \leq 0.05$; [b], $p \leq 0.01$; and [c], $p \leq 0.001$. The n values for each mean were: 155-229 for *Gb*; 115-142 for *Gh tapered*; and 87-97 for *Gh hemisphere*, as sampled from 6 replicates within 3 trials.

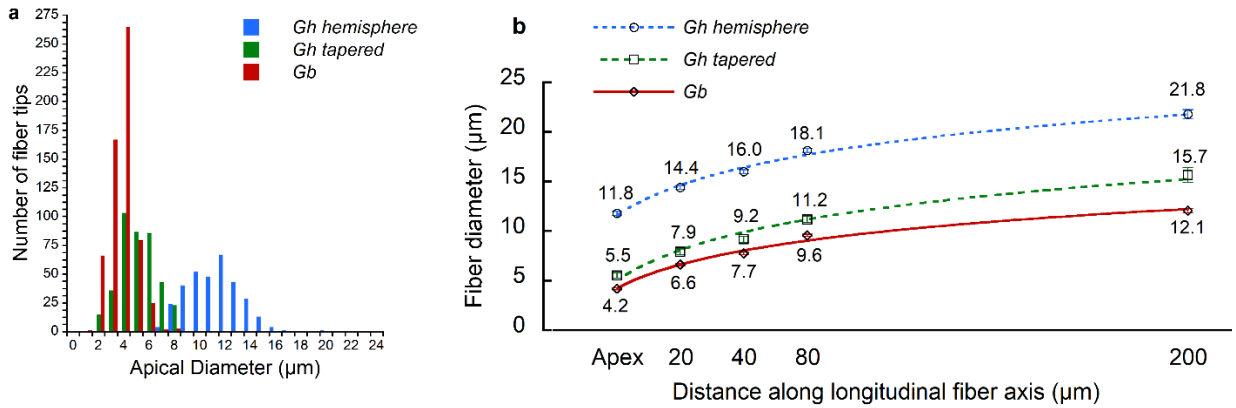

Figure 1. Three fiber tip populations within two cotton species are recognized by their tip shape and diameter at 4 DPA. **a** Frequency distribution of apical diameters of *Gh tapered* (green), *Gh hemisphere* (blue), and *Gb* (red). **b** Average apical diameter, as measured by the diameter of curvature, and average fiber diameter at 20, 40, and 80 µm. Measurements were made on fibers of ovules cultured at 2 DPA. Data for the apex, 40 µm, and 200 µm are repeated from Pierce et al., 2019. Error bars are 95% confidence intervals. Measurements at each location were different between all three tip types ($p < 0.001$).

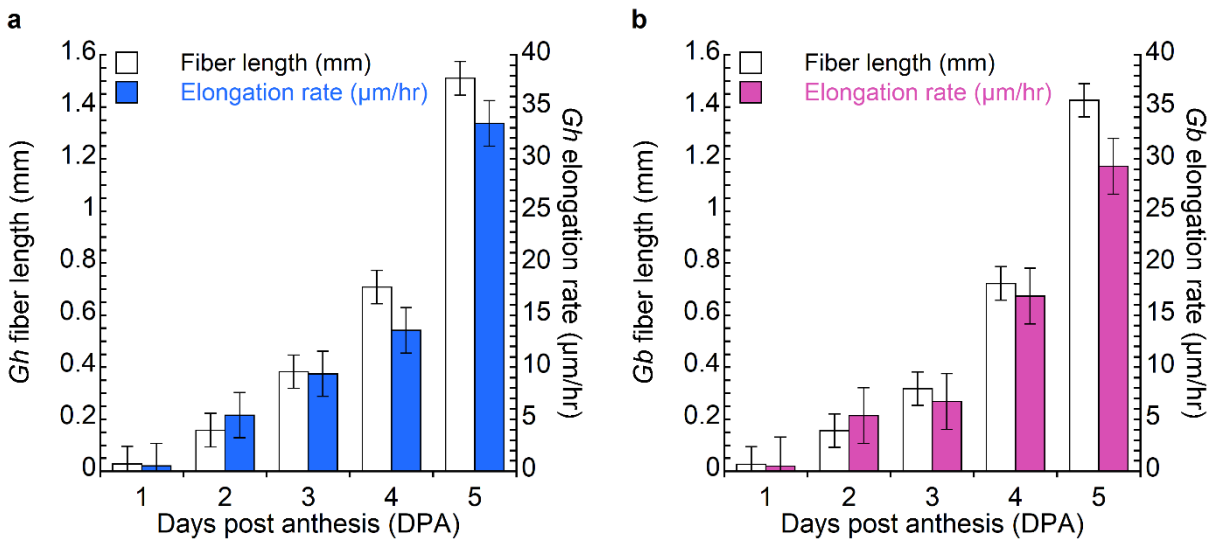

Figure 2. Mean *in planta* fiber lengths and elongation rates. **a**, *Gh* and **b**, *Gb* from 1 DPA through 5 DPA. The rate of elongation increases along with fiber length during this period of development in both species. n = 27-30 measurements per group. Error bars are 95% confidence intervals.

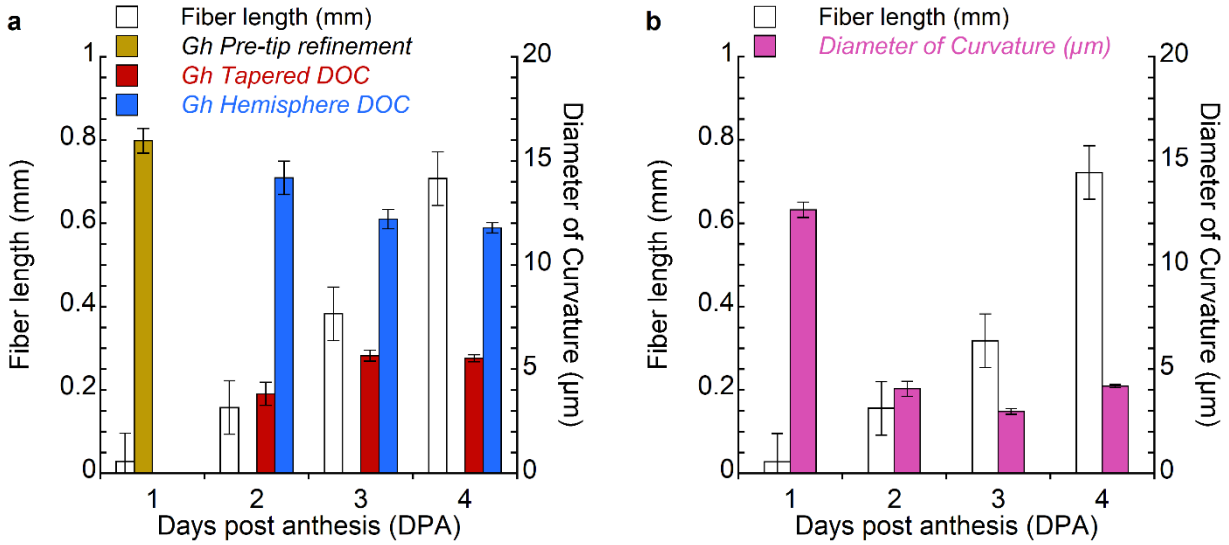

Figure 3. Mean *in planta* fiber length and diameter of curvature (DOC) at the apex over time. **a**, For *Gh*, the DOC at 1 DPA is inclusive of all fibers prior to any tip tapering (called the torpedo stage). **b**, For *Gb*, tip tapering also occurs between 1 and 2 DPA, following a similar trend to *Gh tapered* tips. The DOC for *Gh* and *Gb* at 1 DPA are significantly different from one another according to ANOVA ($F_{(1, 58)} = 4.01$, $p < 0.001$). For fiber length, n = 27-30 for all groups. For DOC, n = 30-35 for 1-2 DPA, 91-210 for 3 DPA, and 326-609 for 4 DPA. Error bars are 95% confidence intervals. Fibers were measured from ovules harvested at the same time of day.

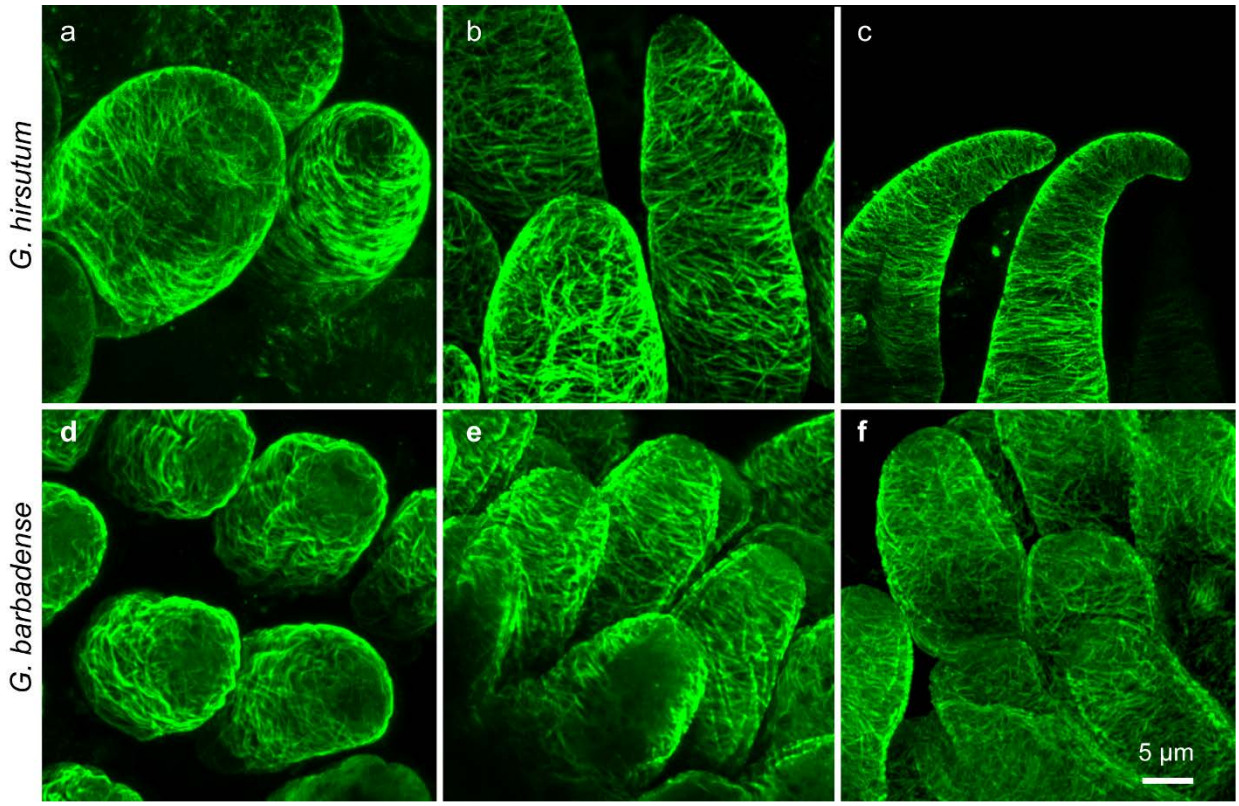

Figure 4. Indirect immunofluorescence of 1 DPA cotton fibers of *G. hirsutum* and *G. barbadense* using an α-tubulin antibody. **a-c**, Fiber cells of *G. hirsutum* through can be seen in stages that represent **a**, the beginning of elongation, **b**, early tip refinement, and, **c**, tip tapering. **d-f**, *Gossypium barbadense* cells progress through similar stages but more closely resemble fibers of *Gh* that do not taper at this time.

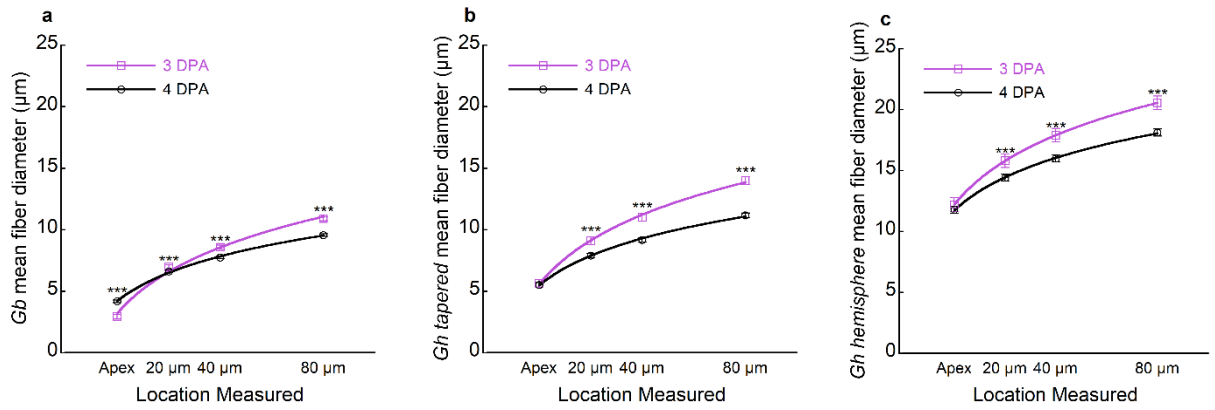

Figure 5. Change in diameter of three fiber tip types between 3 and 4 DPA *in vitro*. Mean diameters for *Gb* tips, *Gh tapered* tips, and *Gh hemisphere* tips are shown for 3 DPA (magenta lines) and 4 DPA (black lines). **a,** The *Gb* tips showed the least overall change between 3 and 4 DPA, although significant narrowing at 4 DPA occurred at 20 - 80 µm. (The effect at 20 µm was minimal). The apical diameter of *Gb* tips uniquely increased between 3 and 4 DPA. **b** and **c,** The apical diameters were indistinguishable at 3 and 4 DPA in both *Gh* tip types, but both the *Gh tapered* and *Gh hemisphere* tips narrowed behind the apex after 3 DPA. For 3 DPA tips, n = 91, 148, or 210 for *Gh hemisphere*, *Gh tapered*, or *Gb* tips, respectively. For 4 DPA tips, n = 326, 393, or 609 for *Gh hemisphere*, *Gh tapered*, or *Gb* tips, respectively. Asterisks indicate significant differences between paired measurement groups for one location and tip type as determined by the Games-Howell test: *, $p \leq 0.05$; **, $p \leq 0.01$; and ***, $p \leq 0.001$. Error bars are 95% confidence intervals.

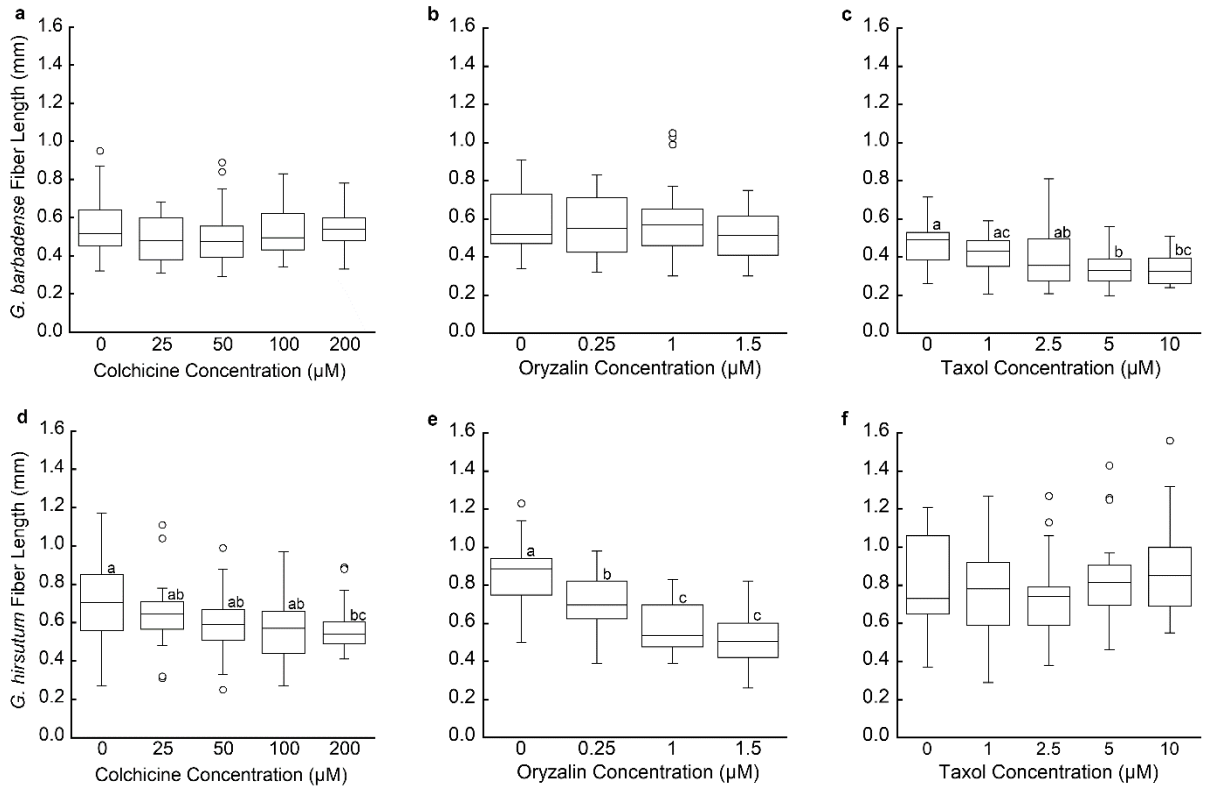

Figure 6. Fiber length for *Gb* and *Gh* ovules treated with microtubule antagonists from 2-4 DPA. Panel labels indicate: **a, b, c** *Gb;* **d, e, f** *Gh;* **a, d** colchicine; **b, e** oryzalin; and **c, f** taxol. Only the microtubule stabilizer taxol reduced fiber length in *Gb (*ANOVA, $F(4, 160) = 3.28$, $p = 0.01$). Inhibitors of microtubule polymerization, colchicine and oryzalin, reduced length in *Gh:* for colchicine (ANOVA, $F(4, 160) = 3.28$, $p < 0.001$) or for oryzalin (ANOVA, $F(3, 92) = 25$, $p < 0.001$). Groups with a common letter do not differ significantly as determined by Tukey's HSD test.

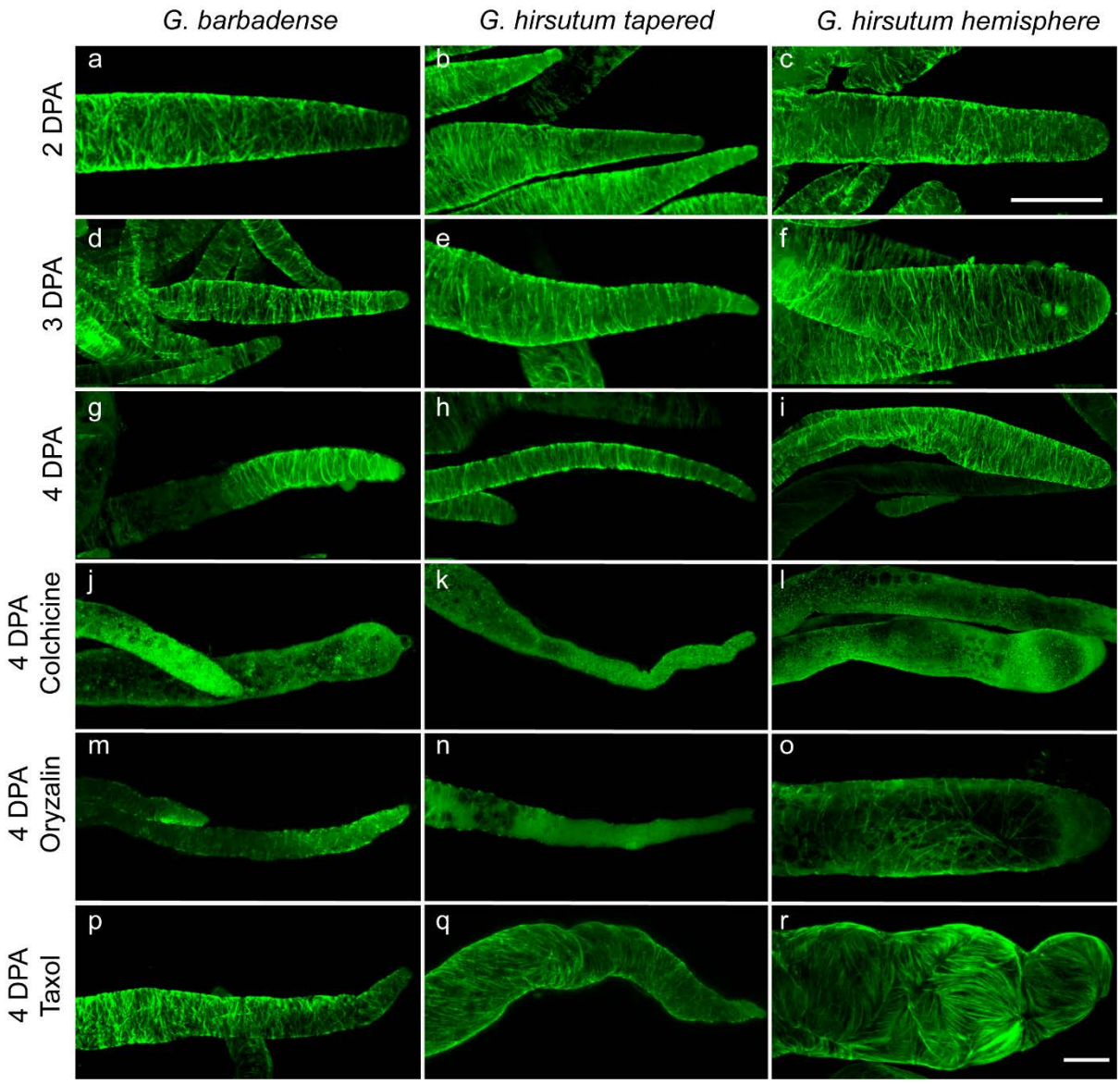

Figure 7. Indirect immunofluorescence using an α-tubulin antibody in the tip of three types of cotton fibers with and without treatment with microtubule antagonists. The three tip types; *Gb*, *Gh tapered*, and *Gh hemisphere* are shown in the left, middle and right columns respectively. Each fiber tip type is shown at the different time-points: **a-c,** 2 DPA, **d-f,** 3 DPA, and **g-i,** 4 DPA. The bottom rows show 4 DPA fibers treated with **j-i,** colchicine, **m-o,** oryzalin, or **p-r,** Taxol. The 2 DPA tips are from *in planta* fibers at the time of culture, whereas 3 and 4 DPA tips are from cultured fibers. To facilitate comparisons, the images for control and colchicine-treated tips at 4 DPA are repeated from a prior publication (Pierce et al., 2019). The images for 2-3, and 4 DPA fibers come from 2 or 3 trials, respectively, and each image displayed is representative of a group of 25 - 30 images. The scale bar (10 µm) in the top right applies to panels **a-c**, the scale bar (10 µm) in the bottom right applies to panels **d-r**.

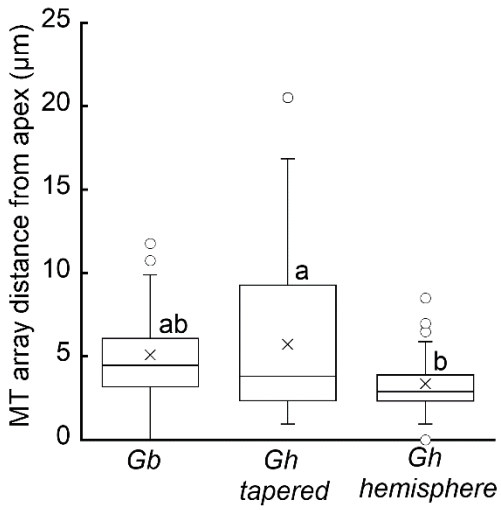

Figure 8. Distance of the transverse microtubule array from the apex of three tip types at 4 DPA. The microtubules in the *Gh hemisphere* fibers were on average closer to the apex as compared to *Gh tapered*. *Gh tapered* tips had a larger range of microtubule distance from the apex than any other tip type. The mean values for both *Gh* tips were not significantly different than the *Gb* tips. n=25-52 fibers of each tip type. Means with a common letter do not differ significantly, as determined by Welch's ANOVA ($F_{(2,75)} = 5.84$; $p = 0.005$) followed by the Games-Howell test.

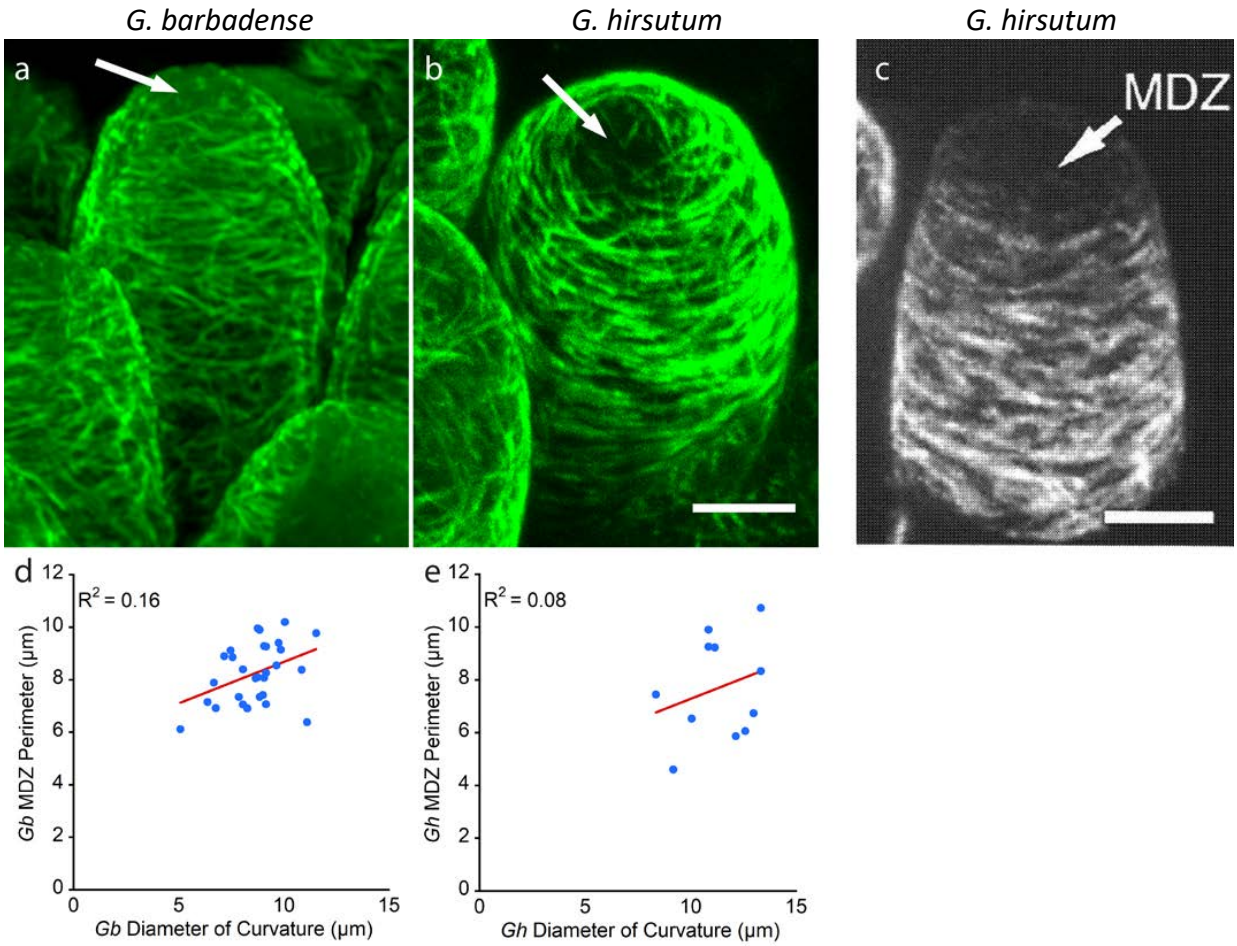

Figure 9. A microtubule depleted zone (MDZ) develops at the apex of cotton fibers as they transition from initiation to polar elongation. **a, b, c** Immunofluorescence images of fibers during early-stage polar elongation (1 DPA). **a,** *Gb* fiber showing the MDZ (arrow) with transverse MTs below the apex. **b,** *Gh* fiber showing a MDZ (arrow) and a predominantly transverse arrangement of MTs. **c,** An image of a *Gh* fiber with a MDZ (arrow) included in a patent application (US 2016/0230180 A1, 2016). **d, e,** Linear regression analysis and calculation of R^2 values showed that MDZ perimeter explained only 16% or 8% of the variance in apical diameter for *Gb* (**d**) or *Gh* (**e),** respectively, during the first phase of polar elongation. n = 29 (*Gb*) and 11 (*Gh*). Scale bar = 5 µm.

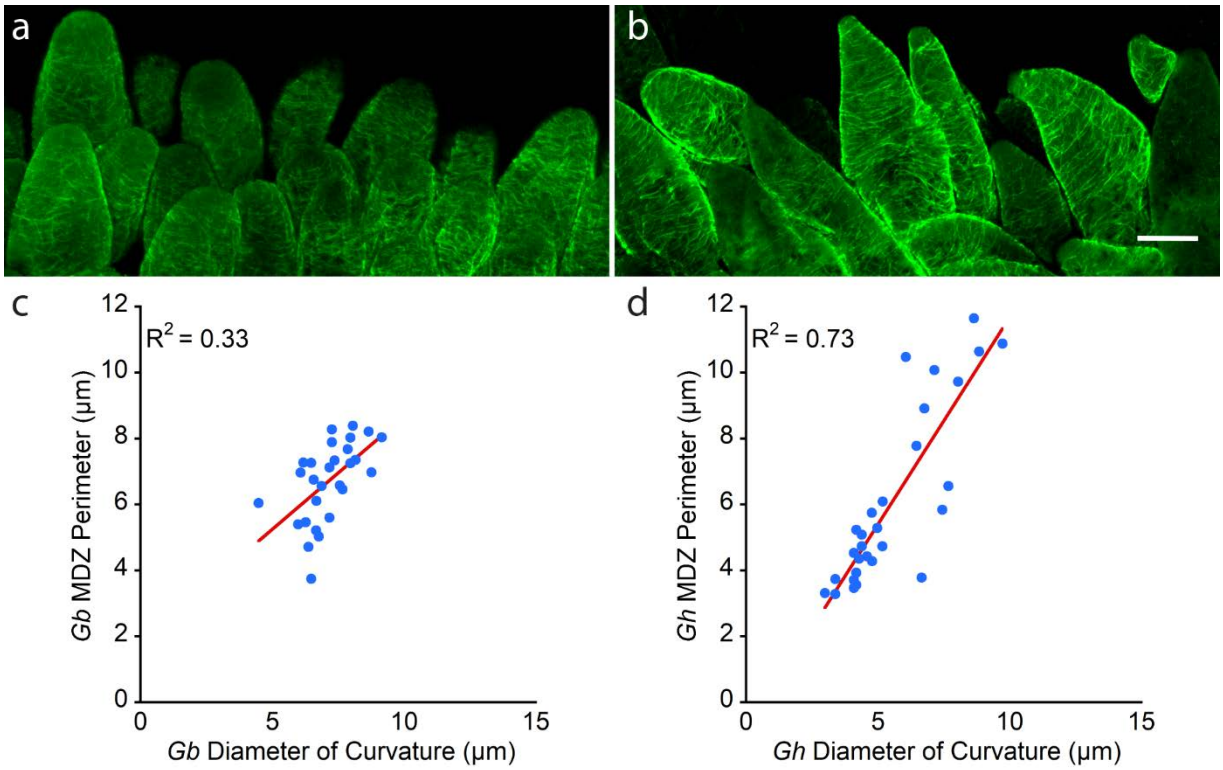

Figure 10. Linear regression analysis and calculation of R^2 values between fiber apical diameter and the MDZ perimeter during visible tip tapering. **a,** For *Gb* tips at 1.5 DPA, the MDZ perimeter explains 33% of the variation in apical diameter. **b,** For *Gh tapered* tips at 1 DPA, the MDZ perimeter explains 73% of the variation in apical diameter. n = 28 (*Gb*) or 29 (*Gh tapered*). *Gh hemisphere* fibers were not included in the analysis because only 2 of 29 (7%) of the *Gh hemisphere* fibers imaged showed a clear MDZ, as opposed to 88% or 68% of *Gb* and *Gh tapered* fiber respectively.

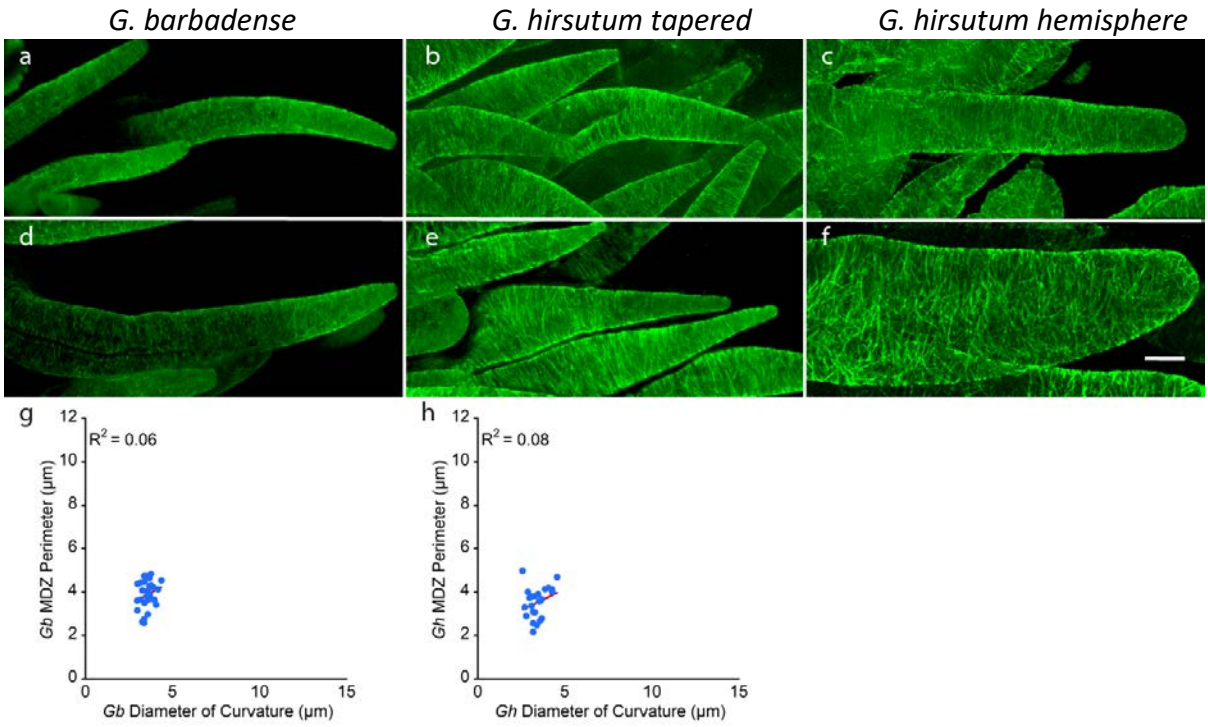

Figure 11. By 2 DPA, transverse microtubule arrays dominated all fiber tip types and MDZ perimeter no longer had a linear relationship to apical diameter. **a, d** *Gb* and **b, e** *Gh tapered* tips had generated their narrow tips by this time. **c, f** *Gh hemisphere* tips had blunt tips at this time. **e, f** Linear regression analysis showed virtually no relationship between MDZ and apical diameter for *Gb* or *Gh tapered* tips after their formation. A plot for *Gh hemisphere* tips is not present due to scarcity of a clear MDZ. Panel f shows a collapsed *Gh hemisphere* fiber appearing wider than it would be in cylindrical form, but such fibers were not included in measurements or linear regression analysis. For **e, f**, n = 30 (*Gb*) or 24 (*Gh tapered*). Scale bar = 10 µm for all images.

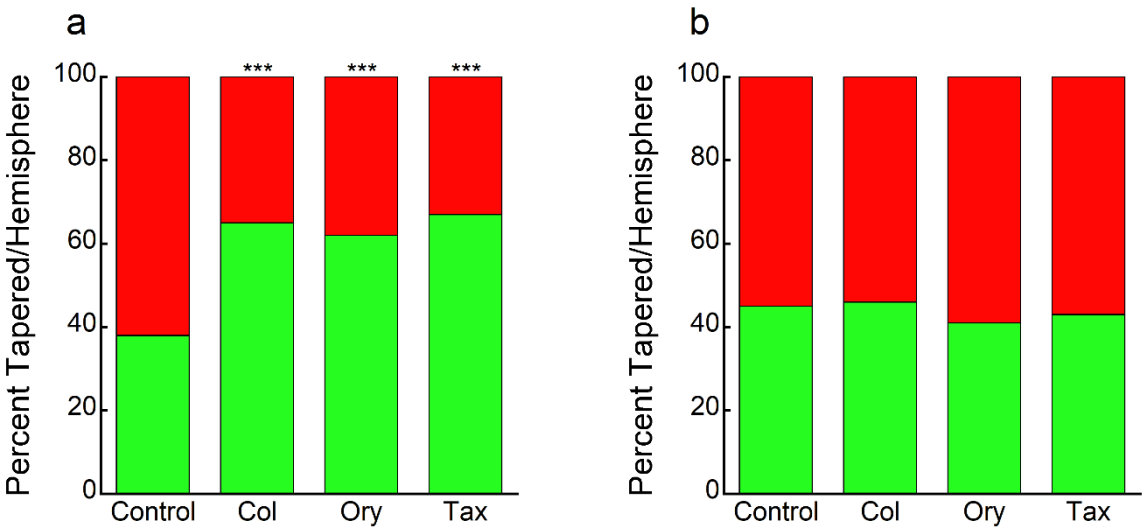

Figure 12. Change in ratio of *tapered* to *hemisphere* fiber tips in *Gh* with and without microtubule antagonists at 3 and 4 DPA. **a**, The percentage of *Gh tapered* fiber tips (red) was reduced when ovules were treated with microtubule antagonists at 1 DPA (Chi-square; $p < 0.001$). **b**, The ratio of *Gh tapered* to *hemisphere* fibers (green) was not changed when ovules were treated at 2 DPA. For 3 DPA *tapered* and *hemisphere* fiber tips, n = 77-148 and 91-152, respectively. For 4 DPA *tapered* and *hemisphere* fiber tips, n = 114-393 and 87-326, respectively. These graphs show data in Tables 1-6. Fiber tips were measured on 10-12 ovules from at least 6 replicates within 3 trials.

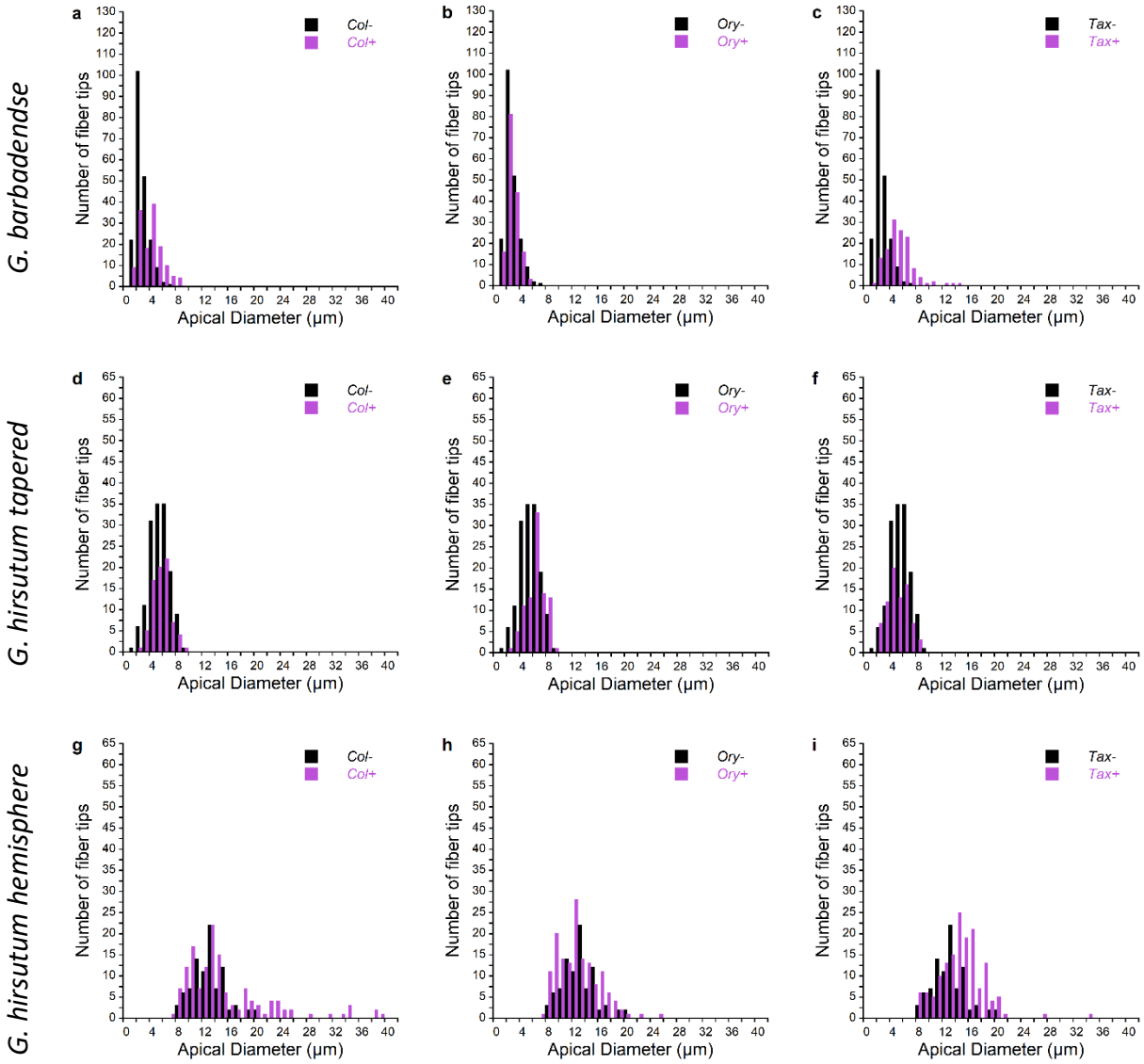

Figure 13. Histograms showing the distribution of apical diameters of three tip types with and without treatment with microtubule antagonists at 1 DPA. The microtubule antagonists used were colchicine (Col), oryzalin (Ory), and Taxol (Tax), and measurements were made at 3 DPA. **a-c**, The distribution of *Gb* apical diameters shifted upwards when treated with colchicine and Taxol but was unaffected by oryzalin. **d-f**, The distribution of apical diameters in *Gh tapered* fiber tips was not changed by treatment with any microtubule antagonist. **g-i**, The apical diameter distribution of *Gh hemisphere* fibers was either **g**, skewed from large diameter outliers or **i**, shifted upwards when treated with colchicine or Taxol respectively.

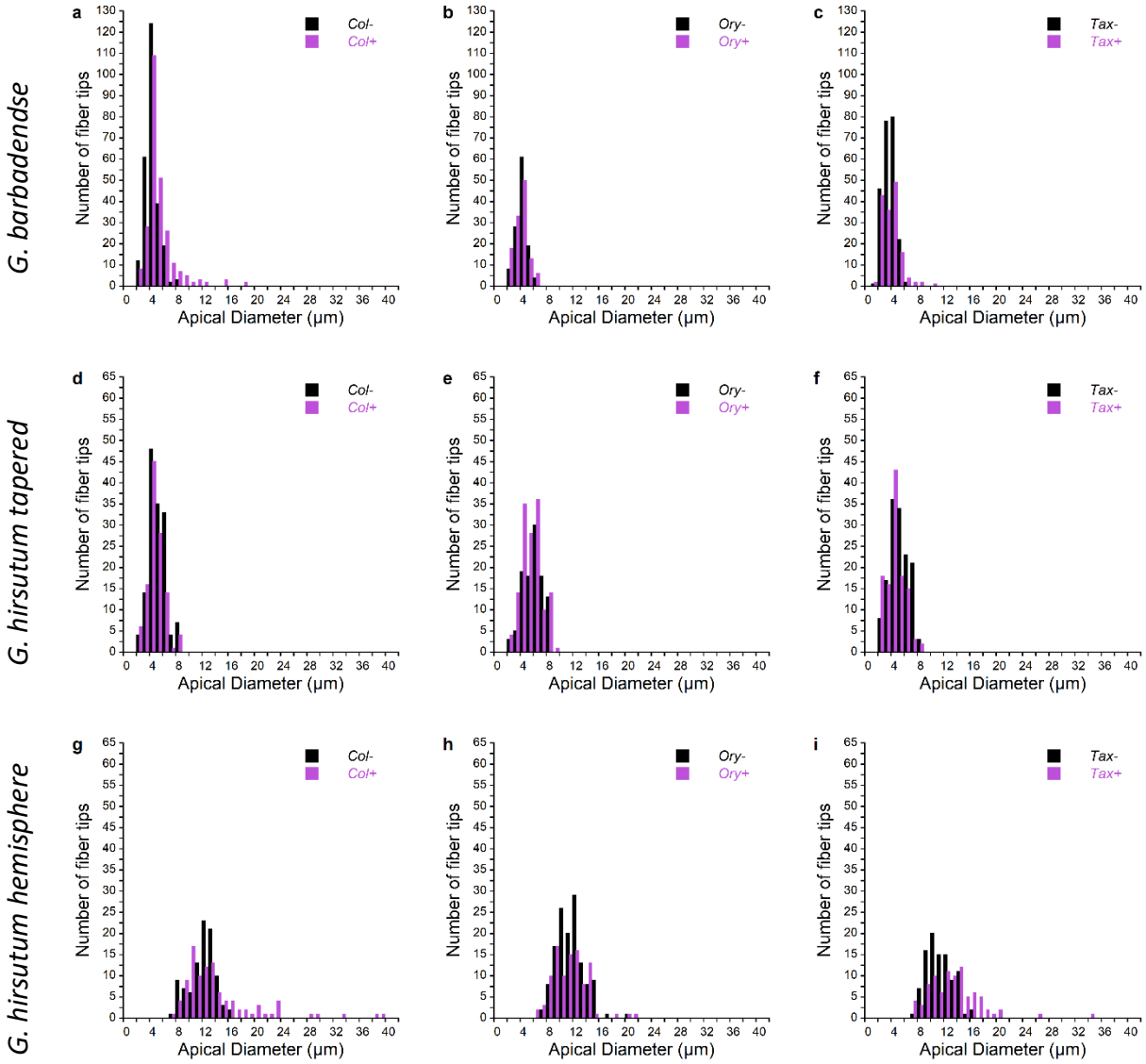

Figure 14. Histograms showing the distribution of apical diameters of three tip types with and without treatment with microtubule antagonists at 2 DPA. The microtubule antagonists used were colchicine (Col), oryzalin (Ory), and Taxol (Tax), and measurements were made at 4 DPA. **a-c**, The distribution of *Gb* apical diameters was skewed towards a higher mean diameter when treated with colchicine. **d-f**, The distribution of apical diameters in *Gh tapered* fiber tips was not changed by treatment with any microtubule antagonist. **g-i**, Similar to fibers treated at 1 DPA, the apical diameter distribution of *Gh hemisphere* fibers treated at 2 DPA was either **g**, skewed or **i**, shifted towards a larger apical diameter when treated with colchicine or Taxol respectively.

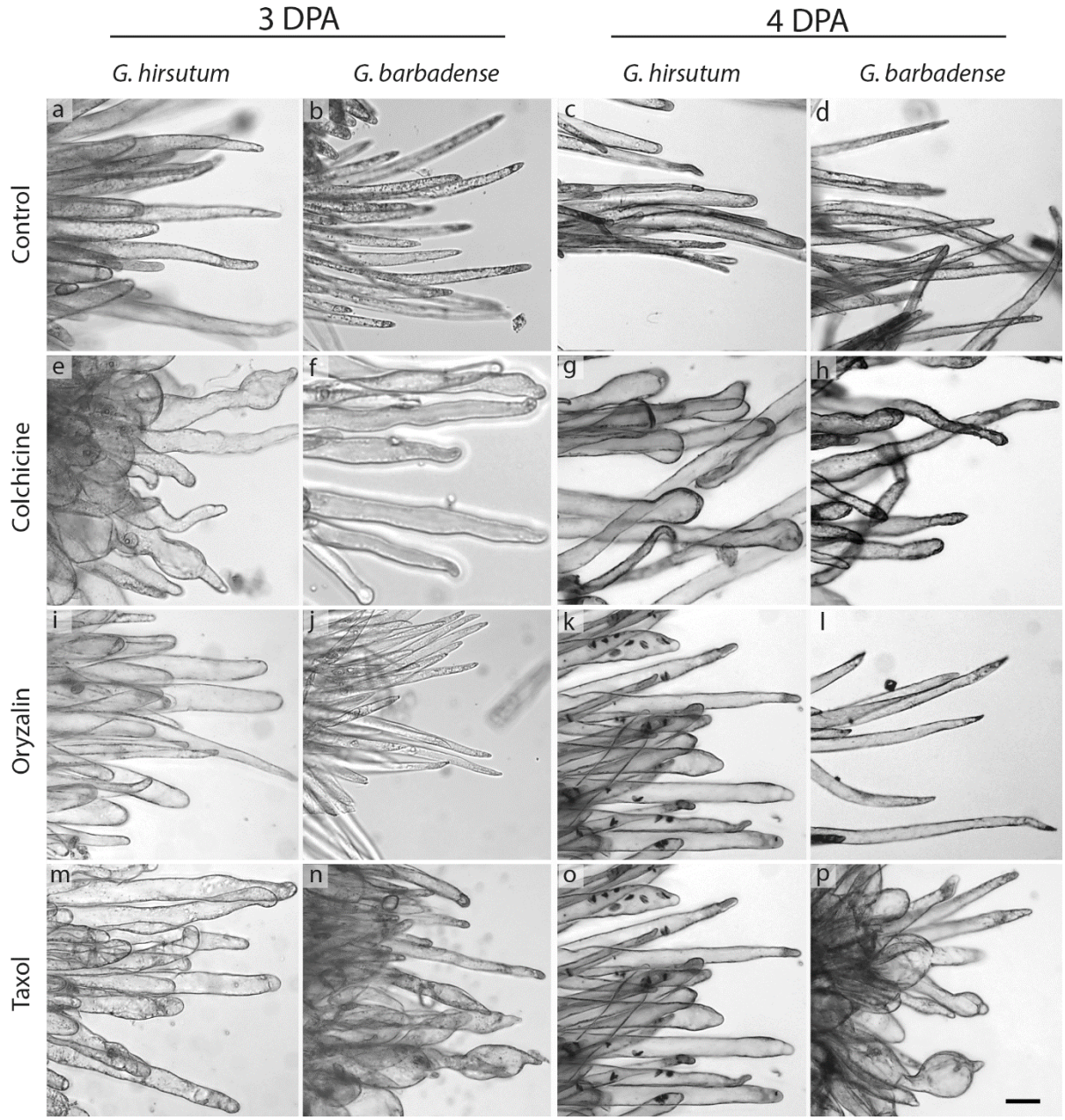

Figure 15. Changes in morphology for cotton fibers of *Gh* and *Gb* when cultured from either 1-3 DPA or 2-4 DPA. **a-d,** Control fibers for both species illustrate the two different tip types present on *Gh* compared to the uniform *Gb* fiber tips. **e-h,** Colchicine treatment consistently resulted in swelling for both species at all time-points. **i-l,** Oryzalin treatment frequently caused swelling in *Gh* but *Gb* did not swell at either time point. **m-p,** Taxol treatment resulted in general swelling and/or swelling of discrete regions while adjacent regions remained relatively normal. The scale bar (20 μm) applies to all images.

Figure 16. Average changes in diameter of 3 DPA fibers after being treated with microtubule antagonists at 1 DPA. Shapes are to scale for each of the four locations measured. Numerical values for the control (blue) are the average diameter at that location. The significant increases in diameter after treatments (green for colchicine, magenta for oryzalin, and orange for Taxol) as compared to control are indicated by numerical percentages (a, $p \leq 0.05$; b, $p \leq 0.01$; and c, $p \leq 0.001$). Statistical analysis by Welch's ANOVA followed by the Games-Howell test.

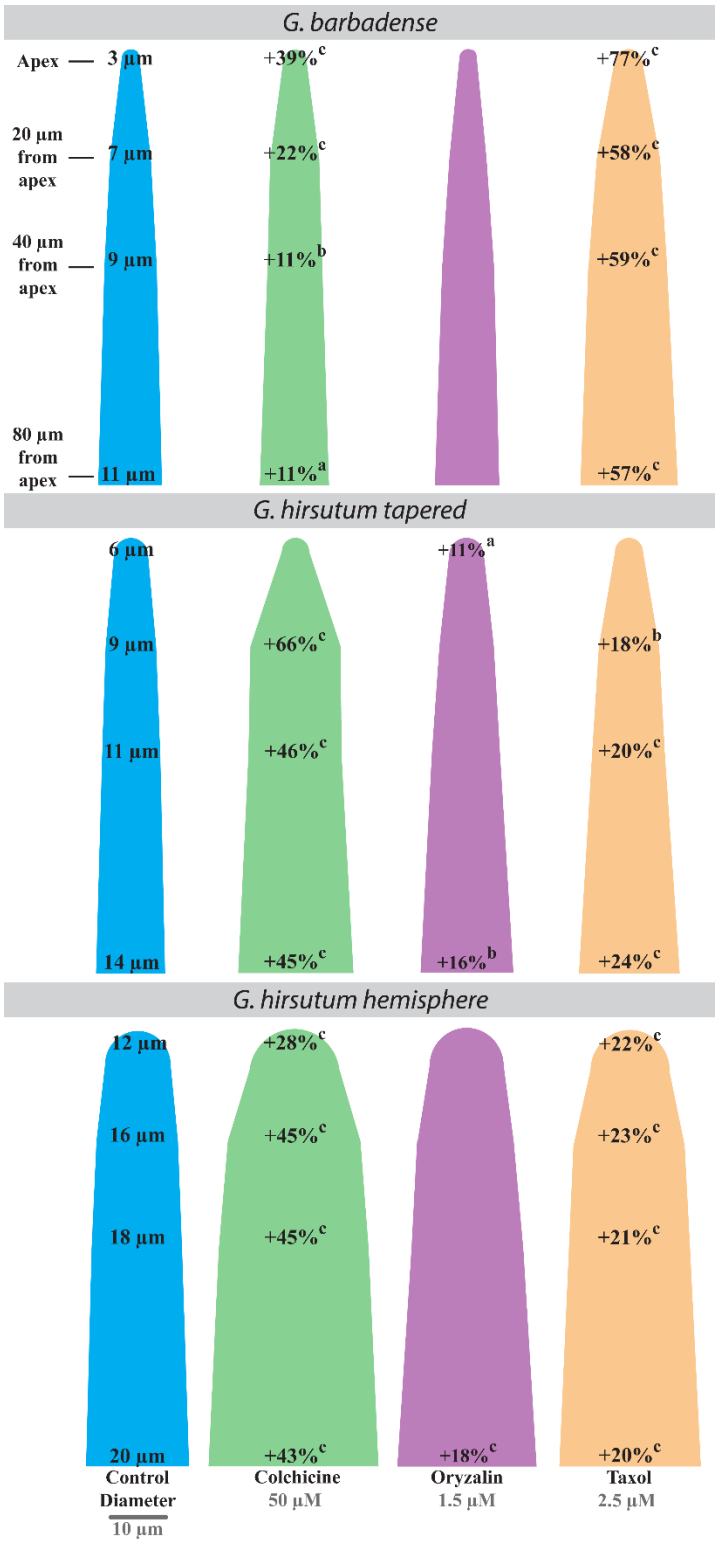
G. barbadense
Apex
3 µm
+39%c
+77%c
20 µm from apex
7 µm
+22%c
+58%c
40 µm from apex
9 µm
+11%b
+59%c
80 µm from apex
11 µm
+11%a
+57%c
G. hirsutum tapered
6 µm
+11%a
9 µm
+66%c
+18%b
11 µm
+46%c
+20%c
14 µm
+45%c
+16%b
+24%c
G. hirsutum hemisphere
12 µm
+28%c
+22%c
16 µm
+45%c
+23%c
18 µm
+45%c
+21%c
20 µm
+43%c
+18%c
+20%c
Control
Diameter
10 µm
Colchicine
50 µM
Oryzalin
1.5 µM
Taxol
2.5 µM

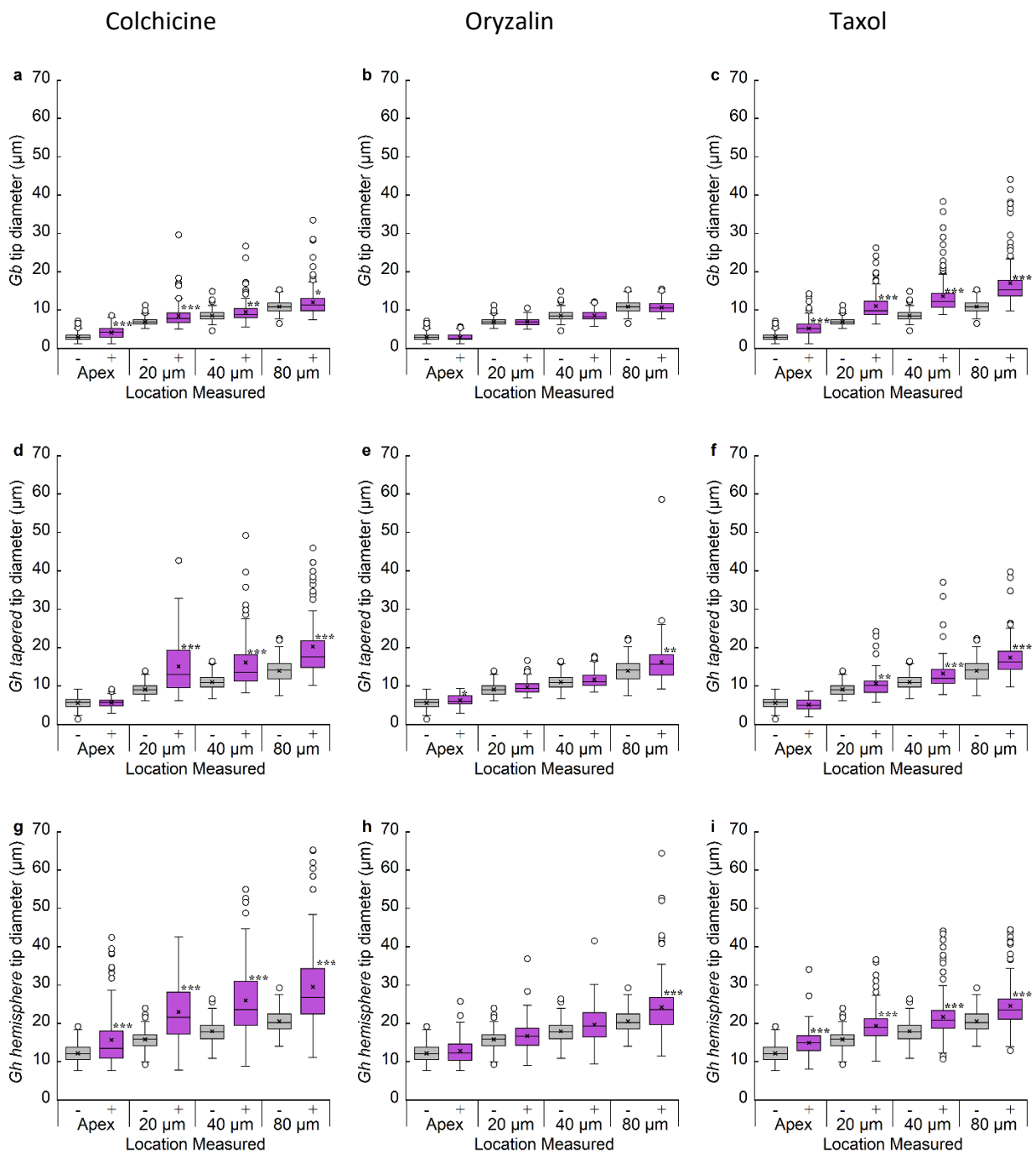

Figure 17. Box plots of fiber tip measurements at four locations in three tip types with and without microtubule antagonists. Ovules at 1 DPA were cultured with (magenta boxes) and without (grey boxes) microtubule antagonists, and tips were measured at 3 DPA. Results are shown for **a-c,** *Gb* tips), **d-f,** *Gh tapered* tips, and **g-i,** *Gh hemisphere* tips with and without **a, d, g,** colchicine, **b, e, h,** oryzalin, or **c, f, i,** taxol. Asterisks (see Fig. 5) indicate significant differences between the control and treatments for each tip type, location, and antagonist, as determined by Games-Howell test. Replication is shown in Tables 1-3.

Figure 18. Average changes in diameter of 4 DPA fibers after being treated with microtubule antagonists at 2 DPA. Shapes are to scale for each of the four locations measured. Numerical values for the control (blue) are the average diameter at that location. The significant increases in diameter after treatments (green for colchicine, magenta for oryzalin, and orange for Taxol) as compared to control are indicated by numerical percentages (a, $p \leq 0.05$; b, $p \leq 0.01$; and c, $p \leq 0.001$). Statistical analysis by Welch's ANOVA followed by the Games-Howell test.

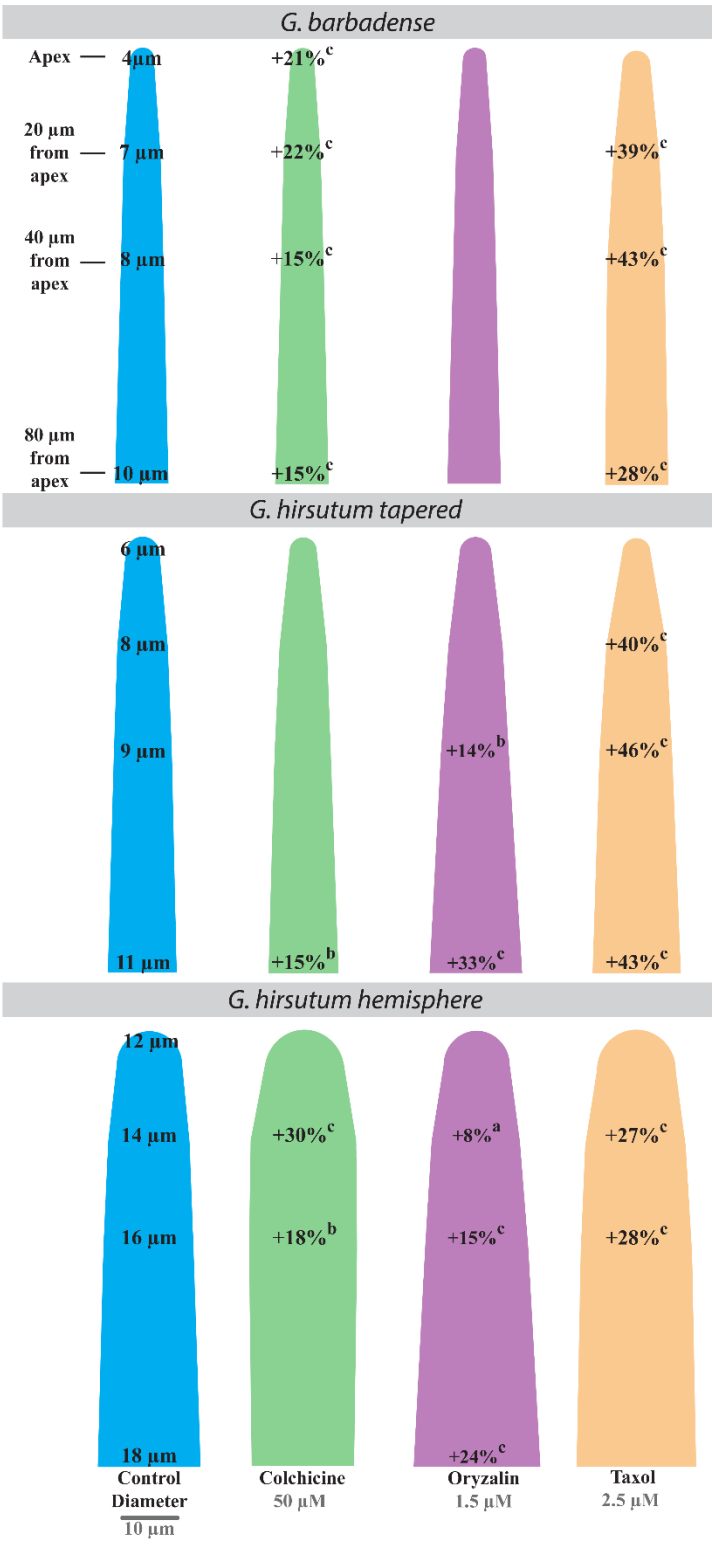
G. barbadense
Apex
4µm
+21%c
20 µm from apex
7 µm
+22%c
+39%c
40 µm from apex
8 µm
+15%c
+43%c
80 µm from apex
10 µm
+15%c
+28%c
G. hirsutum tapered
6 µm
8 µm
+40%c
9 µm
+14%b
+46%c
11 µm
+15%b
+33%c
+43%c
G. hirsutum hemisphere
12 µm
14 µm
+30%c
+8%a
+27%c
16 µm
+18%b
+15%c
+28%c
18 µm
+24%c
Control
Diameter
10 µm
Colchicine
50 µM
Oryzalin
1.5 µM
Taxol
2.5 µM

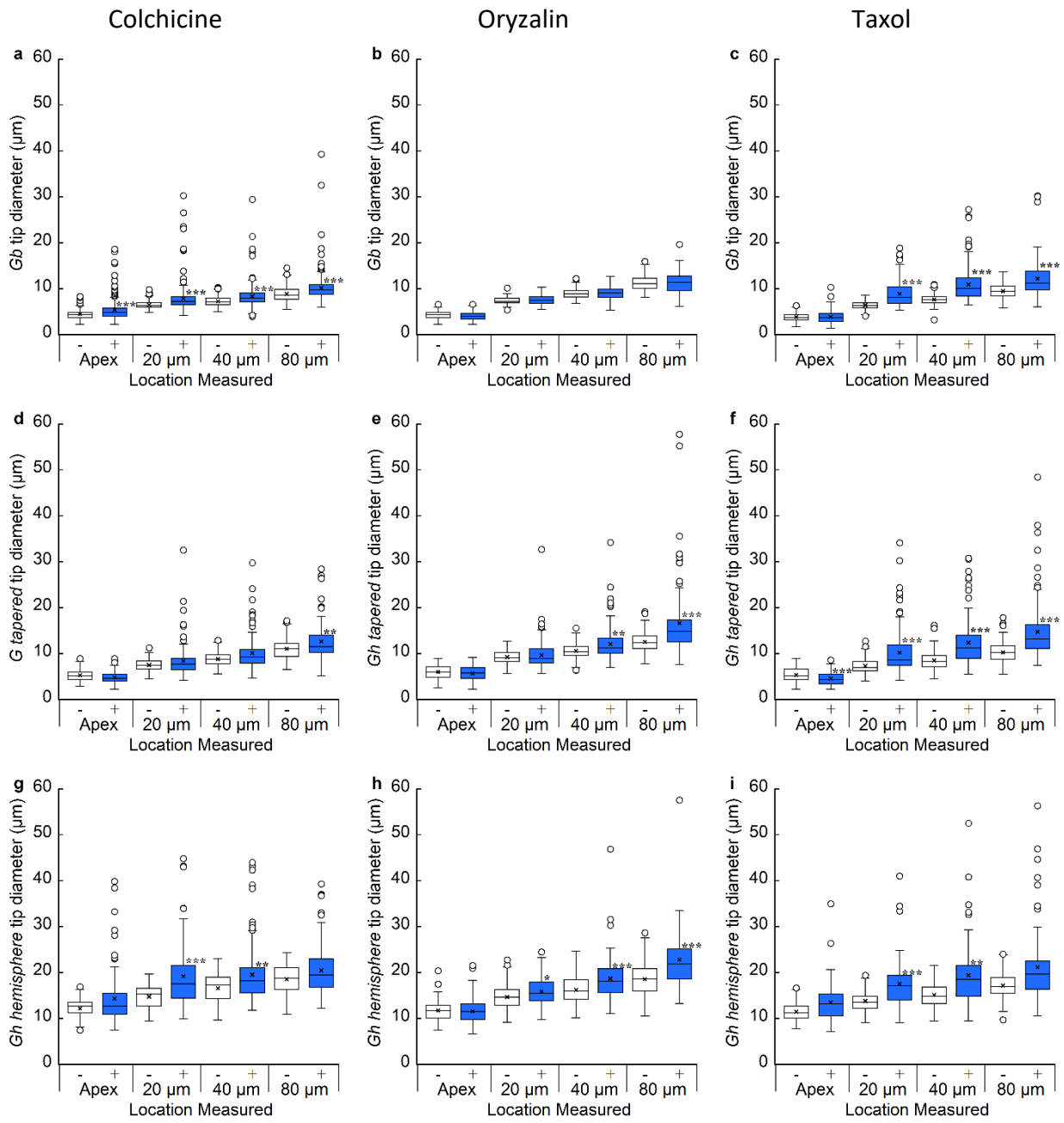

Figure 19. Box plots of fiber tip measurements at four locations in three tip types with and without microtubule antagonists. Ovules at 2 DPA were cultured with (blue boxes) and without (white boxes) microtubule antagonists, and tips were measured at 4 DPA. Results are shown for **a-c,** *Gb* tips, **d-f,** *Gh tapered* tips, and **g-i,** *Gh hemisphere* tips with and without **a, d, g,** colchicine, **b, e, h,** oryzalin, or **c, f, i,** taxol. Asterisks (see Fig. 5) indicate significant differences between the control and treatments for each tip type, location, and antagonist, as determined by Games-Howell test. Replication is shown in Tables 4-6.

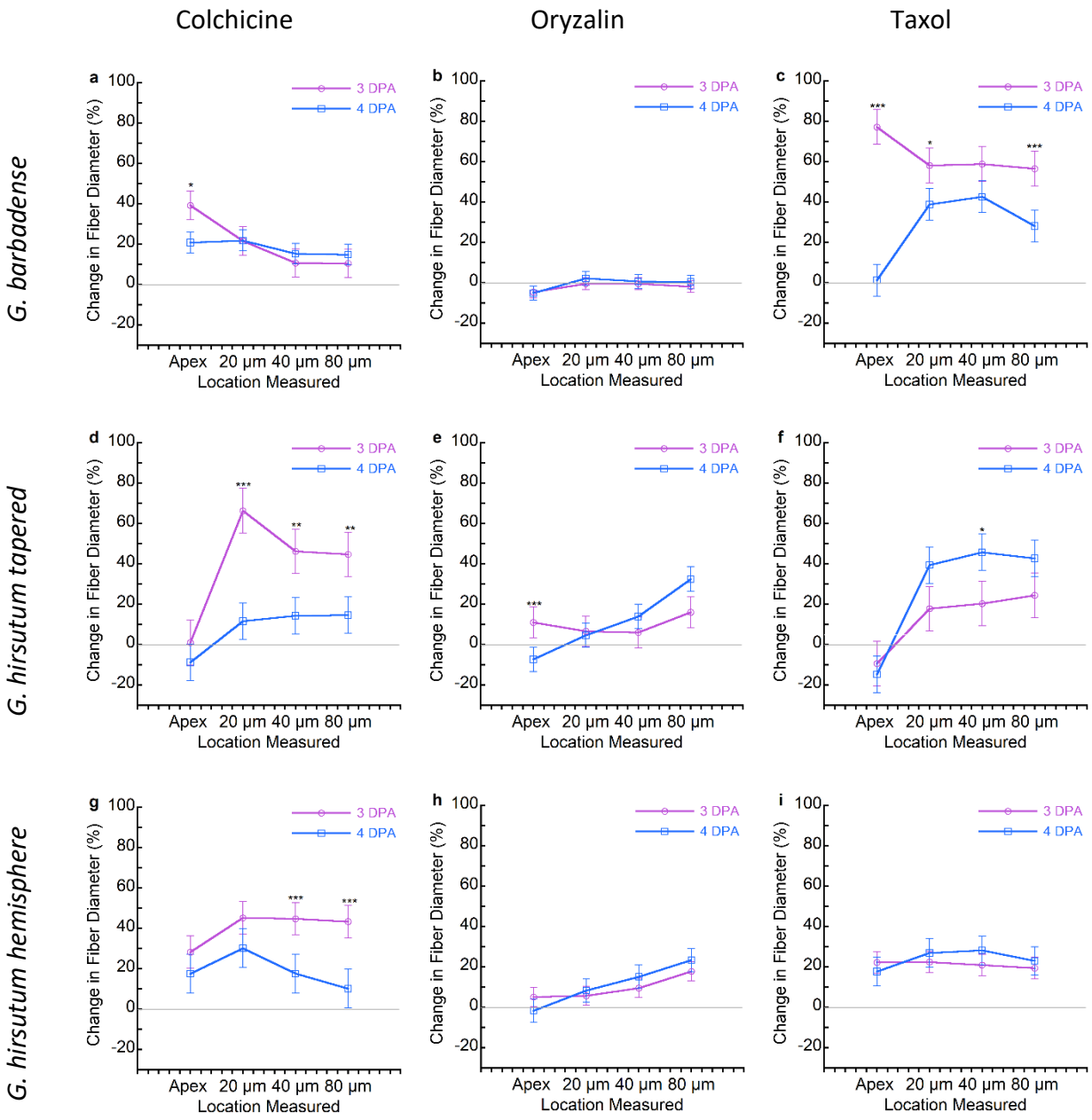

Figure 20. Comparison of the percent changes of treated versus control tip diameters when microtubule antagonists were added at 1 DPA or 2 DPA. In each case, measurements were made 48h later (3 DPA or 4 DPA) at the apex and 20, 40, and 80 µm behind it. Results are shown for **a-c,** *Gb* tips, **d-f,** *Gh tapered* tips, and **g-i**, *Gh hemisphere* tips after the addition of **a, d, g,** colchicine, **b, e, h,** oryzalin, or **c, f, i,** Taxol. The grey line at zero indicates no difference between the two experiments. Asterisks (see Fig. 5) indicate significant differences between percent changes observed at 3 or 4 DPA for each tip type, location, and antagonist as determined by Welch's ANOVA followed by the Games-Howell test. Replication for 3 DPA is shown in Tables 1-3 and Tables 4-6 for 4 DPA. Error bars represent the 95% confidence interval.

REFERENCES

Avci, U., Pattathil, S., Singh, B., Brown, V. L., Hahn, M. G., & Haigler, C. H. (2013). Cotton Fiber Cell Walls of *Gossypium hirsutum* and *Gossypium barbadense* Have Differences Related to Loosely-Bound Xyloglucan. *PLoS ONE*, *8*(2). https://doi.org/10.1371/journal.pone.0056315

Constable, G., Llewellyn, D., Walford, S. A., & Clement, J. D. (2015). Cotton breeding for fiber quality improvement. In V. M. V. Cruz & D. A. Dierig (Eds.), *Industrial Crops, handbook for plant breeding* (pp. 191–232). New York: Springer. https://doi.org/10.1007/978-1-4939-1447-0

Huang, Q., Wang, H., Gao, P., Wang, G., & Xia, G. (2008). Cloning and characterization of a calcium dependent protein kinase gene associated with cotton fiber development. *Plant Cell Reports*, *27*(12), 1869–1875. https://doi.org/10.1007/s00299-008-0603-0

Ma, C., Li, C., Ganesan, L., Oak, J., Tsai, S., Sept, D., & Morrissette, N. S. (2007). Mutations in α-tubulin confer dinitroaniline resistance at a cost to microtubule function. *Molecular biology of the cell*, 18(12), 4711-4720. https://doi.org/10.1091/mbc.e07-04-0379

McDonald, J. H. (2014). *Handbook of Biological Statistics* (3rd ed.). Baltimore, Maryland: Sparky House Publishing.

Naylor, G. R., Stanton, J. H., & Speijers, J. (2014). Skin comfort of base layer wool garments. Part 2: Fiber diameter effects on fabric and garment prickle. *Textile Research Journal*, *84*(14), 1506–1514. https://doi.org/10.1177/0040517514523174

Park, S., Szumlanski, A. L., Gu, F., Guo, F., & Nielsen, E. (2011). A role for CSLD3 during cell-wall synthesis in apical plasma membranes of tip-growing root-hair cells. *Nature Cell Biology*, *13*(8), 973–980. https://doi.org/10.1038/ncb2294

Pierce, E. T., Graham, B. P., Stiff, M. R., Osborne, J. A., & Haigler, C. H. (2019). Cultures of *Gossypium barbadense* cotton ovules offer insights into the microtubule-mediated control of fiber cell expansion. *Planta*, *249*(5), 1551–1563. https://doi.org/10.1007/s00425-019-03106-5

Seagull, R. W. (1995). Cotton fiber growth and development : Evidence for tip synthesis and intercalary growth in young fibers. *Plant Physiology*, *14*, 27–38.

Stewart, J. M. (1975). Fiber Initiation on the Cotton Ovule. *American Journal of Botany*, *62*(7), 723–730.

Stiff , M. R., & Haigler, C. H. (2016). Cotton fiber tips have diverse morphologies and show evidence of apical cell wall synthesis. *Scientific Reports*, *6*, 27883. https://doi.org/10.1038/srep27883

Stiff, M. R., & Haigler, C. H. (2012). Recent Advances in Cotton Fiber Development. *Flowering and Fruiting in Cotton*, 163–192.

Szymanski, D. B. (2016). *US 2016/0230180 A1*. US.

Tiwari, S. C., & Wilkins, T. A. (1995). Cotton (*Gossypium hirsutum*) seed trichomes expand via a diffuse growing mechanism. *Canadian Journal of Botany*, *73*, 746–757. https://doi.org/10.1139/b95-081

Wu, S. Z., & Bezanilla, M. (2018). Actin and microtubule cross talk mediates persistent polarized growth. *Journal of Cell Biology*, *217*(10), 3531-3544.

Yanagisawa, M., Alonso, J. M., & Szymanski, D. B. (2018). Microtubule-Dependent Confinement of a Cell Signaling and Actin Polymerization Control Module Regulates Polarized Cell Growth. *Current Biology*, *28*(15), 2459-2466.e4. https://doi.org/10.1016/j.cub.2018.05.076

Yanagisawa, M., Desyatova, A. S., Belteton, S. A., Mallery, E. L., Turner, J. A., & Szymanski, D. B. (2015). Patterning mechanisms of cytoskeletal and cell wall systems during leaf trichome morphogenesis. *Nature Plants*, *1*(3), 15014. https://doi.org/10.1038/nplants.2015.14

Yu, Y., Wu, S., Nowak, J., Wang, G., Han, L., Feng, Z., Mendrinna, A., Ma, Y., Wang, H., Zhang, X., Tian, J., Dong, L., Nikoloski, Z., Persson, S., Kong, Z. (2019). Live-cell imaging of the cytoskeleton in elongating cotton fibres. *Nature Plants*, *5*(5), 498–504. https://doi.org/10.1038/s41477-019-0418-8

Zaiontz, C. (2019). Real Statistics Resource Pack. Retrieved from www.real-statistics.com

CHAPTER 4

Summary Conclusions

- Differences between three distinct cotton fiber tip types between two species were quantified according to the shape of the apical domain and fiber diameter behind the apex. The fiber tips characterized were *Gossypium barbadense* type, *G. hirsutum tapered* type, and *G. hirsutum hemisphere* type.

- Differences in microtubule regulation of shape between fiber tip types are highlighted by the unique response of *G. hirsutum tapered* tips to colchicine-induced microtubule disruption.

- Transverse microtubule arrays are established by 1 DPA in all three fiber tip types coinciding with an increase in fiber elongation rate. Rearrangement of the microtubule array to achieve the transverse alignment is critical for maintaining fiber diameter.

- Microtubules are critical for maintaining apical diameter in *G. barbadense* and for maintaining diameter behind the apex in *both species*.

- The apical dome shape is being established about 24 hours after fiber initiation in all tip types, but tip shape becomes less dependent on microtubules by 2 DPA in *Gh* tip types.

- A strong, positive, linear relationship exists between the shape of the apical dome and perimeter of the MDZ in well-developed *G. hirsutum tapered* fibers at 1 DPA, similar to what was reported for *Arabidopsis* trichome branches

Ongoing Investigations

- We are working to more precisely determine the times of microtubule dependence or independence of early cotton fiber elongation and tip shape formation (Aniko Verbrugge and Ethan Pierce).

- The function and arrangement of actin filaments are being characterized during early fiber development in the three tip types. Fluorescent staining, pharmacological disruption of actin, and microscopy are being used to investigate the role of actin in tip refinement, elongation, and fiber diameter (Ben Graham, Appendix 1).

- Cellulose synthesis inhibitors are being used to determine the role of cellulose in regulating early fiber diameter and tip shape (Ethan Pierce). Immunofluorescence of microtubules after cellulose synthesis disruption will be used to test a proposed tight connection between cellulose synthesis and cortical microtubules in young cotton fibers.

- The origin of the two tip types in *G. hirsutum* is being investigated by surveying tip morphology in a variety of ancestral cotton lines and early breeding accessions (Laine Hill).

- In collaboration with a bioinformatician (Daniel Restrepo-Montoya, Ben Graham), a group of genes identified in the literature as differentially expressed in fiber between *G. hirsutum* and *G. barbadense* is being investigated. The genes being studied are all involved in cytoskeletal regulation or have been implicated in processes related to plant cell shape control. The genes are being cross-referenced with all available cotton genome sequences while surveying for available expression data linked with fiber qualities.

Future work

Future work should begin with determining the time point at which *Gb* fibers begin to refine their apices to reduce their apical diameter by 2 DPA. *Gossypium hirsutum tapered* fibers begin reducing their apical diameter by the morning of 1 DPA, but this was not as apparent in *Gb*. In fact, *Gb* fibers appeared to elongate while minimally or gradually altering their apical diameter without an obvious tapering effect by the morning of 1 DPA. Observations made 12 hours later, on the evening of 1 DPA, showed increased tapering in *Gb*, but it still did not appear developmentally equivalent to 1 DPA *Gh tapered* fibers. Increasing the temporal resolution, by observing *Gb* fibers throughout the evening of 1 DPA until the tapering can be observed at 2 DPA, will provide a more complete developmental timeline for *Gb* fiber tips. Additionally, the relationship between the apical diameter and MDZ of *Gh hemisphere* fibers at 1 DPA should be determined. Increased sampling and imaging of *Gh hemisphere* fiber tips may overcome the lower occurrence of a clear MDZ in this fiber type.

Differences in the amount and distribution of cell wall components in cotton fibers should be examined for any correlation with microtubules presence, position, and pattern. These data may identify a link between microtubules and the secretion of cellulosic and non-cellulosic cell wall components, which has not been established in cotton fiber. Live-cell imaging of developing cotton fibers with fluorescent markers for the cytoskeletal components would also provide great insight into how this process is regulated. Recent work has shown that the transgenic lines can be created to conduct this research and that live-cell imaging can be achieved, although the methods remain obscure (Yu et al., 2019). Comparing the microtubule angle to the cellulose microfibril angle at a stage in cotton fiber development, analogous to that of the newly branching *Arabidopsis* trichome, would also test for a tip-biased diffuse growth mode in cotton fiber, as is proposed for trichomes (Yanagisawa et al., 2018, 2015).

A greater understanding of the cytoskeletal dynamics during early polar elongation may reveal parts of the regulatory network involved in shape determination. Live-cell imaging of cytoskeletal dynamics, within the context of the *G. hirsutum tapered* and *hemisphere* fibers, might provide clues into the morphogenesis of the two fiber tip types. Developing transgenic lines of *G. barbadense* with fluorescent reporters for the cytoskeleton would allow direct comparisons to the ideal fiber tip type. This information would deepen our understanding of cotton fiber morphogenesis, allowing more efficient efforts toward improving the fiber quality.

Given that the most analogous polar elongating cell to cotton fibers seems to be the *Arabidopsis* trichome branch, at least during early development, genes implicated in trichome shape control should be investigated in cotton. Virus-induced gene silencing (VIGS) is an effective genetic tool in cotton (Tuttle et al., 2015). Alternatively, cotton orthologues could be expressed in corresponding *Arabidopsis* mutants. If cotton genes products are able to rescue mutant phenotypes in *Arabidopsis*, as is the case with GhKINESIN 4A (Kong et al., 2015), that may provide critical clues to the function of these genes in cotton, while also improving our understanding of cotton shape formation. The increasing availability and quality of genome sequences in cotton should be an encouraging sign for future functional gene characterization in cotton using molecular genetic techniques commonly employed today.

Compelling questions

- What are the relative amounts and distribution of crystalline cellulose and pectin types in each cotton fiber tip type? Is the amount or distribution of any of these cell wall components impacted by microtubule or actin filament disruption?

- Do cortical microtubules and crystalline cellulose align early in cotton fiber development? If so, at what DPA does this begin?

- At what point in domestication did *G. hirsutum* begin to exhibit the two morphologically distinct tip types? Are there ancestral lines or accessions that possess only one tip type?

- Are there differences in expression of genes implicated in coordinating apical cell wall synthesis between *G. barbadense* and *G. hirsutum* during the time of tip shape formation?

- What is the localization of the proteins and protein complexes that might be involved in shape control in developing cotton fiber?
    - ARP2/3 complex – actin nucleation
    - W/SRC complex – activation of ARP2/3
    - SPK1 – promotes actin network formation at the apical plasma membrane
    - Myosin VIII

- Can VIGS be used to silence genes that are possibly related to tip refinement and shape control in cotton fiber? Will reduced expression of these genes in cotton fiber result in similar phenotypic defects to those found in other polar elongating cells of the corresponding mutants in other species?

REFERENCES

Kong, Z., Ioki, M., Braybrook, S., Li, S., Ye, Z. H., Lee, Y. R., Hotta, T., Chang, A., Tian, J., Wang, Guangda, Liu, B. (2015). Kinesin-4 Functions in Vesicular Transport on Cortical Microtubules and Regulates Cell Wall Mechanics during Cell Elongation in Plants. *Molecular Plant*, *8*(7), 1011–1023. https://doi.org/10.1016/j.molp.2015.01.004

Tuttle, J. R., Haigler, C. H., & Robertson, D. (2015). Virus-induced gene silencing of fiber-related genes in cotton. In *Plant Gene Silencing* (pp. 219-234). Humana Press, New York, NY. https://doi.org/10.1007/978-1-4939-2453-0_16

Yanagisawa, M., Alonso, J. M., & Szymanski, D. B. (2018). Microtubule-Dependent Confinement of a Cell Signaling and Actin Polymerization Control Module Regulates Polarized Cell Growth. *Current Biology*, *28*(15), 2459-2466.e4. https://doi.org/10.1016/j.cub.2018.05.076

Yanagisawa, M., Desyatova, A. S., Belteton, S. A., Mallery, E. L., Turner, J. A., & Szymanski, D. B. (2015). Patterning mechanisms of cytoskeletal and cell wall systems during leaf trichome morphogenesis. *Nature Plants*, *1*(3), 15014. https://doi.org/10.1038/nplants.2015.14

Yu, Y., Wu, S., Nowak, J., Wang, G., Han, L., Feng, Z., Mendrinna, A., Ma, Y., Wang, H., Zhang, X., Tian, J., Dong, L., Nikoloski, Z., Persson, S., Kong, Z. (2019). Live-cell imaging of the cytoskeleton in elongating cotton fibres. *Nature Plants*, *5*(5), 498–504. https://doi.org/10.1038/s41477-019-0418-8

APPENDIX

Appendix A

In *Gh* fibers, transversely oriented microtubules have been observed throughout the fiber by TEM. They extend to within micrometers of the apex at an angle that coincides with that of cellulose microfibrils (Seagull, 1986, 1995). However, similar to tip growing cells, actin filaments form longitudinal arrays through the center of the cotton fiber with smaller microfilaments branching out toward the cell cortex. This actin network is essential for fiber elongation (Li et al., 2005; Seagull, 1990). The actin arrangement also exhibits signs of a mixed growth mode with components of diffuse and tip growth (Yu et al., 2019). Unfortunately, these observations were not made in the context of the two tip morphologies we now know to be present in *Gh*, nor was any direct comparison made to fiber tips in *G. barbadense* (Stiff & Haigler, 2016).

Arabidopsis trichome branches have similar cytoskeletal arrangements to those observed in cotton fiber (Tian et al., 2015; Yanagisawa et al., 2015). Trichome branches have been shown to elongate by cell wall remodeling at the apex and along the flanks of the branch exhibiting growth modes indicative of highly polarized diffuse growth. There are, however, stark differences in the development and morphological fate of trichome branches and cotton fibers that can complicate direct comparisons. *Arabidopsis* trichome branches refine their apical diameter to a point much smaller than those observed in the relatively stable cotton fiber apices. The final length of trichome branches is also only a fraction of the final length achieved by the cotton fiber types being studied here, although, it does seem likely that there are analogous regulatory components at play in both systems.

Actin filaments are a part of the cytoskeleton that are largely responsible for transporting cell wall material to the point of exocytosis (Ketelaar, 2013; Smith & Oppenheimer, 2005). Actin filaments and microtubules often work in conjunction with one another to coordinate proper cell expansion (Petrasek & Schwarzerová, 2009; Takeuchi et al., 2017). Considering this, by documenting any changes in the actin patterning after microtubule antagonism, we can determine to what degree, if any, actin filaments rely on an established microtubule array to maintain or regulate their natural organization. Changes in the actin filament array caused by pharmacologically-induced disorganization or inhibition of the microtubule array may be partly responsible for the changes in cotton fiber morphology.

In the two narrow tip types, *Gb* and *Gh tapered*, cortically located actin was organized in long axially oriented filaments that terminated at the apex. In *Gh hemisphere* fiber tips, actin is also cortically located and axially oriented, but the actin filaments formed a loop near the apex that could not be resolved in the narrow tip types (Fig. 1a – 1c). This loop structure is similar to what was observed near the apex of elongating *Arabidopsis* root hairs (Zhang et al., 2014). I imaged *Gh* tips after being treated with microtubule antagonists for 48 hours. When treated with the microtubule inhibitors colchicine or oryzalin, the actin signal appeared either diminished or disorganized (Fig. 1d – 1g). When treated with Taxol, actin organization appeared to maintain an organization similar to the controls (Fig. 1h & 1i). These results indicate that the microtubule array must be intact for actin to assume normal organization. This may signify an important interplay between the two cytoskeletal components in developing cotton fiber. Ovules of *Gb* were not available for culture and microtubule antagonist treatment at the same time, therefore, their assessment is still pending.

Actin staining

Fibers were fixed for 1 hour in 4% formaldehyde in KMCP buffer (70 mM KCl, 1 mM $MgCl_2$, 1 mM $CaCl_2$, and 100 mM Pipes, pH 6.5). Ovules with fiber attached were rinsed (2 x 5 min) and then incubated in 0.5% (w/v) ultrapure pectinase in 1x KMCP buffer (Worthington Biochem. #LS004298). Following two more rinses (2 x 5 min) the ovules were treated with 0.1% Triton X-100 in KCMP buffer for 10 minutes. After two rinses (2 x 10 min) ovules were incubated with 1% BSA in KMCP with AlexaFluor488-Phalloidin (ThermoFisher Scientific) for 1 hour then rinsed again prior to mounting in ProLong Gold antifade mountant (ThermoFisher Scientific).

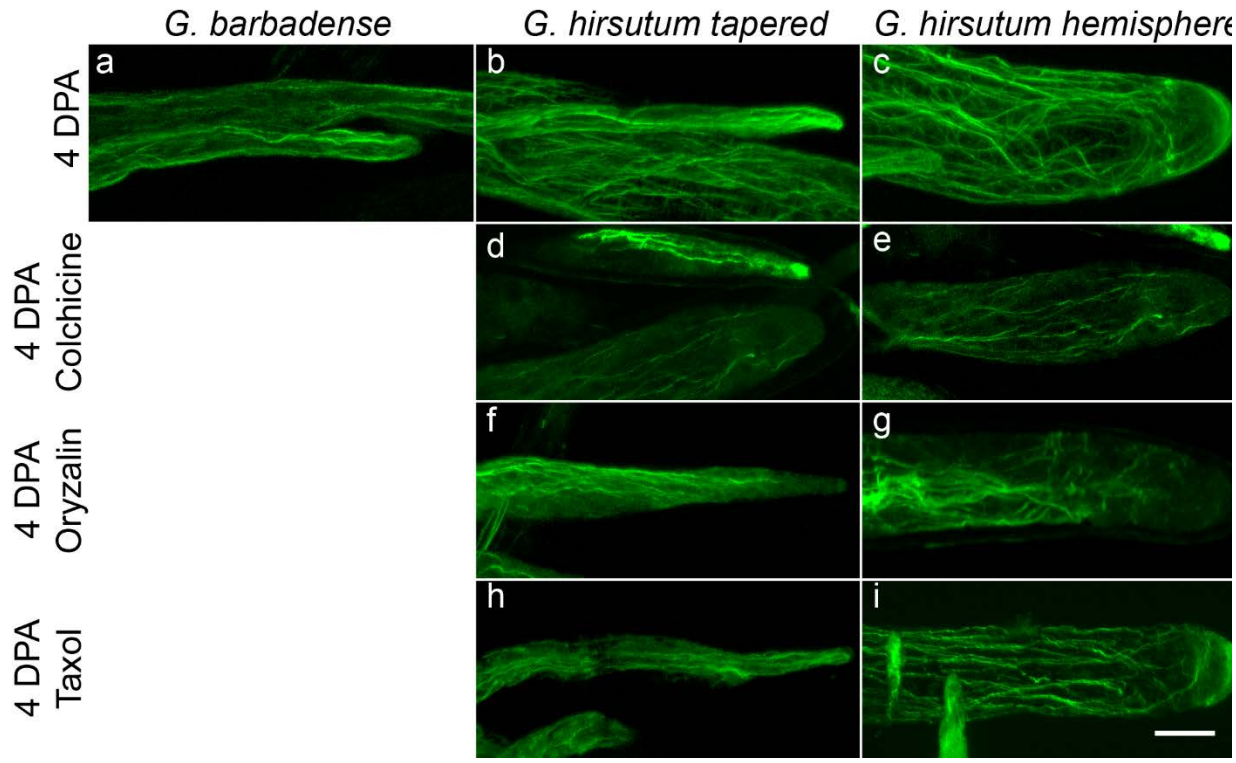

Figure 1. Actin organization in three cotton fiber tip types. Fiber tips of *Gh* were also stained for actin after treatment with microtubule antagonists. **d, e** Colchicine, **f, g** oryzalin, and **h, i** Taxol treated fiber cells of *G. hirsutum*. The scale bar (10 µm) applies all images.

REFERENCES

Ketelaar, T. (2013). The actin cytoskeleton in root hairs: All is fine at the tip. *Current Opinion in Plant Biology*, *16*(6), 749–756. https://doi.org/10.1016/j.pbi.2013.10.003

Li, X., Fan, X., Wang, X., Cai, L., & Yang, W. (2005). The cotton ACTIN1 gene is functionally expressed in fibers and participates in fiber elongation. *The Plant Cell*, *17*(3), 859–875. https://doi.org/10.1105/tpc.104.029629.subapical

Petrasek, J., & Schwarzerová, K. (2009). Actin and microtubule cytoskeleton interactions. *Current Opinion in Plant Biology*, *12*(6), 728–734. https://doi.org/10.1016/j.pbi.2009.09.010

Seagull, R. W. (1986). Changes in Microtubule Organization and Wall Microfibril Orientation during Invitro Cotton Fiber Development - an Immunofluorescent Study. *Canadian Journal of Botany-Revue Canadienne De Botanique*, *64*(7), 1373–1381.

Seagull, R. W. (1990). The effects of microtubule and microfilament disrupting agents on cytoskeletal arrays and wall deposition in developing cotton fibers. *Protoplasma*, *159*(1), 44–59. https://doi.org/10.1007/BF01326634

Seagull, R. W. (1995). Cotton fiber growth and development : Evidence for tip synthesis and intercalary growth in young fibers. *Plant Physiology*, *14*, 27–38.

Smith, L. G., & Oppenheimer, D. G. (2005). Spatial Control of Cell Expansion By the Plant Cytoskeleton. *Annual Review of Cell and Developmental Biology*, *21*(1), 271–295. https://doi.org/10.1146/annurev.cellbio.21.122303.114901

Stiff , M. R., & Haigler, C. H. (2016). Cotton fiber tips have diverse morphologies and show evidence of apical cell wall synthesis. *Scientific Reports*, *6*, 27883. https://doi.org/10.1038/srep27883

Takeuchi, M., Staehelin, L. A., & Mineyuki, Y. (2017). Actin-Microtubule Interaction in Plants. *Cytoskeleton-Structure, Dynamics, Function and Disease. InTechOpen*, 33-54. https://doi.org/http://dx.doi.org/10.5772/66930

Tian, J., Han, L., Feng, Z., Wang, G., Liu, W., Ma, Y., Yu, Y., Kong, Z. (2015). Orchestration of microtubules and the actin cytoskeleton in trichome cell shape determination by a plant-unique kinesin. *ELife*, *4*(8), 1–22. https://doi.org/10.7554/eLife.09351

Yanagisawa, M., Desyatova, A. S., Belteton, S. A., Mallery, E. L., Turner, J. A., & Szymanski, D. B. (2015). Patterning mechanisms of cytoskeletal and cell wall systems during leaf trichome morphogenesis. *Nature Plants*, *1*(3), 15014. https://doi.org/10.1038/nplants.2015.14

Yu, Y., Wu, S., Nowak, J., Wang, G., Han, L., Feng, Z., Mendrinna, A., Ma, Y., Wang, H., Zhang, X., Tian, J., Dong, L., Nikoloski, Z., Persson, S., Kong, Z. (2019). Live-cell imaging of the cytoskeleton in elongating cotton fibres. *Nature Plants*, *5*(5), 498–504.

https://doi.org/10.1038/s41477-019-0418-8

Zhang, Y., Sheng, X., Meng, X., & Li, Y. (2014). The circular F-actin bundles provide a track for turnaround and bidirectional movement of mitochondria in *Arabidopsis* root hair. *PLoS ONE*, *9*(3). https://doi.org/10.1371/journal.pone.0091501